



**LOW TEMPERATURE OPTIMIZATION OF COPPER
RECOVERY FROM E-WASTE**

BY

Motaoana Francis Khashole

Submitted in fulfilment of the academic requirements of

Master of Science

in Chemical Engineering

College of Agriculture, Engineering and Science

University of KwaZulu-Natal,

Durban

South Africa

January 2021

As the candidate's supervisor, I have/have not approved this thesis/dissertation for submission.

PREFACE

The experimental work described in this dissertation carried out at the University of KwaZulu-Natal in the College of Agriculture, Engineering and Science (CAES) at the Department of Chemical Engineering, Howard College Campus, Durban, from February 2019 to July 2020, under the supervision of Dr Mbuyu Ntunka and Dr Malusi Mkhize.

These studies represent original work by the author and have not otherwise been submitted in any form for any degree or diploma to any tertiary institution. Where use has made of the work of others, it is duly acknowledged in the text.

Signed: Dr Mbuyu Ntunka

Date:

COLLEGE OF AGRICULTURE, ENGINEERING AND SCIENCE

DECLARATION 1 - PLAGIARISM

I, Motaoana Francis Khashole, declare that

1. The research reported in this thesis, except where otherwise indicated, is my original research.
2. This thesis has not been submitted for any degree or examination at any other university.
3. This thesis does not contain other persons' data, pictures, graphs or other information, unless specifically acknowledged as being sourced from other persons.
4. This thesis does not contain other persons' writing, unless specifically acknowledged as being sourced from other researchers. Where other written sources have been quoted, then:
 - a. Their words have been re-written but the general information attributed to them has been referenced
 - b. Where their exact words have been used, then their writing has been placed in italics and inside quotation marks, and referenced.
5. This thesis does not contain text, graphics or tables copied and pasted from the Internet, unless specifically acknowledged, and the source being detailed in the thesis and in the References sections.

Signed

.....

ACKNOWLEDGEMENTS

I would like to thank my mother and father; you are the ones who pushed me to do this postgraduate degree. I dedicate this work to you. I would also like to thank my supervisors (Dr Mbuyu Ntunka and Dr Malusi Mkhize), I learnt so much from you both; and not just school knowledge. I deeply thank you. Ntsejoa Koma, thank you for the editorial work you did and pushing me on days I felt like slugging. To my friends, thank you all for your emotional support. Lastly, I would like to thank myself for not giving up and always finding the courage to go to the lab each day. And to those I am forgetting to mention, thank you all.

ABSTRACT

The purpose of the report is to provide a detailed investigation on the recycling of copper from waste electronic Printed Circuit Boards (PCBs). The roles played by leaching agent, temperature, time, particle size, and hydrogen peroxide (parameters) towards the recovery of copper are also explored. Other objectives include investigating the type of material being studied by performing a sieve analysis, investigating the effects of different leaching agents, and use of TGA to characterise the electronic waste (e-waste). PCBs recycling does not only address the issue of finite resources but also serves as an alternative way of obtaining resources (urban mining) with minimal harm to the environment compared to traditional mining. In this study, e-waste recovery has three major steps, the liberation of materials from e-waste, characterization of e-waste, and hydrometallurgical processing. E-waste recycling also helps tackle the problem of landfilling and pollution and is the fastest rising waste source is electronic waste and electronic waste processing for metal recovery is a recycling technique, and it creates job opportunities.

From the analysis of the particle size distribution, the coefficient of curvature was 2.56, and the coefficient of uniformity was 2.91, this indicates that the PCBs are not well distributed. This limits the study in that not sufficient size classes (there were significant differences in size classes) were represented in the PCBs. Furthermore, the thermogravimetric analysis (TGA) found that the ash content within the PCB increases with an increase in size class. When comparing the acid mediums under which the PCBs were leached, it was seen that; nitric acid conditions bring about more dissolution of the target metals. Under nitric acid conditions, copper, iron, and nickel fractions dissolved were 0.2391, 0.0047, and 0.0006 respectively. Under sulphuric acid and hydrogen peroxide, copper, iron and nickel metal fractions dissolved were 0.17568, 0.00364, and 0.00046 respectively. However, nitric acid was not explored beyond preliminary runs because of its hazardous nature (it was used to investigate more parameters that are paramount to e-waste processing); it is more toxic than sulphuric acid with hydrogen peroxide. Aqua regia is a highly corrosive combination of nitric acid and hydrochloric acid and has been used to fully dissolve metals within PCBs. This allowed for the recovery of copper from the leaching processes to be determined, the maximum recovery of copper was found under using the central composite design with conditions: hydrogen peroxide at 18 volume%, the temperature at 30⁰C, time at 120 minutes, and the particle size of 0.75mm. Amongst the parameters, hydrogen peroxide volume percentage was found to be the most significant parameter. The recovery of copper was found to be 36.1%.

Contents

PREFACE.....	ii
DECLARATION 1 - PLAGIARISM	iii
ACKNOWLEDGEMENTS.....	iv
ABSTRACT.....	v
CHAPTER 1	- 1 -
1.1 INTRODUCTION	- 1 -
1.2 PROBLEM STATEMENT	- 7 -
1.3 RESEARCH MOTIVATION	- 7 -
1.4 AIM.....	- 9 -
1.4.1 Objectives	- 9 -
1.5 HYPOTHESIS	- 9 -
1.6 THESIS OUTLINE.....	- 10 -
CHAPTER 2: LITERATURE REVIEW	- 11 -
2.1 LITERATURE REVIEW	- 11 -
2.1.1 Dismantling.....	- 13 -
2.1.2 Size reduction.....	- 14 -
2.1.3 Physical separation.....	- 17 -
2.1.4 Complete dissolution of metals.....	- 19 -
2.1.5 Hydrometallurgical processes	- 19 -
2.1.6 Kinetics	- 21 -
2.1.7 Bio-hydrometallurgical processes.....	- 24 -
2.1.8 Pyrometallurgical processes.....	- 25 -
2.1.9 Novel technologies.....	- 26 -
2.1.10 E-waste in developing countries	- 29 -
2.1.11 Metal recovery strategies	- 30 -
2.1.12 Experimental Designs for Optimization.....	- 32 -
CHAPTER 3: MATERIALS AND METHODS	- 34 -
3.1 EXPERIMENTAL METHOD.....	- 34 -
3.1.2 Liberation of e-waste material	- 34 -
3.1.3 Characterization of e-waste.....	- 35 -
3.1.4 Hydrometallurgical processing	- 36 -
CHAPTER 4: RESULTS AND ANALYSIS.....	- 42 -

4.1 LIBERATION OF MATERIALS.....	- 42 -
4.2 CHARACTERIZATION OF E-WASTE.....	- 44 -
4.3 HYDROMETALLURGICAL PROCESSING	- 47 -
4.3.1 Nitric acid media.....	- 50 -
4.3.2 Sulphuric acid media.....	- 54 -
CHAPTER 5	- 72 -
5.1 CONCLUSIONS.....	- 72 -
5.2 RECOMMENDATIONS	- 73 -
REFERENCES	- 74 -
APPENDICES	- 78 -
A.....	- 78 -
B.....	- 81 -
B.1 HYDROMETETALLURGICAL PROCESSING: Iron (Nitric Acid conditions).....	- 82 -
B.2 HYDROMETALLURGICAL PROCESSING: Nickel (Nitric acid conditions).....	- 83 -
B.3 ANALYSIS IN MINITAB (Nitric acid leaching conditions)	- 84 -
B.3.1 Iron Yield	- 85 -
B.3.2 Nickle Yield	- 88 -
B.4 HYDROMETALLURGICAL PROCESSING: Iron (H ₂ SO ₄ and H ₂ O ₂ conditions).....	- 90 -
B.5 HYDROMETALLURGICAL PROCESSING: Nickel (H ₂ SO ₄ and H ₂ O ₂ conditions).....	- 92 -
B.6 ANALYSIS IN MINITAB (Nickel (H ₂ SO ₄ and H ₂ O ₂ conditions)	- 94 -
B.6.1 Iron Yield	- 94 -
B.6.2 Nickle Yield	- 98 -
B.7 SURFACE PLOTS.....	- 100 -
B.7.1 Interaction Plots.....	- 108 -

List of Tables

<i>Table 1.1: Main components of a typical WEEE.....</i>	<i>- 1 -</i>
<i>Table 1.2: E-waste sources and their health effects</i>	<i>- 2 -</i>
<i>Table 1.3: WEEE production from each continent.....</i>	<i>- 4 -</i>
<i>Table 1.4: Weight composition and value distribution of metals (in brackets) from different WEEE.....</i>	<i>- 5 -</i>
<i>Table 1.5: Comparison of Metal content between Ores and PCBs</i>	<i>- 8 -</i>
<i>Table 1.6: Toxic elements present in an average computer</i>	<i>- 9 -</i>
<i>Table 3.1: Method used in this thermogravimetric analysis.....</i>	<i>- 35 -</i>
<i>Table 3.2: Lab acids used for leaching.....</i>	<i>- 38 -</i>
<i>Table 3.3: Full factorial design of experiment</i>	<i>- 39 -</i>
<i>Table 3.4: Parameters and their levels.....</i>	<i>- 40 -</i>
<i>Table 3.5: Full factorial design of experiment</i>	<i>- 40 -</i>
<i>Table 4.1: Particle size distribution of the waste PCBs after crushing.....</i>	<i>- 42 -</i>
<i>Table 4.2: Results of leached copper in nitric acid</i>	<i>- 48 -</i>
<i>Table 4.3: Results of leached copper in sulphuric acid and hydrogen peroxide.....</i>	<i>- 49 -</i>
<i>Table 4.4: Coded Coefficients.....</i>	<i>- 51 -</i>
<i>Table 4.5: Regression Equation in Uncoded Units</i>	<i>- 51 -</i>
<i>Table 4.6: Coded Coefficients.....</i>	<i>- 55 -</i>
<i>Table 4.7: Regression Equation in Uncoded Units</i>	<i>- 56 -</i>
<i>Table 4.8: Parameters and their levels.....</i>	<i>- 58 -</i>
<i>Table 4.9: Central composite Design</i>	<i>- 58 -</i>
<i>Table 4.10: Results of leached copper in sulphuric acid and hydrogen peroxide.....</i>	<i>- 60 -</i>
<i>Table 4.11: Analysis of Variance.....</i>	<i>- 62 -</i>

<i>Table 4.12: Model Summary</i>	- 62 -
<i>Table 4.13: Regression Equation in Uncoded Units</i>	- 63 -
<i>Table B.1: Leached Iron for different runs under nitric acid condition</i>	-80-
<i>Table B.2: Leached Nickel for different runs under nitric acid conditions</i>	-82-
<i>Table B.3: Coded coefficients (Fe)</i>	-84-
<i>Table B.4: Regression equation in uncoded units (Fe)</i>	-85-
<i>Table B.5: Coded coefficients (Ni)</i>	-88-
<i>Table B.6: Regression equation in uncoded units (Ni)</i>	-89-
<i>Table B.7: Leached Iron for different runs under sulphuric acid and hydrogen peroxide</i>	-90-
<i>Table B.8: Leached Nickel for different runs under sulphuric acid and hydrogen peroxide</i> ...	-92-
<i>Table B.9: Coded coefficients (Fe)</i>	-94-
<i>Table B.10: Regression equation in uncoded units (Fe)</i>	-95-
<i>Table B.11: Coded coefficients (Ni)</i>	98-
<i>Table B.12: Regression equation in uncoded units (Ni)</i>	-99-

List of Figures

<i>Figure 1.1: Weight fraction of materials within e-waste.....</i>	<i>6</i>
<i>Figure 2.1: Unit operations in the treatment of WEEE.....</i>	<i>- 12 -2</i>
<i>Figure 2.2: Mechanical processes for the recycling of waste PCBs.....</i>	<i>- 13 -3</i>
<i>Figure 2.3: Image showing a populated and depopulated (from manual dismantling) PCBs....</i>	<i>14</i>
<i>Figure 2.4: A schematic of how a hammer crusher works.....</i>	<i>16</i>
<i>Figure 2.5: The extraction of Cu from TV boards in the presence and absence of hydrogen peroxide.....</i>	<i>- 20 -0</i>
<i>Figure 2.6: A schematic of a spherical particle.....</i>	<i>23</i>
<i>Figure 2.7: A schematic showing the unit operations in advanced pyrometallurgy.....</i>	<i>27</i>
<i>Figure 3.1: A schematic of the experimental set-up.....</i>	<i>37</i>
<i>Figure 3.2: A schematic of the experimental set-up for filtration.....</i>	<i>- 42 -1</i>
<i>Figure 4.1: Particle size distribution.....</i>	<i>- 44 -</i>
<i>Figure 4.2: TGA curve of unreacted PCBs of size class -125+180μm.....</i>	<i>- 78 -6</i>
<i>Figure 4.3: Mass loss for unreacted PCB size classes.....</i>	<i>49</i>
<i>Figure 4.4: Normal plot of the effects.....</i>	<i>56</i>
<i>Figure 4.5: Normal plot of the effects.....</i>	<i>60</i>
<i>Figure 4.6: Percentage copper recovered.....</i>	<i>67</i>
<i>Figure 4.7: Percentage copper recovered.....</i>	<i>68</i>
<i>Figure 4.8: Percentage copper recovered.....</i>	<i>69</i>
<i>Figure 4.9: Percentage copper recovered.....</i>	<i>70</i>
<i>Figure 4.10: Percentage copper recovered.....</i>	<i>71</i>
<i>Figure 4.11: Percentage copper recovered.....</i>	<i>72</i>
<i>Figure 4.12: Percentage copper recovered.....</i>	<i>73</i>

<i>Figure 4.13: Main effects plot for % Cu dissolved.....</i>	<i>74</i>
<i>Figure A.1: TGA curve of unreacted PCBs of size class -850+500μm.....</i>	<i>109</i>
<i>Figure A.2: TGA curve of unreacted PCBs of size class -1400+1000μm</i>	<i>110</i>
<i>Figure B.1: Iron fraction within PCB (3,125g).....</i>	<i>81</i>
<i>Figure B.2: Leached nickel for different runs under nitric acid conditions.....</i>	<i>83</i>
<i>Figure B.3: Normal Plot effects.....</i>	<i>86</i>
<i>Figure B.4: Pareto Chart of the effects</i>	<i>87</i>
<i>Figure B.5: Normal Plot of effects.....</i>	<i>- 89 -</i>
<i>Figure B.6: Pareto Chart of the effects</i>	<i>- 90 -</i>
<i>Figure B.7: Iron fraction within Pb(3,125g).....</i>	<i>- 91 -</i>
<i>Figure B.8: Nickel fraction within the PCB(3,125).....</i>	<i>93</i>
<i>Figure B.9: Normal Plot of the effects.....</i>	<i>96</i>
<i>Figure B.10: Pareto Chart of the effects Fe, alpha=0,05</i>	<i>97</i>
<i>Figure B.11: Normal Plot of the effects Ni, alpha=0,05</i>	<i>- 99 -</i>
<i>Figure B.12: Pareto Chart of the effects Ni, alpha=0.05.....</i>	<i>- 100 -</i>
<i>Figure B.13: Surface Plots of %Cu dissolved</i>	<i>- 101 -</i>
<i>Figure B.14: Surface Plot of %Cu dissolved Vs Temperature. Hydrogen peroxide vol%.....</i>	<i>- 102 -</i>
<i>Figure B.15: Surface of %Cu dissolved Vs Time. Hydrogen peroxide vol%</i>	<i>- 103 -</i>
<i>Figure B.16: Surface Plot of %Cu dissolved VS particle size. Hydrogen peroxide vol%.....</i>	<i>- 104 -</i>
<i>Figure B.17: Surface Plot of %Cu dissolved VS time. Temperature</i>	<i>- 105 -</i>
<i>Figure B.18: Surface Plot of %Cu dissolved vs Particle size. Temperature</i>	<i>- 106 -</i>
<i>Figure B.19: Surface Plot of %Cu vs Particle size. Time.....</i>	<i>- 107 -</i>
<i>Figure B.20: Interaction Plot for %Cu dissolved.....</i>	<i>- 108 -</i>

List of abbreviations

PCB: Plastic Circuit Board

E- Waste: Electronic Waste

TGA: Thermogravimetric Analysis

ICP-OES: Inductively Coupled Plasma Optimal Emission Spectrometry

WEEE: Waste Electric and Electronic Equipment

CRT: Cathode Ray Tube

PVC: Polyvinyl Chloride

DNA: Deoxyribonucleic Acid

EOL: End of Life

UN: United Nations

IT: Information Technology

PC: Personal Computer

LED: Light Emitting Diode

REE: Rare Earth Elements

MS: Magnetic Separation

EDS: Eddy Current Separation

ACS: Air Current Separation

CES: Corona Electrostatic Separation

AAS: Atomic Absorption Spectrometry

ICPMS: Inductively Coupled Plasma Mass Spectrometry

HHM: HNO + HF + Microwave Energy

SPF: Sodium Peroxide Fusion

RRE: Resource Recovery Efficiency

NMF: Non-Metallic Fraction

BFRs: Brominated Flame Retardants

NMP: Non-Metallic Powder

LCA: Life Cycle Assessment

GFRP: Glass Fiber Reinforced Plastic

CHAPTER 1

1.1 INTRODUCTION

Continuous technology advancements have accelerated the obsolescence of numerous electronic and electrical products, thus generating waste (Zhang, Schnoor and Zeng, 2012). Moreover, rapid technological innovations accelerate the frequent replacement of electronic products. The market is too big for technological products, hence the rate of disposal for current technologies is too high (Diaz *et al.*, 2016). Therefore, the rate of generation of electronic waste is significant and mainly due to the short period of ownership of these electronic products. The waste produced from the disposal of these electrical products poses a significant concern with respect to the environment, economy, and the human health. For example, groundwater contamination. What makes this waste more challenging is the different sources it comes from.

There are several sources of e-waste. E-waste can be obtained from the general public, the government, and the private (industrial) sectors. Important government sectors such as Defense and Healthcare are estimated to be responsible for generating large volumes of e-waste; explaining why the government sector is experiencing such rapid growth as a prominent source of e-waste (Ari, 2016). Another source of e-waste is imports, especially in developing countries as they act as dump sites for developed countries. Table 1.1 shows the main components of a typical Waste Electric and Electronic Equipment (WEEE) (L. Zhang & Xu, 2016). From table 1.1, PCBs are the main components in most WEEE.

Table 1.1: Main components of a typical Waste Electric and Electronic Equipment (Zhang & Xu, 2016)

TYPICAL WEEE	MAIN COMPONENTS
Refrigerator	Tubes, liners, condenser, wires, refrigerant
Air conditioner	Heat exchanger, motor, compressor, copper pipe, PCBs, Wires, refrigerant
Washer	Tub, drain hose, motor, wires, salt waste
Television	Deflection yoke, demagnetized coil, speaker, PCBs, wires, CRTs, LCD
Computer	Speaker, battery, storage medium, PCBs, wires, CRTs, LCD
Cell phones	Plastic enclosure, battery, storage medium, PCBs, wires, LCD
Printer/duplicator	Roller, toner, PCBs, wires, toner cartridge

PCBs are composed of three types of material, a non-conductive substrate, printed conducting tracks, and components mounted on the substrate (Bizzo, Figueiredo and De Andrade, 2014). Using conductive pathways etched from copper sheets laminated on a non-conductive substrate, PCBs are used to mechanically help and electronically link electronic components (Zeng *et al.*, 2012). They are employed in the manufacturing of business machines, computers, communication, and home equipment (Zeng *et al.*, 2012). Three primary material types can be recovered from PCBs, recyclable metals such as copper and aluminum, recyclable polymeric material, and ceramic material (Bizzo, Figueiredo and De Andrade, 2014). An electronic waste (e-waste) is defined as an unwanted electronic product that has been disposed of or which no longer meets the needs of the owner (Associates, 2006). E-waste releases toxic material into the environment (Associates, 2006). More than 1000 toxic substances associated with e-waste are known, barium, lead, cobalt and manganese; just to name a few (Abdelbasir *et al.*, 2018). These toxic materials affect both the ecosystem and humans. In addition, most of the e-waste ends up in landfills. Table 1.2 shows the source of these toxic materials and their effects, specifically on human beings (Ari, 2016). Due to the non-metallic fraction in the e-waste being non-biodegradable, it rapidly accumulates in landfills. Therefore, increasing the cost of waste disposal (Associates, 2006). E-waste recycling through use in manufacturing processes of electronic products significantly reduces the impacts of greenhouse gases emissions compared to using virgin resources to manufacture electronic products (Associates, 2006).

Table 1.2: Electronic waste sources and their health effects (Ari, 2016)

E-waste sources	Constituents	Health effects
Solder in PCBs, glass panels, and gaskets in computer monitors	Lead	Causes damage to the nervous system, circulatory system, and kidney. Also affects brain development in children.
Chip resistors and semiconductors	Cadmium	Causes neural damage.
Relays and switches, PCBs	Mercury	Cause chronic damage to the brain and respiratory and skin disorders.
Corrosion protection of untreated galvanized steel plates,	Hexavalent chromium	Causes bronchitis and DNA damage

decorator, or hardener for steel housing		
Cabling and computer housing	Plastics including Polyvinyl chloride (PVC)	Affects the reproductive system and immune system and leads to hormonal disorder.
The plastic housing of electronic equipment and circuit boards	Brominated flame retardants	Disrupts endocrine system functions.
The front panel of Cathode-ray Tubes (CRTs)	Barium, phosphor, and heavy metals	Causes muscle weakness and damage to the heart, liver, and spleen.
Motherboard	Beryllium	Carcinogenic in nature and causing skin diseases.

E-waste management is a significant concern, since safely and sustainable disposal of End of Life (EOL) e-waste is still a considerable challenge. Novel technologies are required to deal with safely and sustainable disposal of e-waste. E-waste is mainly categorized as hazardous waste, i.e, a heterogeneous mixture of materials and metals. Therefore, e-waste disposal requires specialized skills to minimize/eliminate negative impacts on the environment and humans (Ari, 2016).

Recovery and recycling of obsolete electronic materials are proving to be a rather lucrative business as metals such as gold, silver, palladium and other high-value metals make up some of the components of e-waste (Ari, 2016). According to the United Nations (UN), in 2012, about 50 million tons of e-waste were created worldwide; that's an average of 151 pounds per human (Ari, 2016) and the figure is growing by about 45 million tons/year (Zhang & Xu, 2016b). Of the 50 million tons, China contributed 11.1 million tons, America 10 million tons, and the United Kingdom 1.3 million tons. In the past decade, about 4000 tons/hour of e-waste were generated worldwide (Ari, 2016). In 2017, the global e-waste generation was estimated to be 65.4 million tons, an increase from 20 million in 2000 (Tatarants *et al.*, 2017). As already highlighted earlier, the drastic increase in the generation of WEEE is a result of entirely new electronic products with high popularity and also them being integrated into almost every sphere of human life (Tatarants *et al.*, 2017). According to the European Union (EU), it produced 8.3-9.1 million tons of e-waste by 2005 and is projected to increase to 12.3 million tons by (Sethurajan *et al.*, 2019). Table 1.3 shows the total WEEE that was produced by each continent in 2017 (Deveci and Yazici, 2018). These numbers prove why recovery and recycling of obsolete electronics are essential and why it is a global challenge.

Table 1.3: Waste Electric and Electronic Equipment production from each continent (Deveci and Yazici, 2018)

Continents	Amount (in million tonnes)	Amount (kg/inch.)
Africa	1.9	1.7
America	11.7	12.2
Asia	16	3.7
Europe	11.6	15.6
Australia	0.6	15.2

South Africa is running out of space for waste disposal due to rapid growth in solid waste and a shortage of suitable land to dispose of (Africa, 2018). Studies state that as little as 5.2 percent of households in 2015 recycled waste, despite the benefits and need for recycling (Africa, 2018). Looking at e-waste in South Africa (SA), the trace of e-waste proved to be challenging before there were government regulations on how to deal with e-waste. Most help came due to the implementation of SA's National Management Act 59 of 2008; it provides guidelines on how e-waste should be treated. In 2007, the total computer distribution was 29815 tons, while for phones was 1875 tons (A. Finlay, 2008). Information Technology (IT) products had a market value of R280 Billion. From the distributed IT, the resultant e-waste was 3061.6 kg (A. Finlay, 2008). Currently, each individual in SA generates about 6.2 kg/year of e-waste and the department of environmental affairs estimates the current total e-waste at about 360000 tons/year.

The SA e-waste recycling industry has not yet reached a point where most of the components are recovered for reuse, which is why current e-waste professionals are exporting fractions of personal computer (PC) boards to European and other global markets to be paid a full return on investment; SA is effectively exporting jobs (Media, 2018). To curb the export of e-waste, Ewasa has embarked on a programme. The programme is coupled to the outcomes of Operation Phakisa on the chemicals and waste economy of South Africa. It has partnered with local technology experts in various sectors to take locally available technology in SA and develop it into a world-class commercial solution for the beneficiation of metals from PC boards found in e-waste (Media, 2018).

The major component of the obsolete and discarded electronic scrap is the Printed Circuit Board (PCB). It is composed of non-metals (plastics, epoxy resins, glass) > 70%, copper at about 16%, iron (ferrite) at about 3%, Nickel at 2%, Silver at 0.05%, gold at 0.03%, palladium at 0.01% and other rare earth metals at <0.01%

(Ari, 2016). These materials and metals on the PCB are attached to the board by a solder containing lead and tin (Zeng *et al.*, 2012). It is difficult to provide a generalized material composition and for the entire waste stream, given the wide range of materials found in WEEE (Ari, 2016). Table 1.4 shows the weight composition and value distribution of metals from different WEEE (Zhang & Xu, 2016). Minerals that are present in trace amounts are expressed in ppm. Most research, however, looks at five content categories: ferrous metals, non-ferrous metals, glass, plastics, and others. Metal contents of PCBs are varied in different kinds of literature and this is because metals' content especially precious metal contents of PCBs are varied with age, origin, and manufacturer (Zhang *et al.*, 2012). The composition within PCBs is 30% metal, 30% plastic, and 30% ceramic material while (Kumar *et al.*, 2014) has it at 40% organic, 30% metal, and 30% ceramics (Pietrelli *et al.*, 2018). The main components of many electronic systems are PCBs, which contribute about 30 percent of the total electronic scrap produced (Abdelbasir *et al.*, 2018). Metals account for 60% within the WEEE, 15.21% is for plastics and CRTs, and Light Emitting Diode (LED) screens making up 11.87% (Zhang & Xu, 2016). Figure 1.1 shows the material's fraction in e-waste, and as can be seen, it is consistent with what other researchers found (Ari, 2016).

Table 1.4: Weight composition and value distribution of metals (in brackets) from different Waste Electric and Electronic Equipment (Zhang & Xu, 2016)

Electronic waste	Content and value distribution for different WEEE (%) (in brackets)							
	Weight (%)				Weight (ppm)			
	Fe	Cu	Al	Pb	Ni	Ag	Au	Pd
TV board scrap	28 (4)	10 (39)	10 (13)	1 (2)	0.3 (5)	280 (6)	20 (25)	10 (6)
PC board scrap	7 (0)	20 (10)	5 (1)	1.5 (0)	1 (1)	1000 (64)	250 (5)	110 (15)
Mobile phone scrap	5 (0)	13 (8)	1 (0)	0.3 (0)	0.1 (0)	1380 (5)	350 (67)	210 (19)
DVD player scrap	62 (17)	5 (35)	2 (4)	0.3 (1)	0.05 (1)	115 (4)	15 (33)	4 (4)
PC main board scrap	4.5 (0)	14.3 (6)	2.8 (0)	2.2 (0)	1.1 (2)	639 (2)	566 (81)	124 (8)

PCBs scrap	12 (1)	10(19)	7 (4)	12 (1)	0.85 (6)	280 (3)	110 (66)	-
TV scrap (CRTs removed)	-	3.4 (82)	1.2 (9)	0.2 (2)	0.038 (4)	20 (3)	<10 ((-)	<10 (-)
Calculator scrap	4 (1)	3 (12)	5 (6)	0.1 (0)	0.5 (8)	260 (6)	50 (64)	5 (3)
Portable audio scrap	23 (3)	21 (78)	1 (1)	0.14 (0)	0.03 (0)	150 (3)	10 (12)	4 (2)
Typical electronic device scrap	8 (0)	20 (5)	2 (0)	2 (0)	2 (2)	2000 (3)	1000 (87)	50 (2)
E-scrap sample	27.3 (1)	16.4 (22)	11 (5)	1.4 (1)	-	210 (2)	150 (65)	20 (4)

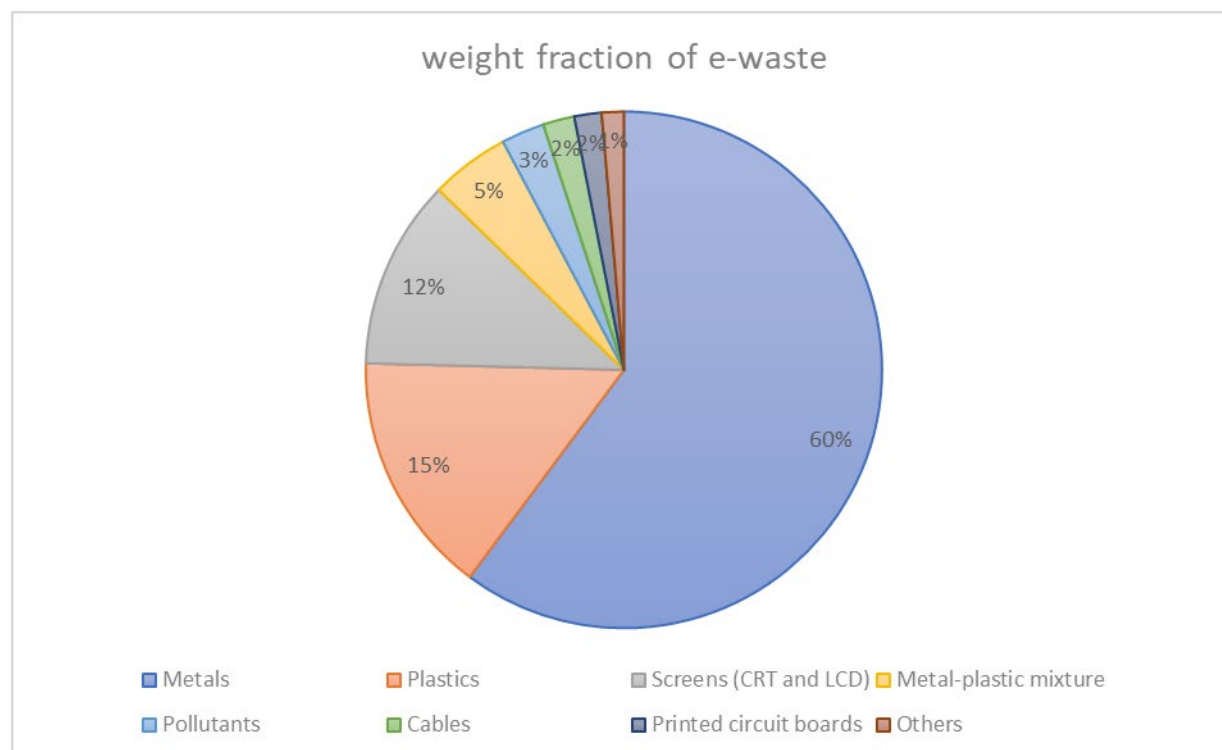


Figure 1.1: Weight fraction of materials within electronic waste (Ari, 2016)

A previous study found that e-waste contains rarer and nobler metals than traditional mines which partially satisfy the global metal demand, especially in regions where resource shortages persist (Zhang et al., 2012).

The demand for raw materials in the developing world has created a problem. However, it has encouraged the recovery of useful materials from e-waste by small operators without adequate pollution control equipment and technology; thus stimulating the transboundary flow of e-waste (Zhang et al., 2012). This kind of metal recovery from informal industries is referred to as artisanal recycling. Example of such processes includes open burning of manually separated PCBs followed by leaching of metals using acid baths (Ilankoon *et al.*, 2018).

1.2 PROBLEM STATEMENT

E-waste management is a global challenge and more so to economically emerging or developing countries. When the e-waste material is disposed of in landfills, the risk of exposing the soil to toxic chemicals such as lead and mercury which contaminate the soil; increases. E-waste contains non-metallic fractions that are non-biodegradable, therefore impact the environment negatively. In addition, e-waste recycling saves landfill space and creates jobs. Recycling WEEE also means less secondary waste and the recycling process consumes less energy than mining for metals from natural resources (Zhang & Xu, 2016).

1.3 RESEARCH MOTIVATION

The present work will be valuable to society as e-waste recovery conserves natural resources. Natural resources are finite and with e-waste recycling, less dependence on natural resources will be exploited since valuable metals can be obtained from discarded electronics. Recycling e-waste protects the surroundings and promotes proper management of toxic chemicals and helps reduce e-waste from landfills. E-waste recycling is an emerging and rapidly growing industry, and the present study aims to contribute to resolving e-waste challenges for the benefit of society. The metal of interest from e-waste in this study is copper. One of the world's most used metals is copper. This is because of its corrosion-resistant nature, ability to conduct electricity, machinability, and that it's malleable. In this study, parameters that affect the rate and extent of copper recoveries such as time, temperature, agitation speed, and leachate concentration will be studied to optimize the copper leaching process (Lee *et al.*, 2018).

The mining industry faces a plethora of challenges, one of them being that most of the rare earth metals that are being mined are finite resources. E-waste recycling offers a comprehensive solution to that problem (urban mining). Table 1.5 shows the metal content in PCBs compared to ores (Bizzo, Figueiredo and De Andrade, 2014). Spent PCBs contain a significant concentration of different critical, base, and precious metals, allowing them to be used as sources for such metals (Sethurajan *et al.*, 2019). A PCB on a personal computer can contain up to 20% copper and 250ppm gold which are 25-250 for gold and 20-40-fold for copper when compared with natural ores (Tuncuk *et al.*, 2012). Furthermore, it tackles the ever-increasing problem of world pollution. According to Wirefly.org, the average cellphone user gets a new one every 18 months, and a 100 million cellphones are tossed in the trash every year (U.S) (Crashers, 2011). It is further

reported that 112 000 computers and laptops are discarded every day; that is 41.1 million in a year (Crashers, 2011).

Table 1.5: Comparison of Metal content between Ores and Printed Circuit Boards (Bizzo, Figueiredo and De Andrade, 2014)

Metal	Ore %	PCBs %
Copper	0.5-3.0	12.0-29.0
Zinc	1.7-6.4	0.1-2.7
Tin	0.2-0.85	1.1-4.8
Lead	0.3-7.5	1.3-3.9
Iron	30-60	0.1-11.4
Nickel	0.7-2.0	0.3-1.6
Gold	0.0005	0.0029-0.112
Silver	0.0005	0.01-0.52

The reason why this research focuses on computer PCBs as the source of e-waste is that about 28-30% of the PCB content is metal, with 10-20% copper and precious metals accounting for 0.3-0.4% (Abdelbasir *et al.*, 2018). Also, due to the rate at which computers are being discarded. According to statistics, in the United States of America (USA) 500 million tons of computers were discarded between 1997 and 2007 and in Japan, 610 million tons of computers became obsolete by the end of 2010 (Zhang & Xu, 2016). In terms of products, the electronic and electrical industry is one of the most innovative; this is reflected by the rate at which electronic devices become obsolete (Bizzo, Figueiredo and De Andrade, 2014).

Table 1.6 shows the toxic elements present in an average computer (Ari, 2016). It supports the claim that the recycling of WEEE minimizes the volume of landfills and prevents pollution of the soil (Tuncuk *et al.*, 2012). PCBs account for about 3% of nearly 50 million tons per year global WEEE (Sethurajan *et al.*, 2019). In addition, they have been identified as posing a global environmental challenge and contributing to the depletion of precious and base metals (Kumar *et al.*, 2014). The treatment of WEEE for metal recovery is critical for reducing the footprint of carbon and materials, copper from conventional mining has a high carbon footprint; nearly 4 kg of CO₂ is produced for 1 kg of copper (Tuncuk *et al.*, 2012). The United Nations reported that precious metals deposits in the e-waste are 40-50 times richer than that found in ore mined from the natural resources. This proves that e-waste recycling is more efficient than mining.

Table 1.6: Toxic elements present in an average computer (Ari, 2016)

Element	Quantity (g)
Plastics	7240
Lead	1980
Mercury	0.693
Arsenic	0.410
Cadmium	2.961
Chromium	1.980
Barium	9.920
Beryllium	4.940

1.4 AIM

The research project aims to optimize the recovery process of copper from e-waste (computer PCBs) at low temperatures using hydrometallurgical processes (chemical). Also, to investigate the effectiveness played by the leaching reagent in the leaching process.

1.4.1 Objectives

- Investigate the type of material being studied by performing a sieve analysis. This will involve the PCBs being depopulated and being crushed by a Zerma crusher.
- Investigate the effects of different leaching agents (nitric acid and sulphuric acid with hydrogen peroxide)
- Investigate the effect of other leaching process conditions such as leaching time, particle size, hydrogen peroxide volume percent, and temperature.
- TGA will also be used to characterize the E-waste. TGA analysis will be done on e-waste prior to leaching.

1.5 HYPOTHESIS

The use of highly concentrated acids, for longer leaching times, small size classes, and at increased temperatures are anticipated to yield higher metal recoveries (copper). Also, using low concentrated acids, for shorter leaching times, with bigger size classes, and at low temperatures is anticipated to yield low metal recoveries.

1.6 THESIS OUTLINE

Chapter 1: Introduction, this chapter identifies problems associated with electronic waste that require urgent resolve.

Chapter 2: Literature review, this chapter offers an analysis of the available published works in electronic waste processing. A general overview of e-waste problems and the different methods used to deal with them.

Chapter 3: Materials and methods, this chapter will provide the procedure for physical separation, e-waste characterisation procedure, and hydrometallurgical processing procedure for e-waste.

Chapter 4: Results and discussion, this section elaborates on the results that are were found in the physical separation, characterisation, and hydrometallurgical processing of e-waste.

Chapter 5: Conclusion, conclusive remarks are provided and highlighting significant observations from the experiments conducted. Also, recommendations for further research work are given.

CHAPTER 2: LITERATURE REVIEW

2.1 LITERATURE REVIEW

In Taiwan, it is reported that an e-waste recycling plant can recover useful material from the main machines and monitors of scrap computers to the extent of 94.75wt% and 45.99wt% respectively (Ari, 2016). For these levels of material extraction to be maintained, the electronic scrap industry needs a steady supply of scrap, a cost-effective technology for material recovery facility, and stable demand for recycled material. In an attempt to achieve a cost-effective technology and simplicity, steps on how to recover metals from e-waste have been studied. Figure 2.1 shows the major steps that are involved in WEEE recycling (Sethurajan *et al.*, 2019).

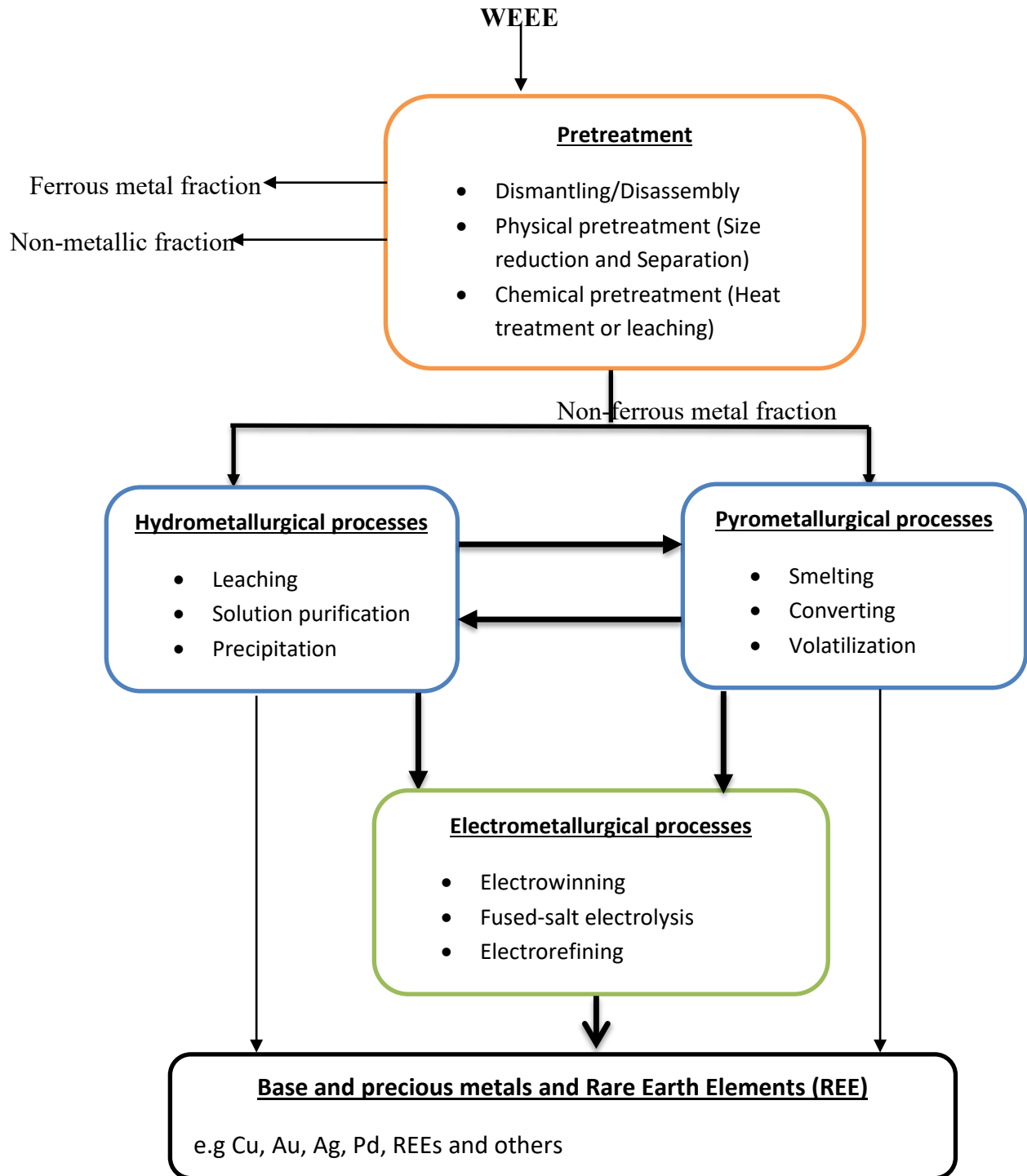


Figure 1.1: Flow diagram for processing of Waste Electric and Electronic Equipment (Sethurajan *et al.*, 2019)

2.1.1 Dismantling

The major steps in e-waste recovery are the liberation of materials of e-waste together with physical separation techniques, e-waste classification, and further processing of recovered metals. In the liberation of metals from WEEE, manual dismantling is preferred if there is no litter emission of pollutants (Ruan and Xu, 2016). Figure 2.2 shows the two major steps in PCB mechanical recycling and was taken from (Zeng *et al.*, 2012). The most enticing dismantling method research is the use of robots, but sadly, the complete implementation of automation of dismantling for PCB recycling is full of frustrations (Zeng *et al.*, 2012). Selective dismantling is a necessary method since it is possible to reuse components and dismantle dangerous components (Zeng *et al.*, 2012).

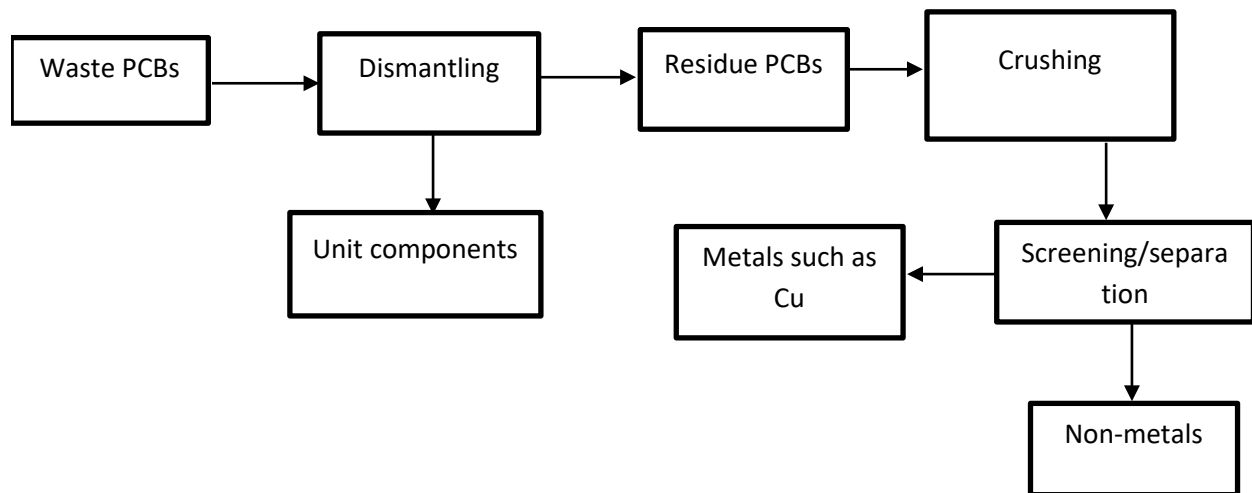


Figure 2.2: Mechanical processes for the recycling of Waste Printed Circuit Boards (Zeng *et al.*, 2012)

As it has already been echoed, e-waste is a heterogeneous material, owing to its complexity; metal liberation from e-waste is a difficult process (Jha *et al.*, 2010). Since metallic elements are often covered on PCBs with different plastic or ceramic materials, a mechanical pretreatment process is first needed to expose metals of interest to the leaching reagent's action and thus facilitate their efficient extraction (Tuncuk *et al.*, 2012). The most common point of these disassembly technologies is that the solder left on the board is retrieved by subjecting it to a temperature much higher than the molten point of the solder. Manual dismantling includes manual handling, manual crushing, and manual disassembly by a screwdriver. In developing countries, manual dismantling is preferred due to labor costs; even though manual dismantling emits hazardous material which brings health risks to humans and the environment.

The risks include exposure to noise, heavy metals, and chemical contaminants. Dismantling aims to selectively separate valuable parts for recycling while getting rid of deleterious components (Deveci and Yazici, 2018). The biggest waste dismantling Centre is in China, treating about 2 million tons of waste, valuable metallic materials are directly recycled during the manual dismantling process, while hazardous materials are collected for safe disposal (Deveci and Yazici, 2018). The e-waste is manually handled and crushed and can further be dismantled using screwdrivers. The adverse effect of this process is exposure to hazardous material which can be bad for one's health (Ruan and Xu, 2016). Figure 2.3 shows populated and depopulated computer PCBs that were manually dismantled in the lab. From figure e below, it is seen that depopulated PCBs already aluminium metals that are seen on the populated PCB.



Figure 2.3: Image showing a populated and depopulated (from manual dismantling) Printed Circuit Boards

2.1.2 Size reduction

Upon manual dismantling, the e-waste is subjected to a crushing unit (Ruan and Xu, 2016). The purpose of crushing e-waste is to liberate its material. The choice of a crusher for liberating materials of e-waste is determined primarily by the characteristics of the material (Deveci and Yazici, 2018). These characteristics include hardness, strength, and particle size. In general, e-waste contains broad two-dimensional sizes of metal and plastic, and shearing, grinding, and impact forces are suitable for liberating materials of e-waste (Ruan and Xu, 2016). Therefore, a hammer crusher is often used. A hammer crusher works in a way that materials fed to the cavity of the crusher are subjected to a shearing force from the hammer and then rapidly thrown to the impact plate for breaking down (Ruan and Xu, 2016). The large size materials are acted on

by the grinding force from the hammer and impact plate (Ruan and Xu, 2016). Figure 2.4 shows a schematic of how a hammer crusher works (Ruan and Xu, 2016). The Energy consumption of a hammer crusher is represented by the equation 2.1 (Ruan and Xu, 2016).

$$E = 2340m \left(\frac{1}{D_2} - \frac{1}{D_1} \right) \quad (\text{Ruan and Xu, 2016}) \quad (2.1)$$

Where;

- m is the mass of a single feeding material
- D_1 is the size (m) of a single feeding material before crushing
- D_2 is the average size (m) of the crushed material
- 2340 is the equation constant

This means that the consumption of energy is determined by the scale of the crushed materials. The crushing process is energy-intensive and thus increases the temperature in the crusher cavity, the high temperature not only speeds up the hammer and impacts plate abrasion, but also the risk of plastic pyrolysis (Ruan & Xu, 2016). Thus, a condensing system; usually of circulating water is employed in the crusher.

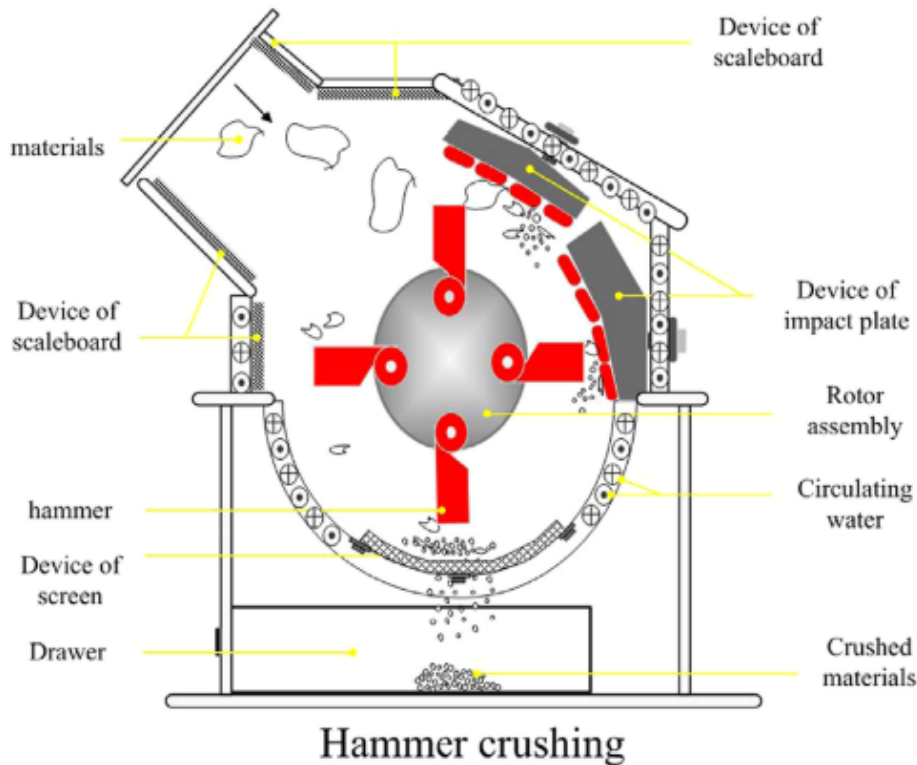


Figure 2.4: A schematic of how a hammer crusher works (Ruan & Xu, 2016)

While crushing, excessive crushing will cost more energy and pulverize the metals smaller; this makes separation hard (Ruan & Xu, 2016). Also, inadequate crushing will deteriorate the liberation minerals within the e-waste and as such decrease the recovery of metals. The degree of size reduction depends on the recovery process chosen in that relatively coarse material can easily be smelted, whereas fine size reduction is inherently needed by physical separation and hydrometallurgical processes for successful metal recovery (Tuncuk et al., 2012). Although processing large waste PCBs would eliminate dust generation and thus providing a more environmentally friendly approach, reducing the size of waste PCBs is beneficial to recycling costs (Kumar et al., 2014). It should also be noted that size reduction reduces the purity of recovered metals, purity levels of less than 98% copper for PCBs that were reduced in size were recorded and, above 99% purity for PCBs that were not treated to size reduction (Pietrelli et al., 2018). It is documented that it was possible to achieve almost complete copper release from computer PCBs at a particle size less than 2mm and poor release at coarser fractions was due to the association of copper pins with plastics and the encapsulation of copper wire segments with plastics (Tuncuk et al., 2012). Another challenge for size reduction and physical separation is the low recovery of base and precious metals which report to the $-75\mu\text{m}$ fraction generated during comminution (Ogunniyi et al., 2009). Depending on the particle size of material from the crusher, an appropriate physical separation technology will be employed

for different size classes. Only after physical separation and characterization can further processing techniques are performed.

2.1.3 Physical separation

Having researched and patented a dry separation method for recovering precious metals from PCBs, their method is based on a two-step grinding of boards; followed by air current centrifugal classification for gravity separation and electrostatic separation (Ari, 2016). Physical separation processes in the recycling of E-waste benefit from low capital and operating costs. E-waste is a heterogeneous mixture, with materials having different physical properties; it is these properties that are exploited to separate metals from a non-metallic fraction (Deveci & Yazici, 2018). Of other separation techniques, electrodynamic separation was studied. This is a process by which electric field forces separate two or more solid phases of different physical properties by electric field forces. It is stated that this technique can achieve copper products with grades ranging from 93% to 99% and recovery from 95% to 99% (Ari, 2016). It was further proposed that an eddy-current method for recovering aluminum metals from PCBs and personal computer scrap (Ari, 2016). The eddy-current method worked in such a way that materials on the high-force eddy-current separator, an aluminum concentrate out of personal computer scrap can be obtained with a purity of 85% while maintaining a recovery of more than 90% (Ari, 2016). Another important physical separation technique is gravity separation. Gravity separation exploits the differences in specific gravity of materials; the use of heavy liquids allows liberated metals to separate from plastics (Deveci & Yazici, 2018). Table 2.1 gives a summary of the physical separation techniques that are mostly used in industry (Zhang & Xu, 2016). Separation techniques are highly dependent on the size of the materials being separated. Table 2.2 shows which separation technique is most effective for different size fractions (Sethurajan et al., 2019).

Table 2.1: Summary of physical separation techniques (Zhang & Xu, 2016)

Physical separation method	Character of separation	Main advantages and disadvantages
Magnetic separation (MS)	Separation of ferrous metals	MS was most suitable separating steel or iron but not suitable of non-ferrous metals
Eddy current separation (EDS)	Separation of ferrous and non-ferrous metals	EDS was encouraged to recover non-ferrous metallic particles and

			hard to separate ferrous metals /other metals
Air current separation (ACS)	Separation of light particles from heavy particles		Wind velocity, particle size, particle density, etc. were the critical influences for ACS
Corona electrostatic separation (CES)	Separate metallic particles (size from 0.2mm to 1mm) from non-metallic particles		The movement trajectory and collection position of metallic particles in CES were hard to predict and compute

Table 2.2: Physical separation methods and their dependence on particle size (Sethurajan et al., 2019)

Method	Exploited property	Particle size (mm)
MS	Magnetic susceptibility	<5
Electrostatic separation	Electrical conductivity	0.1-5
ECS	Electrical conductivity/specific gravity	>5
Gravity separation	Specific separation	0.05-10
Flotation	Surface properties	0.075-1

It must be noted that no individual physical separation technology has proven to be sufficient for recovering total metals from e-waste (Ruan & Xu, 2016). Apart from the already discussed separation technologies, there is air current separation, froth flotation, vacuum metallurgy separation, and electrostatic separation. Although pre-treatment of e-waste is vital, part of critical and precious elements is lost during the pre-treatment processes; mainly as dust (Sethurajan et al., 2019). This is one of the most important detractions of physical separation processes as 10-35% of valuable metals are lost (Tuncuk et al., 2012). The key reasons for these losses are the inadequate release of metals due to the intimate association of valuable metals with plastics, the generation of fines ($-75 \mu\text{m}$) during size reduction, and the inefficiency of separation processes from the fine fractions (Tuncuk et al., 2012). Complete dissolution reactions are performed to determine the amount of each metal within the PCB. This is where the use of wet spectroscopy

methods such as Atomic absorption spectroscopy (AAS), inductively coupled plasma mass spectrometry (ICP-MS), and inductively coupled plasma optical emission spectrometry (ICP-OES) is required.

2.1.4 Complete dissolution of metals

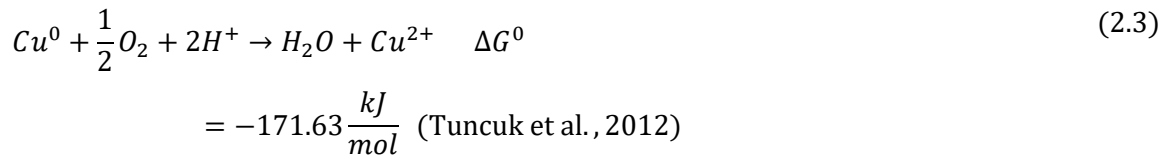
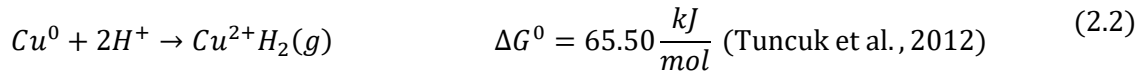
For complete dissolution of metals, the PCB is subjected to a very aggressive and corrosive media which can virtually dissolve most if not all metals' matrix contained within the PCB. Aggressive combinations such as aqua-regia are considered. $\text{HNO}_3 + \text{HF}$ + microwave energy (HHM) and sodium peroxide fusion (SPF) followed by HCl dissolution were studied alongside aqua-regia for their ability to dissolve metals (Ogunniyi et al., 2009). Of the three solutions, sodium peroxide fusion followed by HCl dissolution was found to be the most aggressive, dissolving all metals (Ogunniyi et al., 2009). However, it was not used because the resulting solution from complete dissolution using SPF could not be analyzed by ICP-MS/OES. Hot aqua-regia is preferred over HHM and SPF because it can give analysis liquor for all elements and the produce is less hazardous compared with using HHM (Ogunniyi et al., 2009). Aqua regia is used to obtain the largest volume of copper and gold from PCBs (Tuncuk et al., 2012).

2.1.5 Hydrometallurgical processes

Over the past two decades, extractive metallurgy processes (pyro-metallurgy, hydrometallurgy, electrometallurgy, and their combinations) have been used for processing and recovering precious and base metals from e-waste (Ghodrat et al., 2016). The key steps in hydrometallurgical processing consisted of a sequence of solid material acid leaching procedures. Hydrometallurgical processing in metal recovery is the dissolution of metals into solution using acids/bases/salts, purification of the leach solution to remove impurities by solvent extraction, adsorption, or ion exchange (Deveci & Yazici, 2018). In a solution that was then subjected to separation and purification processes such as impurity precipitation, solvent extraction, adsorption, and ion exchange to isolate and concentrate the metals of interest, selected elements were leached out (Ghodrat et al., 2016). Hydrometallurgical processes are used because they are relatively cheap (make use of low temperatures), more accurate and predictable, and much easier to control (Popescu et al., 2014). The reason why hydrometallurgical processes have high metal recoveries is due to their stability for small-scale applications (Tuncuk et al., 2012). Following the hydrometallurgy procedures, the solutions were treated to electrorefining processes and chemical reduction for the recovery of metals (Ghodrat et al., 2016).

In WEEE, metals are present as native and/or alloys; this is of practical importance for the selection and production of an effective leaching method (Tuncuk et al., 2012). A widely used method of recovering metals from e-waste is that makes use of an oxidative leaching process. Figure 2.5 illustrates the dissolution of metallic copper in the presence and absence of hydrogen peroxide as an oxidant in acidic sulfate media (Tuncuk et al., 2012). It is seen from figure 2.5 that a very limited copper extraction (about 2%) is achieved

in the absence of an oxidant. From equations (2.2) and (2.3), the extraction of copper in the absence of an oxidant is less likely to happen as it is less spontaneous.



Equation (2.3) is more spontaneous, hence why copper gets extracted more readily in the presence of an oxidant. The standard Gibbs free energy (ΔG^0) of equation (2.3) is negative and according to thermodynamics, chemical reactions are spontaneous when the ΔG^0 is negative.

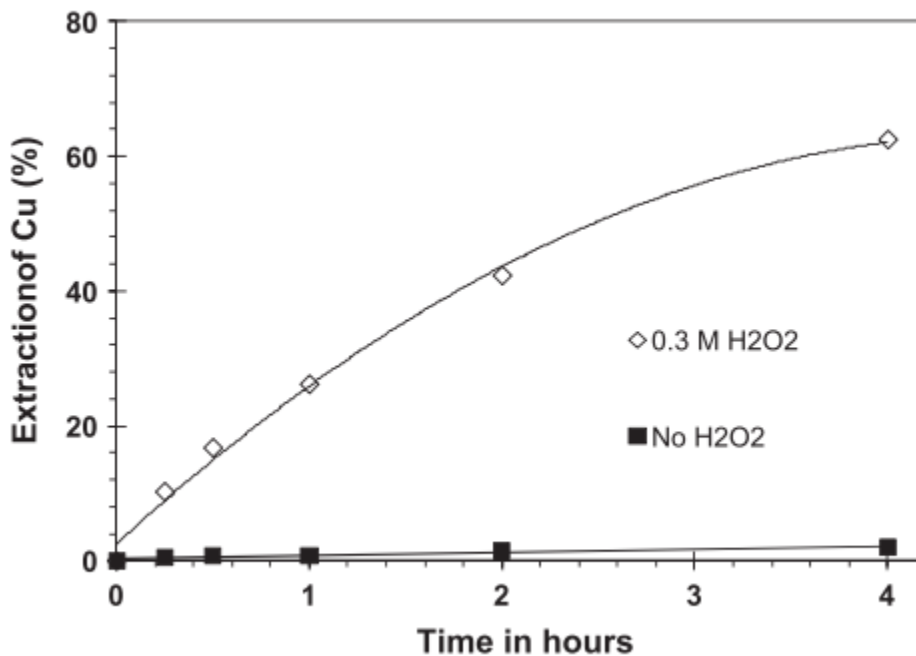


Figure 2.5: The extraction of copper from TV boards in the presence and absence of hydrogen peroxide (Tuncuk et al., 2012)

Hydrogen peroxide is a strong oxidant and the oxidation reaction is highly exothermic ($\Delta H^0 = -411.2$ kJ/mol) and control of temperature is needed (Tuncuk et al., 2012). Previous studies suggest that the concentration of hydrogen peroxide and temperature are the most influential factors affecting the extraction of metals from e-waste (Tuncuk et al., 2012).

However, the hydrometallurgical processes have certain limitations, amongst others; they could not handle a large throughput, they were slow and regarded as complicated, they required extensive mechanical pre-processing of the e-waste and they made use of toxic and corrosive chemicals in large quantities (Ghodrat et al., 2016). Also, hydrometallurgical processes generate sludge and cause heavy metal pollution (Sethurajan et al., 2019). However, Bio-hydrometallurgy on the other hand is still proving to be beneficial as the world's largest copper producer (Chile) uses bioleaching processes to extract the copper (Gentina & Acevedo, 2013).

2.1.6 Kinetics

Reaction kinetics deals with the rate at which a chemical reaction proceeds and thus can be used to model a chemical reaction. Basic methods use the Arrhenius expression and single reaction rate as a parameter (Popescu et al., 2014). However, with the determination of pre-exponential constants (K_0), activation energies, and reaction orders, punctual methods refer to multiple parameter identification for each reaction phase (Popescu et al., 2014). Such techniques, which consider a kinetic specific to homogeneity, are not specific to leaching reactions but are generally used when agreeing that the reactions take place on the leaching metal surface (Popescu et al., 2014).

In a leaching system, there are diffusion processes taking place. Diffusion happens across a gradient if a component is moving from the bulk to the surface; it means that its place of high concentration is the bulk. Diffusion always happens from a place of high concentration to that of low concentration. The rate of a chemical-diffusion reaction can be rate limited by the reaction happening on the surface of the unreacted solid core, the diffusion of the fluid through the reacted surface of the solid particle (ash), or the diffusion of fluid through the external film. A shrinking core model is assumed.

2.1.6.1 External film diffusion controlling

The driving force for the fluid species to be transported from the bulk to the solid core surface will be the concentration of the species in the bulk fluid less concentration of the species in the surface. The concentration of the species on the surface is zero because diffusion through the ash layer happens very rapidly. Thus, the driving force is essentially the concentration of the fluid in the bulk fluid.

Assuming concentration in the bulk fluid is constant, we can make a mole balance;

$$\frac{dN_A}{dt} = -K_b S_{ex} C_{Ab} \quad (\text{Popescu et al. , 2014}) \quad (2.4)$$

Where;

- K_b is the mass transport coefficient
- S_{ex} is the external surface area of the solid particle
- C_{Ab} is the concentration of species A in the bulk fluid
- N_A is the number of moles of species A

If;



And assuming equimolar consumption;

$$N_A = N_B \quad (2.6)$$

Therefore;

$$\frac{dN_B}{dt} = -K_b S_{ex} C_{Ab} \quad (2.7)$$

The equation above allows us to monitor the amount of solid that is being consumed with passing time.

$$N_B = \rho_B V \quad (2.8)$$

Where;

- V is the volume of the spherical particle B
- ρ_B is the density of solid B

$$\frac{d}{dt} \rho_B V = -K_b S_{ex} C_{Ab} \quad (2.9)$$

The volume of a spherical particle is;

$$V = \frac{4}{3} \pi r(t)^3 \quad (2.10)$$

The equation above is substituted into the mole balance to give;

$$\frac{4}{3}\pi 3r^2 \rho_B \frac{dr}{dt} = -K_b S_{ex} C_{Ab} \quad (2.11)$$

Equation (2.11) is simplified and integrated between the changing radii of the particle at any time (t) and radii of the spherical particle (R_0);

$$\frac{1}{3}[R^3 - R_0^3] = \frac{-K_b S_{ex} C_{Ab}}{4\pi \rho_B} \quad (2.12)$$

2.1.6.2 Chemical reaction controlling

In this case, the surface chemical reaction is much slower than reagent diffusion through the diffusion layer. As the presence of a product layer does not affect the progress of the reaction, the quantity of material reacting is proportional to the available surface of the unreacted core.

Assuming a spherical particle below;

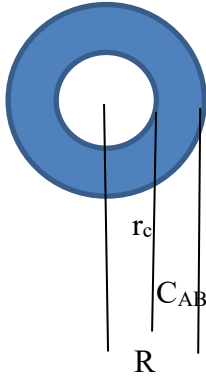


Figure 2.6: A schematic of a spherical particle

At steady state,

$$-\frac{1}{4\pi r_c^2} \frac{dN_B}{dt} = -\frac{b}{4\pi r_c^2} \frac{dN_A}{dt} = -bK_r C_{AB} \quad (2.13)$$

The first-order rate constant for the surface reaction is K_r . We can then write N_B in terms of the shrinking radius and integrate (Muzayanha et al., 2020).

$$-\rho_B \int_R^{r_c} dr_c = bk_r C_{AB} \int_0^t dt \quad (2.14)$$

$$t = \frac{\rho_B}{bk_r C_{AB}} (R - r_c) \quad (2.15)$$

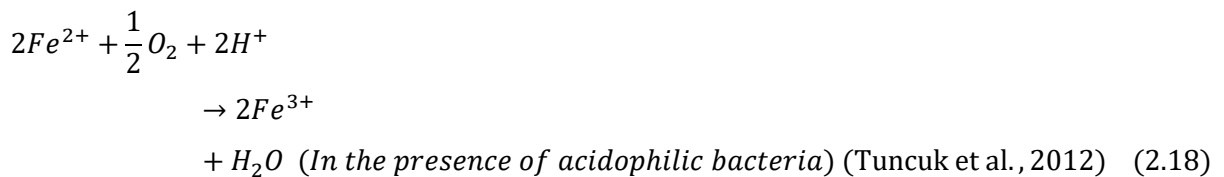
$$t_{comp} = \frac{\rho_B R}{bk_r C_{AB}} \quad (2.16)$$

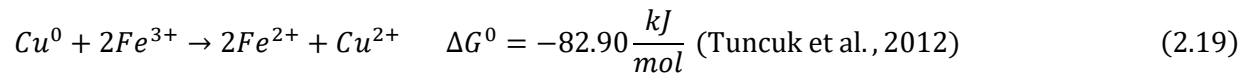
$$\frac{t}{t_{comp}} = 1 - \frac{r_c}{R} = 1 - (1 - X_B)^{1/3} \quad (2.17)$$

2.1.7 Bio-hydrometallurgical processes

In bioleaching, a living organism is involved in the process of metal extraction, and due to the cost-effectiveness of bioleaching; the process is mostly used in low-grade ores. In bioleaching, the most commonly used microbes are thiobacillus ferrooxidance and thiobacillus thiooxidance which are acidophilic bacteria. The influence of bacterial culture on copper leaching from PCBs is vital. It was found that higher recoveries of copper are obtained when thiobacillus ferrooxidance and thiobacillus thiooxidance are mixed together to make one bacterial culture instead of using just thiobacillus ferrooxidance (Sedlakova-kadukova, 2013). The bacteria are important because they can grow and utilize ferrous ion or elemental sulfur to produce ferric ions or sulfuric acid that are important as leaching agents for metal recovery (Sedlakova-kadukova, 2013). The bacteria act as a catalyst. Bioleaching can happen directly or indirectly and there is still much debate over which mechanism is more dominant during the leaching process. Bio-hydrometallurgy and pyro-metallurgy can work hand in hand to attain higher metal recoveries from e-waste recycling.

While bioleaching processes are especially suitable for the treatment of low-grade materials and small-scale applications, they suffer from long residence times for metal extraction, low pulp density, and metal toxicity (Tuncuk et al., 2012). To keep metals in solution, bioleaching processes require that the acidic environment be maintained at a pH lower than 2 (Tuncuk et al., 2012). As already echoed, bioleaching of metals from e-waste is done bioleaching of metals from e-waste is often carried out using iron-oxidizing strains of acidophilic bacteria (Tuncuk et al., 2012). The reactions proceed as follows;





From the bioleaching investigations of dust generated during size reduction of e-waste, it was found that metals including Al, Cu, Zn and Ni could readily be extracted (>90%) by using mesophilic bacteria (Tuncuk et al., 2012).

2.1.8 Pyrometallurgical processes

Though the industry is shifting towards hydrometallurgical processes for metal recovery in e-waste (mainly due to high-grade ores of copper now being limited and pyrometallurgical processes causing more pollution), pyro-metallurgical processes have always been used (as high-grade ores were abundant in the past); these processes involved the use of high temperatures to extract the metals from e-waste. Pyrometallurgy is a conventional WEEE-based technology for the recovery of ferrous and precious metals (Tuncuk et al., 2012). The typical process of pyro-metallurgy processes involved incineration, smelting in furnaces, sintering, melting, and reactions in a gaseous phase at high temperatures to recover the metals (Ghodrat et al., 2016).

E-waste is pumped into a high-temperature furnace during the smelting process and is integrated into a base metal production process (e.g. Cu) where the base metal serves as a carrier for the precious metals (Ghodrat et al., 2016). The impure base metal then undergoes electrorefining to obtain the base metal at high purities and to extract precious metals as part of the sludge by-product through various extraction processes. During the smelting process, elements that easily oxidize (iron, aluminum, and silicon) will form slag. In the process, the plastics and hydrocarbons in the PCBs are burnt and can also serve as a reductant and additional energy source from exothermic reactions (Ghodrat et al., 2016). The ability of pyrometallurgy processes to use the organic compounds as a supplement for coke as a fuel and reducing agent makes them potentially suitable for the treatment of WEEE (Tuncuk et al., 2012). If a robust pollution control system is installed to deal with harmful elements, the combustion of these plastics will become a viable source of energy recovery.

This then shows why pyro-metallurgy processes are used in industry, as they enrich the valuable metals carrier and use plastics as reductant and for their ability to act as additional sources of energy. However, pyrometallurgical processes are not without any negative impacts of their own. Pyrometallurgical processes are energy-intensive and thus require high capital costs, processes lose noble metals into the slag phase and they are also associated with releasing harmful gaseous effluents to the environment (Sethurajan et al., 2019). These effluents' treatment needs large investment in heavy equipment (Kumar et al., 2014). Halogenated flame retardants used in PCBs, leading to the formation of dioxins and furans, volatile metals,

and dust can present environmental problems and are therefore a requirement for off-gas treatment (Tuncuk et al., 2012).

2.1.9 Novel technologies

Conventional methods such as pyrometallurgy and strong acid leaching can have significant defects such as low recovery efficiency and cause harm to human health. Traditional hydrometallurgical processes, for example, produce huge amounts of wastewater and residues and if not handled properly, they can cause serious secondary pollution (Zhang & Xu, 2016). That is why over the past decade, hydrometallurgical technology has paid more attention to environment-friendly recycling metals (Zhang & Xu, 2016). The use of mild leaching agents (mild extraction) and modified technologies were studied. The advantages of these advanced technologies include them being more exact and having relatively low construction costs.

For the modified technology, pyrometallurgical processes were vastly improved in terms of recycling technology and the ability to treat its pollutants (Zhang & Xu, 2016). For this process, crushed e-waste is burnt in a high-temperature furnace, and metals are volatilized by a chemical reaction with impurities converted into slags (Zhang & Xu, 2016). Enriched metals are smelted in furnaces and coarse metal ingots can be obtained, Flash and bath smelting are the two basic and commonly used smelting methods (Zhang & Xu, 2016). Flash smelting utilizes oxygenated gas to facilitate autogenous conditions, while bath smelting relies on the roasting and smelting steps (Zhang & Xu, 2016). Advanced smelting equipment like the Mitsubishi continuous smelter is used. For the conversion in the copper convertors, matte is obtained from blowing air from the tuyeres; this step can oxidize the iron sulfide and convert sulfide to copper (Zhang & Xu, 2016). Refining units make up the last step, their purpose is to get high purity copper in the reverberatory or rotary furnaces. Figure 2.7 below is a schematic showing a summary of steps involved in the advanced pyrometallurgical processes (Zhang & Xu, 2016).

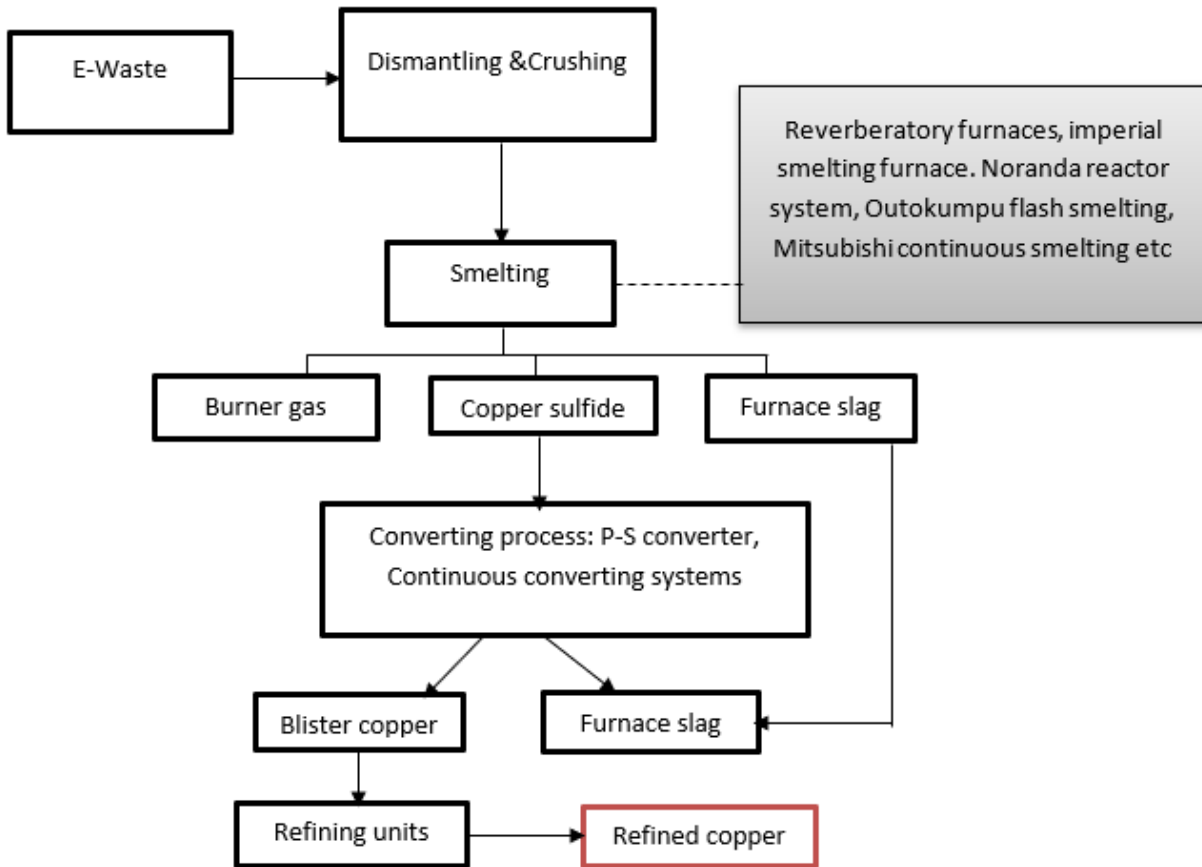
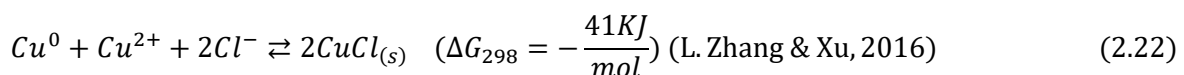
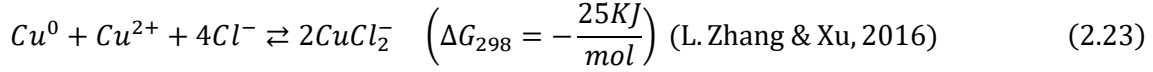


Figure 2.7: A schematic showing the unit operations in advanced pyrometallurgy (Zhang & Xu, 2016)

Mild extraction technology makes use of mild leaching agents for hydrometallurgy, they are more targeted towards metals recovery or pre-treatment, easier to control chemical reaction, and make relatively less pollution than pyrometallurgical processes (Zhang & Xu, 2016). Some of the processes can include leaching process of chlorinating, ammonia-ammonium for copper, and non-cyanide lixivants for leaching Au.

In the chlorinate leaching for copper a chloride medium (HCl-CuCl₂-NaCl) is used to extract copper, cupric ion (Cu²⁺) acting as an oxidant can form stabilization of cuprous (Cu⁺) when an appropriate ligand such as a chloride ion (Cl⁻) was added to sulfate solution (Zhang & Xu, 2016). The reactions proceed as follows:





To obtain maximum metal extraction (greater than 98%) for Cu, the initial concentration of Cu^{2+} should be increased to ≥ 79 mmol/l for a leaching period of more than 120 minutes (Zhang & Xu, 2016).

The ammonia-ammonium leaching for copper (Cu) method has superiority in terms of selectivity towards copper (Zhang & Xu, 2016). Ammonia-ammonium sulfate and chloride systems are used to extract copper from waste PCBs, and the leaching agents are salt solutions of ammonia-ammonium containing Cu(i) and Cu(ii) ammine complexes (Zhang & Xu, 2016). Leaching and purification are the two main steps. Cu is oxidized from Cu(ii) to form (Cu(i)-ammine complex ions during leaching of copper in waste PCBs, resulting from the reduced oxidation-reduction potential during leaching (Zhang & Xu, 2016). The leaching reaction proceeds as follows:

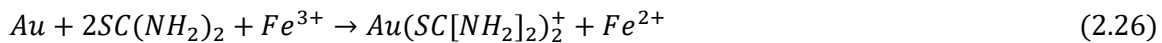


In the purification stage, an electro-winning technology had been proposed to recycle copper in the Cu(I)-ammine complex ($Cu(NH_3)_2^+$). The focus was placed on the leaching mechanism and behavior of copper by electro-winning. The results showed that 98% of copper could be leached under the following conditions: 2kmol/m³ NH_4Cl and 5kmol/m³ NH_3 solution, 0.1kmol/m³ $CuCl_2$ at 30°C (Zhang & Xu, 2016).

Non-cyanide systems aim for overcoming the disadvantages of cyanide leaching of precious metals, several non-cyanide lixivants have been proposed over the years; including thiosulfate and thiourea. As thiourea is used as a gold extraction agent for WEEE, due to its high leaching rate, eco-efficiency, and lower toxicity, it has shown considerable benefit (Zhang & Xu, 2016). The amount of gold leached is dependent on careful optimization and control of pH, thiourea concentration, redox potential, and leaching time (Zhang & Xu, 2016). The reaction proceeds as follows:



The combination of lixivants was also explored and realized that this results in a synergic effect (Zhang & Xu, 2016a). When using ferric sulfate as the oxidant for leaching gold, the effect was more apparent. Gold is leached in an acid thiourea-ferric sulfate solution and can be represented by the reaction below:



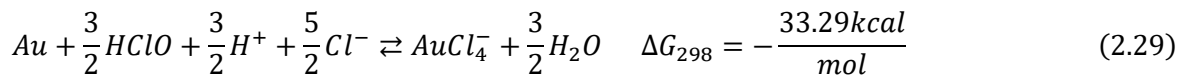
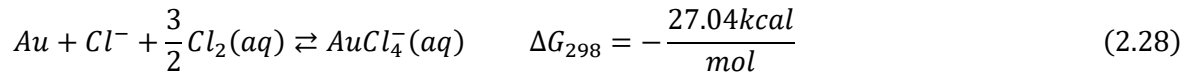
The ferric ion present in acidic thiourea solutions can have a major effect on the reaction kinetics of the gold cementation process. The results from this experiment showed that the leaching rate of gold depended

on the ferric concentration, ferric ion increased significantly the redox potential of the solutions; but the leaching rate kept constant with time when thiourea concentration was below 12g/l and ferric was above 0.1g/l (Zhang & Xu, 2016).

Other promising technologies include electrochemical technology to recover from WEEE base metals and precious metals. Electrochemical processes have high environmental compatibility, are high energy efficient, and make use of minimal chemicals (Zhang & Xu, 2016). A process that uses electro-generated chlorine was developed to carry out the leaching of metals from waste PCBs. Due to the acquisition of high oxidation potential, the process is beneficial for leaching precious metals (Zhang & Xu, 2016). Two cathodes and anodes were used, and hydrochloric acid was poured into the leaching reactor (Zhang & Xu, 2016). The anodic reaction is represented as follows:



And the dissolution of gold reaction as:



With increasing temperature and initial chlorine concentration, the content of leached gold increased and was positive even at low acid concentrations (Zhang & Xu, 2016). However, the leaching of copper was different; leaching increased with increasing concentration of acid and decreasing temperature (Zhang & Xu, 2016).

The advanced technologies are however not without their defects, some being that they particularly single, advanced pyrometallurgical technologies pollute the atmosphere with fine particles (PM_{2.5} and PM₁₀) and mild extraction technology can have low chemical stability (Zhang & Xu, 2016). Although some countries are paving the way in e-waste recovery by successfully implementing these recovery techniques, e-waste recovery is a challenge for developing countries and countries in transition.

2.1.10 E-waste in developing countries

It is known that e-waste has the potential to generate significant environmental and public impacts if disposed of inappropriately, and this is the case for most developing countries. The most contributing factor is the level of technology in such countries, the level of technology in each country determines how a country can deal with its e-waste. There are also instances where developing countries act as dump sites for developed countries. Developed countries have high standards of environmental protection hence the e-

waste not treated is transported to developing countries instead of being treated domestically (Ruan & Xu, 2016). More than 5 million tons were exported from the developed countries to countries in transition such as China and India (Ruan & Xu, 2016).

Due to the lack of technology, informal and semi-formal extraction of metals is prevalent in developing countries. Most developing countries process e-waste to produce a concentrate which is then sold to formal industries in developed countries (Ilankoon et al., 2018). For developing countries, the waste management strategy usually follows two principal routes; disposal directly into conventional landfills and indirectly as residues from efforts to recover or recycle valuables (Ilankoon et al., 2018). The problem with these practices is that they are likely to cause leaching of metal ions and necessitate extended and potentially unsafe storage of electronic waste respectively (Ilankoon et al., 2018). Amongst the efforts used by developing countries to recover valuables is incineration. China is responsible for the largest WEEE recycling via environmentally unfriendly and hazardous primitive methods like incineration (Zhang & Xu, 2016). Common problems associated with incineration are energy consumption and a considerable amount of loss of metals. Furthermore, PCB components include plastics and brominated flame retardants that during incineration emit toxic gases and carcinogenic compounds (Jha et al., 2011).

Botswana, just like many middle-income countries and developing countries has great problems associated with e-waste. Botswana's largest e-waste comes from information communication and technology equipment and with urbanization on the rise; the situation is only getting worse (Mmereki et al., 2015). As in many developing countries, there are no separate collection channels for e-waste and this makes it hard to determine the quantities and types of e-waste (Mmereki et al., 2015). Developed countries are very strict about e-waste policies (accountability), but this is not the case in developing countries which further contributes to problems of e-waste management in developing countries. This research focuses on hydrometallurgical processes being used to recover copper from e-waste even though there is yet to be an industrial scale of hydrometallurgical processing plants with regards to e-waste recovery.

2.1.11 Metal recovery strategies

The form and composition of e-waste are fundamentally complex and heterogeneous, with significant differences in metal and material content (Sethurajan et al., 2019). This makes it hard to develop and implement large-scale processing plants for selective recovery of desired metals. There is also a continual significant change in the composition of e-waste due to technological advancements over the years. To build a mobile and industrial-scale hydrometallurgy processing plant would then require knowledge and experience gained in a variety of chemical processing steps and economic and environmental evaluation of numerous parameters (Sethurajan et al., 2019). Current recycling technologies used by mobile recycling plants do not permit reach of an economic advantage for all valuable metals contained within the e-waste;

this is because recycling plants are mostly focused on a single stream (Sethurajan et al., 2019). The driving force for recycling may not be feasible due to economic reasons and technological limitations, hence the contribution score. Common practice, however, is to place more emphasis on recovering precious metals. Since precious metals make a major contribution to the value of e-waste, their extraction is of primary importance to the economy of a recycling activity (Tuncuk et al., 2012).

The contribution score determines the recyclability of a metal and is related to weight content, environmental hazards associated with the metal, energy consumption, and natural resources depletion (Sethurajan et al., 2019). Although the contribution score is important, the widely used assessment index is the Resource Recovery Efficiency (RRE) (Sethurajan et al., 2019).

$$RRE = \sum_i \left(\frac{E_i F_i}{P_i} \right) \left(\frac{C_i}{R_i} \right) \approx \sum_i (E_i F_i / R_i) \quad (\text{Sethurajan et al., 2019}) \quad (2.30)$$

Where;

- E is %recovery
- F is amount of resource per ton of scrap
- P&C are annual production and consumption of the primary resource
- R is the world reserve of the resource
- i counts the type of resources in the scrap

With equation (2.30) above, it can be determined if it is feasible to recover certain metals within the e-waste. For it to be feasible to recover most of the metals within the e-waste on an industrial scale using hydrometallurgical processes, it would mean that the industry would require manufacturing firms to be highly agile; with the capability of exploiting rapid market changes by increasing flexibility in their physical infrastructure and production processes (Sethurajan et al., 2019).

The process of recovering a metal (recovery technology) is designed according to a specific strategy. The most precious metals are commonly considered as those mainly deserving to be recovered (Pietrelli et al., 2018). These precious metals like gold commonly have the lowest concentrations within the PCB yet they can contribute to the highest portion of the total recoverable e-waste (Diaz et al., 2016). However, it is possible to recover and recycle metals with less value but more markets such as copper. It is more considering given that the gold content in PCBs has gradually decreased thanks to the optimization of the surface conduction mechanism. In the 80s, the gold contact layer was in the range of 1-2.5µm while currently its 0.3-0.6µm and expected to drop (Pietrelli et al., 2018). Based on the information above, an equation to calculate the value share of metals within a PCB is provided below.

$$v_i = 100 \times \frac{w_i Pr_i}{\sum_i w_i Pr_i} \quad (\text{Pietrelli et al., 2018}) \quad (2.31)$$

Where;

- w is weight percent of the metal in the PCB
- Pr is the current price of the metal per tonne
- v is the value share of the metal
- i is the type of metal within the PCB

Using equation (2.31) above, the metal with the most value within the PCB can be calculated.

As already stated earlier, during the processing of e-waste, the metallic fraction is separated from the non-metallic components. Not much attention is paid to the non-metallic fraction (NMF) of the e-waste in this study, but they can also be useful. After the recycling process of waste PCBs, a large volume of NMF mainly consisting of resin and glass fibre enters the waste stream and awaits appropriate treatment (Kwonpongsagoon, 2017). The non-metallic components within the e-waste are fibre-reinforced polymers (FPR) consisting of thermosetting resin and a glass fibre containing silica (Abdelbasir et al., 2018). It is difficult to recover any of these products by simple means, current local and foreign non-metallic powder (NMP) treatment methods include landfills, incineration, and dumping in open scrap yards (Abdelbasir et al., 2018). These NMPs are used as asphalt-modified bitumen to boost the performance of asphalt by resisting the rising traffic load under various climate conditions and resisting permanent deformation (Abdelbasir et al., 2018).

NMF incineration can lead to the development of highly toxic compounds such as polybrominated dibenzodioxins and dibenzofurans, while NMF landfilling will lead to secondary heavy metal contamination and brominated flame retardants (BFRs) leaching into groundwater (Kwonpongsagoon, 2017). Methods that are used as appropriate waste management options for NMF are in accordance with the Life Assessment Cycle (LCA). LCA is a technique to assess the potential environmental impacts associated with a product or service (Kwonpongsagoon, 2017). The methods explored are recycling NMF as a modified Glass Fiber Reinforced Plastic (GFRP), recycling NMF as a new product, landfilling, and incineration (Kwonpongsagoon, 2017).

2.1.12 Experimental Designs for Optimization

An experiment is a test or a series of experiments in which purposeful adjustments are made to a system's input variables such that explanations are observed for changes in the way of the output response (Montgomery, 2017). Design of experiments has several advantages, saves time and budget costs, allows

for a finding of levels of the factors that optimizes the response, want to know the effect of each factor on the response and how the factors may interact with each other and make it possible to predict the responses for given levels of the factors. All experiments should be designed experiments. Some studies, however, are poorly planned and thus ineffectively use valuable resources and result in inconclusive results. Statistically designed experiments allow data to be analyzed effectively, economically, and using statistical techniques; resulting in scientific objectivity when concluding (Montgomery, 2017).

When designing experiments, different strategies are used, best guess approach, one factor at a time approach, and factorial approach. The best guess approach is trial and error and thus can continue indefinitely and it cannot guarantee that the best solution in the experimental work has been found. The one factor at a time approach is inefficient as it requires many test runs and fails to consider any possible interaction between factors. The one factor at a time approach is a prevalent but potentially disastrous type of experimentation, tests are conducted by systematically changing the levels of one factor while holding the levels of all other factors fixed. The optimum level of the first factor is then selected. The same procedure is repeated for all the other factors, it is regarded as easier to implement, more easily understood, and more economical than factorial experiments. These presumptions are generally false as this approach does not provide adequate information on interactions and does not provide efficient estimates of the effects. The factorial approach was invented in 1920s (Montgomery, 2017). It is regarded as the correct, modern, and most efficient approach. In the factorial approach, factors can be varied together, and it can also determine how the factors interact.

The factorial approach has different classes, the 2-level approach, fractional factorial, and response surface methodology. This technique helps experiments to construct mathematical models that predict how input variables interact to produce output variables. As already highlighted, there are advantages to using this approach, it allows the obtaining of prediction equations, screen important variables, and optimize the response. Three basic principles of using this approach include replication, which helps in the estimation of experimental errors and allows for a more precise estimate of the sample mean. Randomization reduces bias and systematic errors and averages out the effects of extraneous factors (Montgomery, 2017). The last principle is blocking, which increases the precision of experiments and factors out variables not studied.

CHAPTER 3: MATERIALS AND METHODS

In this chapter, the methods that are carried out to achieve the objectives of this project are clearly outlined. Liberation of materials from e-waste, characterization of e-waste and, its hydrometallurgical processing was carried out.

3.1 EXPERIMENTAL METHOD

E-waste (waste computer PCBs) recovery entails 3 major steps:

1. Liberation of materials from e-waste.
2. Characterization of e-waste
3. hydrometallurgical processing

3.1.2 Liberation of e-waste material

- Computer boxes were opened using screwdrivers.
- Once opened, further use of screwdrivers was employed to take the PCB out of the computer box.
- The PCB was clamped on vice, and a solder gun was used to remove large components that could not be easily removed. The soldering gun melted the pins of the large plastic components and pliers were used to remove them from the PCB
- Once the Large components were removed, the PCB was removed from the vice, and easy to remove components (capacitors) were removed using pliers
- The depopulated PCBs were then subjected to further depopulating now using screwdrivers (The aim was to remove as much of the small pins on the board as possible)
- E-waste (PCB) was then subjected to a crushing unit for further liberation of the e-waste material. The Zerma grinder was used.
- The output from the grinder had different size-classes thus sieving was carried out to determine the size-classes and mass of the material. Size-classes help in determining the physical separation technique to be used as different sizes of material are more suited to certain separation techniques. The optimum size that yields great recoveries is 0.5mm under the experimental conditions of the authors (Chartterjee, 2009).
- For this experiment, only magnetic separation was used as other physical separation techniques lose metal when used.

After sieving, the e-waste was characterized using the TGA. TGA analysis is done before and after hydrometallurgical processing. The reacted e-waste is also characterized by the ICP machine.

3.1.3 Characterization of e-waste

- To determine the content values of the metals present within the e-waste, characterization will be done with a TGA and using ICP.
- The TGA will be used to analyze the presence of metals at 800°C at optimized conditions and before waste PCBs are processed.

Table 3.1: Method used in this thermogravimetric analysis

Temp. Rate	Hold Temp.	Hold Time	Gas
[C/min]	[C]	[min]	
0.00	30.0	5	1
5.00	110.0	5	1
10.00	800.0	5	2
10.00	900.0	10	2

Table 3.1 describes the method applied for every TGA run that was carried out. Where:

- Gas 1 is nitrogen (inert environment)
- Gas 2 is air (oxygen-rich environment)

The TGA has two crucibles, one which is used as a reference for weighing the mass of the second crucible; The second one is for collecting the sample to be analysed. Before placing the sample in the crucible, the crucible is first weighed, and a sieved sample of the e-waste is placed in a clean crucible (the mass of the sample inside the crucible should not be less than 10mg but also not greater than 20mg). The crucible containing the e-waste is inserted in the TGA to be analysed as per table 3.1.

At the beginning of the run, the temperature is held constant at 30°C for 5 minutes under nitrogen gas conditions; after five minutes, the temperature starts increasing. The temperature increases at 5°C/min till it reaches 110°C and is then held constant for another 5 minutes. This is still in an inert environment. After 5 minutes, the temperature increases at 10°C/min till the temperature in the TGA reaches 800°C where it gets held for 5 minutes in an oxygen-rich (air) environment. Lastly, the temperature is increased at a rate of 10°C/min until the temperature reaches 900°C and it gets held constant for 10 minutes in an oxygen-rich environment.

Once the e-waste had been characterized using the TGA, it was processed using hydrometallurgical techniques.

3.1.4 Hydrometallurgical processing

A complete dissolution experiment was conducted to know the amount of copper that is present on the PCB board. This is necessary as the % recovery will be measured or based on the amount of copper that is found to be present in the boards. For complete dissolution, a very aggressive medium (aqua-regia) is used to ensure that all metals within the board are dissolved. The solid-liquid ratio was kept within an optimum range of 25 – 100g/L(Kumar et al., 2014).

- The cone and quartering sampling technique was used to obtain a 3.125g sample from the crushed PCBs
- The sample was placed in a conical flask
- In a separate beaker, the aqua regia solution that will be used to dissolve the metals was prepared
- Concentrated hydrochloric acid was added to a beaker and in the same beaker nitric acid was added. The volume ratio was 1:1. A stirrer was used for 20 minutes for the color of the solution to turn dark yellow
- 50ml of the aqua regia was added to the 3.125gram PCB board in the conical flask and it was ensured that the conical flask was clamped and with a stirrer in it
- The reaction was allowed to proceed for a maximum of 0.5 hours
- The experiment was triplicated and the amount of dissolved copper from each experiment was determined. The average from the three experiments was taken as the amount of copper present in the PCB board

AQUA REGIA PREPARATION

Aqua regia is a mixture of nitric acid and hydrochloric acid and it is characterized by being very corrosive. Aqua regia is normally prepared as three parts nitric acid and 1-part hydrochloric acid, but in this study; it is prepared as 1-part nitric acid and 1-part hydrochloric acid. When preparing aqua regia, it is advised that you start with hydrochloric acid and add nitric acid.

3.1.4.1 Experimental setup 1

These hydrometallurgical reactions were proceeding by the setup below

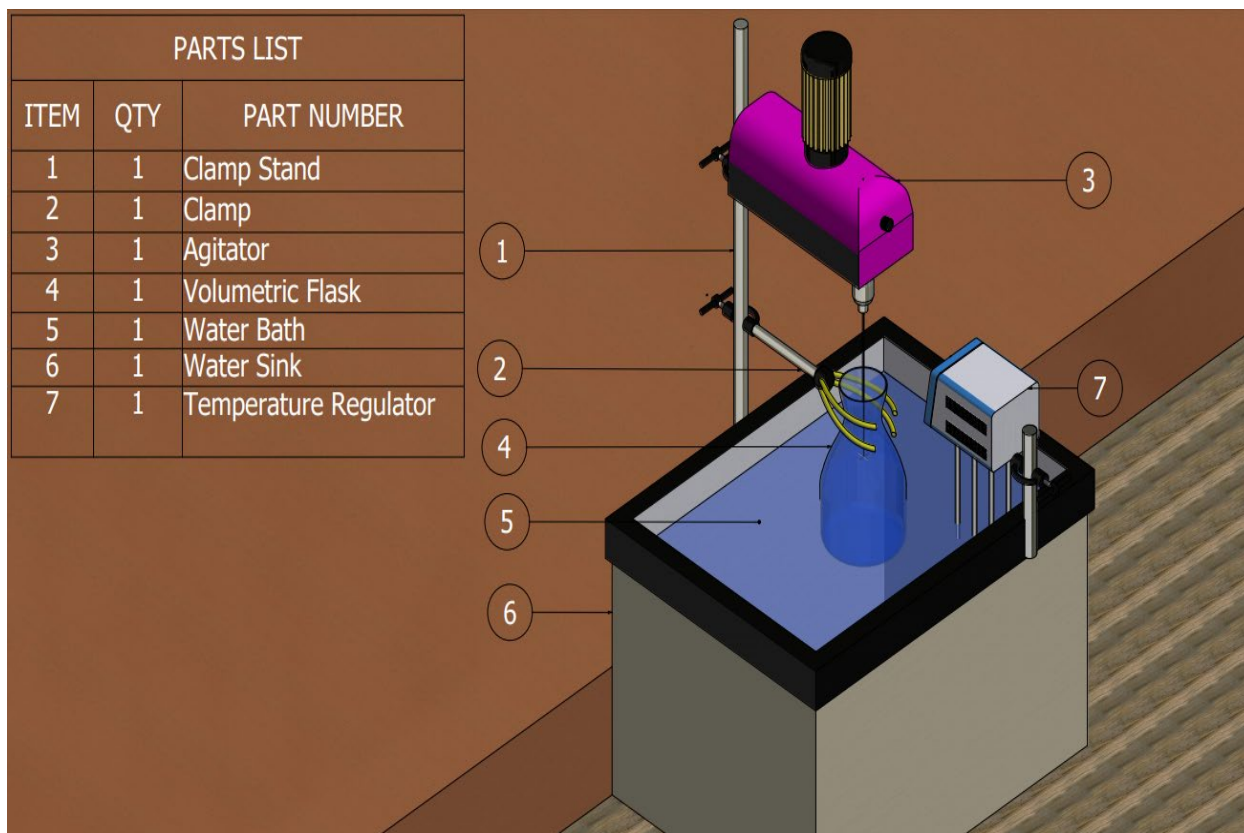


Figure 3.1: A schematic of the experimental set-up

Following the complete dissolution experiments, screening experiments were carried out in the same experimental set-up to determine the most effective leaching agent. Also, due to many parameters being investigated in this study, a Design of Experiment (DoE) was of paramount importance to avoid having to do numerous experiments to investigate the effect of each parameter and to investigate if there were any interactions amongst the parameters. A full factorial design of experiment using two levels was used for the preliminary runs. These preliminary runs were used for screening purposes.

The screening experiments were conducted first under nitric acid conditions then again under sulphuric and hydrogen peroxide conditions. Different acidic mediums were also used to investigate which medium recovered the most metal (to determine the most effective leaching agent). Also, using different acid mediums allowed for more parameters to be investigated. For example, under sulphuric acid and hydrogen peroxide medium, size as a parameter is not investigated; but nitric acid conditions investigate size as a parameter. To conduct these experiments, the lab acids had to be prepared to the desired molarities.

$$\text{Molarity} = \frac{\text{weight fraction} \times \rho}{\text{Molecular weight}} \quad (3.1)$$

Table 3.2: Lab acids used for leaching

	Nitric acid	Sulphuric acid
Weight fraction	0.55	0.98
Acid density (g/L)	1340	1840
Molecular weight (g/mol)	63.01	98.079

Using the information above and the molarity equation (3.1), the molarities of the lab acids were determined;

$$\text{Nitric acid} = 11.697M$$

$$\text{Sulphuric acid} = 18.4M$$

Using the calculated molarities and knowing how much of the PCB is being used in every run, the volume to be used and the molarity of the acid required for a particular run; the amount of lab acid to be diluted is calculated using the equation below.

$$C_1V_1 = C_2V_2 \tag{3.2}$$

In the case where we are using 4M nitric acid, the calculations were done as shown below;

$$V_1 = \frac{4 \times 50}{11.697} = 17.1ml \tag{3.3}$$

The volume of 17.1ml was that of lab acid that will be diluted with distilled water to the final volume of 50ml thus reducing the molarity of the nitric acid from 11.697M to 4M. All the molarity calculations were conducted similarly.

The purpose of screening experiments was to determine which of the parameters being studied was most important to the response variable (%recovery of copper). Full factorial design of experiments was used to determine the weight of each variable on the response variable and as well as if the parameters show any form of interaction. Each parameter was tested at two extreme levels. An orthogonal matrix that shows the number of runs and conditions for each parameter is displayed below. The agitation speed was kept constant at 500rpm.

The DoE below illustrates when nitric acid is being used as the leaching media.

Table 3.3: Parameters and their levels

Control factors (Variables)	Levels	
	Max level (+)	Min level (-)
Time (hrs)	8	2
Temperature (°C)	80	25
Size fraction (mm)	2	6
Concentration (M)	4 (HNO ₃)	1 (HNO ₃)

Table 3.4: Full factorial design of experiment

runs	Time	temperature	concentration	Size class
1	+	+	+	+
2	+	+	+	-
3	+	+	-	+
4	+	+	-	-
5	+	-	+	+
6	+	-	+	-
7	+	-	-	+
8	+	-	-	-
9	-	+	+	+
10	-	+	+	-
11	-	+	-	+
12	-	+	-	-
13	-	-	+	+
14	-	-	+	-
15	-	-	-	+
16	-	-	-	-

Where:

- + represents the maximum level
- - represents the minimum level

The DoE below illustrates when sulfuric acid with hydrogen peroxide is being used as the leaching media. Hydrogen peroxide is being considered as a variable because it was established from the literature that leaching with just sulphuric acid was not economic as close to no leaching occurred. Tables 3.4 and 3.5 show parameters being investigated and the full factorial DoE respectively.

Table 3.3: Parameters and their levels

Control factors (Variables)	Levels	
	Max level (+)	Min level (-)
Time (hrs)	8	2
Temperature ($^{\circ}\text{C}$)	80	25
Hydrogen peroxide volume %	20	4
Concentration (M)	1.2 (H_2SO_4)	0.8 (H_2SO_4)

Table 3.4: Full factorial design of experiment

runs	Time	temperature	concentration	Hydrogen peroxide vol %
1	+	+	+	+
2	+	+	+	-
3	+	+	-	+
4	+	+	-	-
5	+	-	+	+
6	+	-	+	-
7	+	-	-	+
8	+	-	-	-
9	-	+	+	+
10	-	+	+	-
11	-	+	-	+
12	-	+	-	-
13	-	-	+	+
14	-	-	+	-
15	-	-	-	+
16	-	-	-	-

After every screening run, the waste PCBs were removed from the solution first by decanting. The smaller particles of the waste PCBs were then removed from the solution by filtration.

3.1.4.2 Experimental setup 2

The filtration experiment setup was as follows

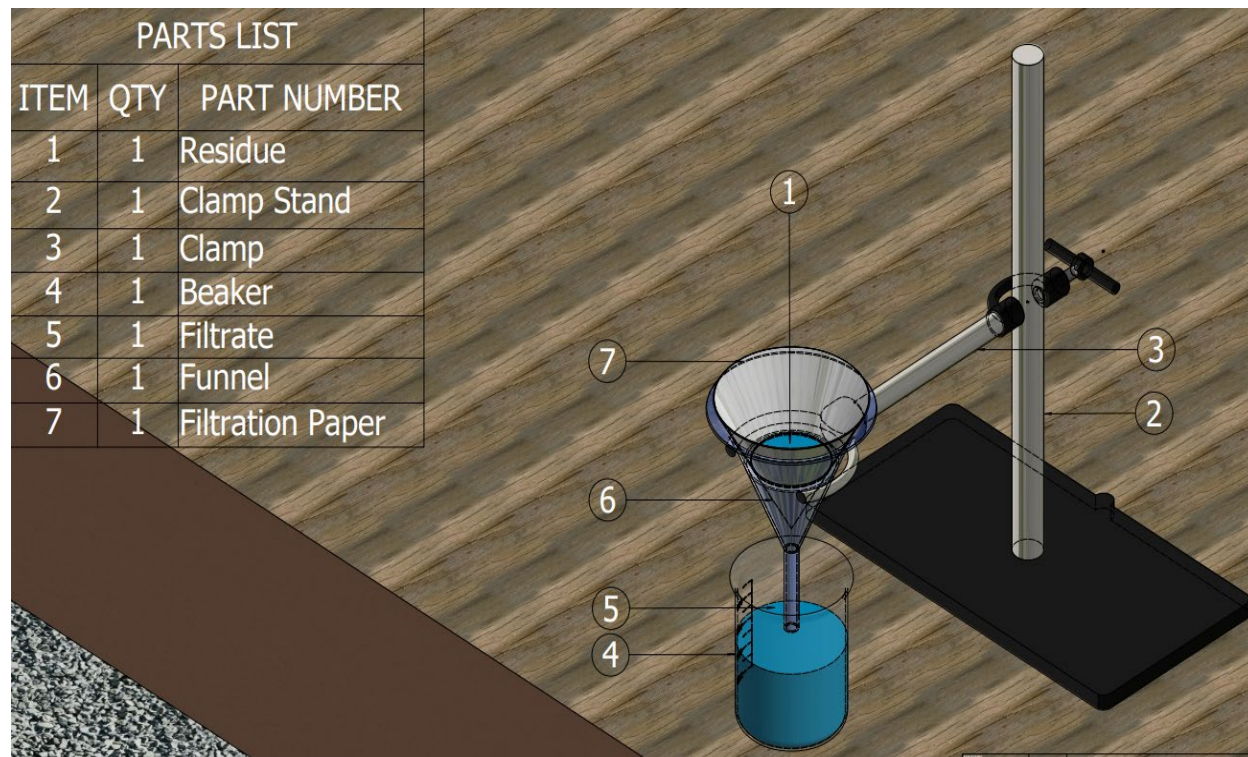


Figure 3.2: A schematic of the experimental set-up for filtration

To determine the amount of metal that is dissolved in the leaching experiments, the solution was diluted and analyzed using an ICP. It was from the ICP analysis that parameters with the most significance on the yield were determined.

Once the parameters that have the most significance on the response variable had been identified, the central composite design was used to investigate the effect of those parameters further. Central composite design because it allows for the addition of axial and center points which will be used to test if there is curvature or high order interactions. The addition of center points will also allow for replication, which is important in determining the error associated with the experiments.

CHAPTER 4: RESULTS AND ANALYSIS

4.1 LIBERATION OF MATERIALS

The particle size distribution of the waste PCBs after crushing is represented by the table and figure below. It shows the representation of size particles after crushing and the range of particles present in the sample. From the graph, we can determine the uniformity coefficient, coefficient of curvature and tell if we are dealing with predominantly fine or coarse particles.

Table 4.1: Particle size distribution of the waste PCBs after crushing

Size class (microns)	Mass (grams)	Mass %	Mass percent passing
-125	3	0.9	0.9
-180+125	6.7	2	2.9
-500+180	16.6	5	7.9
-850+500	22.2	6.7	14.6
-1000+850	9.1	2.8	17.4
-1400+1000	26	7.9	25.3
+1400	246.4	74.7	100

Figure 4.1 shows the particle size distribution

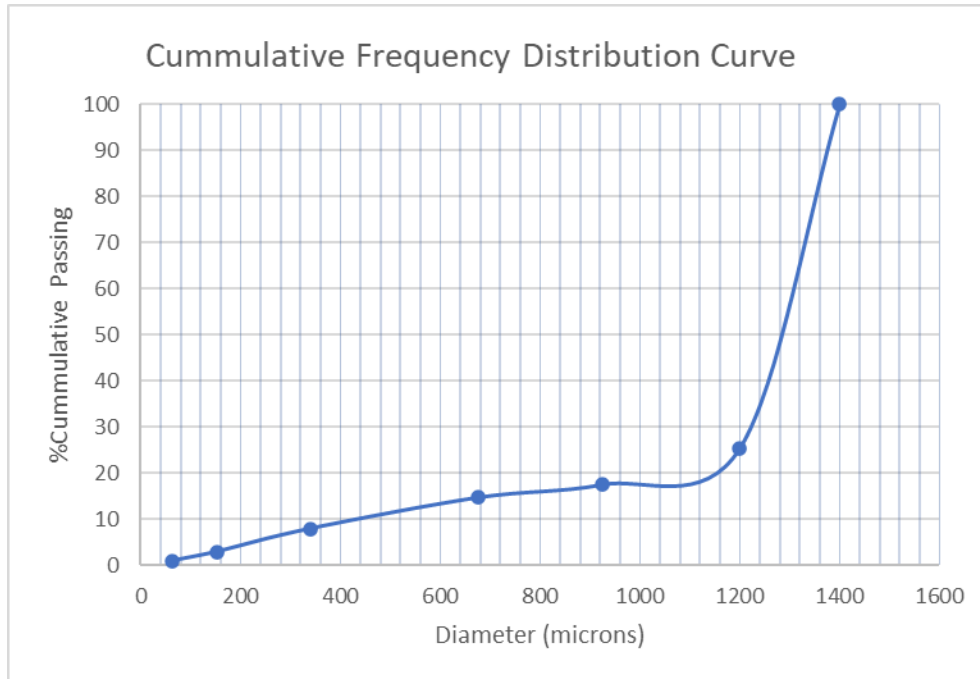


Figure 4.1: Particle size distribution

Using an excel function (Trend), Important parameters were able to be calculated and the importance of those parameters is discussed.

$$d_{10} = 445$$

$$d_{30} = 1212.6$$

$$d_{50} = 1266.1$$

$$d_{60} = 1292.9$$

From the figure 4.1, it is seen that there are no gaps in size classes as all size particles are represented. However, the value of d_{50} gives valuable insight about the sample being analyzed.

$D_{50} = 1266.1$ microns and this means that more than half our sample has a size greater than 1266.1 microns. This means that the sample being used is predominantly coarse.

Using d_{10} , d_{30} and d_{60} it can be determined if the sample is well distributed.

Coefficient of uniformity (C_u):

$$C_u = \frac{d_{60}}{d_{10}} \quad (4.1)$$

Using the equation above:

$$C_u = 2.91$$

Coefficient of Curvature (C_c):

$$C_c = \frac{d_{30}^2}{d_{10} \times d_{60}} \quad (4.2)$$

Using equation (4.2) above:

$$C_c = 2.56$$

For a coarse material sample to be well distributed, $C_u > 4$ and $1 < C_c < 3$. For the sample being analyzed, only one criterion is met ($C_c = 2.56$). This means that the PCB sample is not well distributed. This limits the study in that there were significant differences in size classes (e.g. the size classes in between the coarse particles and the fines are limited).

4.2 CHARACTERIZATION OF E-WASTE

This section contains results of e-waste analyzed by the TGA before hydrometallurgical processing.

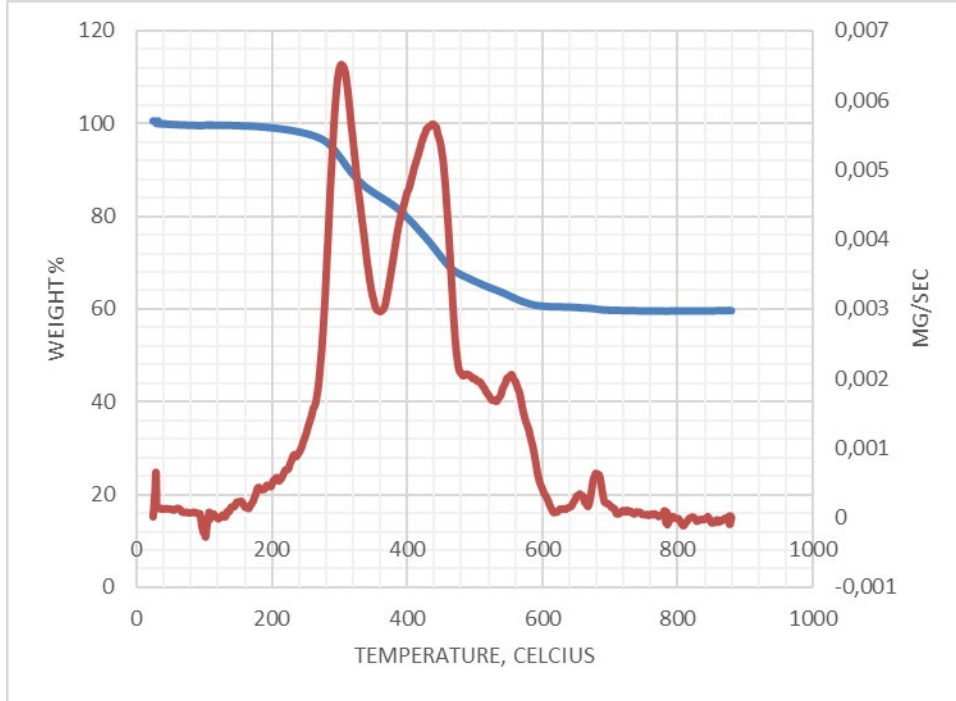


Figure 4.2: Thermogravimetric analysis curve of unreacted Printed Circuit Boards of size class -125+180µm

- Figure 4.2 is a TGA curve of unreacted PCBs of size class -125+180µm

Moisture content (M) is calculated as follows:

$$M = \frac{W - R}{W} \times 100 \quad (4.3)$$

Where:

W is the initial mass when the decomposition starts,

R is the mass measured at temperature X (Temperature X is taken at the centre of the first mass loss plateau)

Volatile matter (O) is calculated as follows:

$$O = \frac{R - S}{W} \times 100 \quad (4.4)$$

Where:

R and W are as defined from equation (4.4) above,

S is the mass measured at temperature Y (Temperature Y should correspond to mass loss plateau for switching atmospheres)

Combustible material content (C) is calculated as follows:

$$C = \frac{S - T}{W} \times 100 \quad (4.5)$$

Where:

T is the mass measured at temperature Z (Temperature Z corresponds to the mass loss of the last plateau)

Ash content (A) is calculated as follows:

$$A = \frac{T}{W} \times 100 \quad (4.6)$$

Using figure 4.2 and the equations (4.3)-(4.7), moisture content, volatile matter content, combustible material content, and ash content are calculated.

$$W = 18.8\text{mg}$$

$$R = 16.6\text{mg}$$

$$S = 13.0\text{mg}$$

$$T = 11.2\text{mg}$$

With the constants above defined, the amounts of different materials can be determined.

$$M = \frac{18.806007 - 16.590176}{18.806007} \times 100 = 11.78\%$$

$$O = \frac{16.590176 - 12.954138}{18.806007} \times 100 = 19.33\%$$

$$C = \frac{12.954138 - 11.214922}{18.806007} \times 100 = 9.25\%$$

$$A = \frac{11.214922}{18.806007} \times 100 = 59.63\%$$

Figure 4.2 shows the decomposition of the PCB, and from the derivative curve, the number of decomposition steps is identified. There are 4 identifiable peaks. Each peak represents a maximum temperature of a decomposition stage and thus the sample has four stages of decomposition. From the table method, gas 1 is nitrogen (inert atmosphere) and gas 2 is air (reactive, oxygen-rich atmosphere).

From the figure, it is seen that the first 3 decomposition stages occur in an inert environment and the last decomposition stage occurs in the reactive atmosphere. The first two peaks are a representation of the decomposition of organic matter and the maximum decomposition temperature for the two stages are 300°C and 440°C respectively. The 3rd decomposition starts at 520°C and ends at 560°C, with peak decomposition occurring around 550°C; the temperature range of this decomposition is similar to that of magnesium, which decomposes at 540°C. In the reactive atmosphere, there is a single decomposition occurring and the maximum of the decomposition is 700°C; this is the decomposition temperature of aluminium. The base material of PCBs is glass re-enforced epoxy and it decomposes at 300°C.

At 101°C, before any decomposition starts, there is a dip in the DTA curve and this is due to the burning off of volatiles and H₂O. From the weight % curve, the mass loss is around 40%. This means the residue content of the PCB is around 60% and within the residue is where reinforcements and char are found. There can also be the presence of metals like tin and iron, which start decomposing at 1473K.

TGA analysis for other size classes was conducted similarly. The TGA curves and analysis of these size classes are in the appendix section (Appendices A).

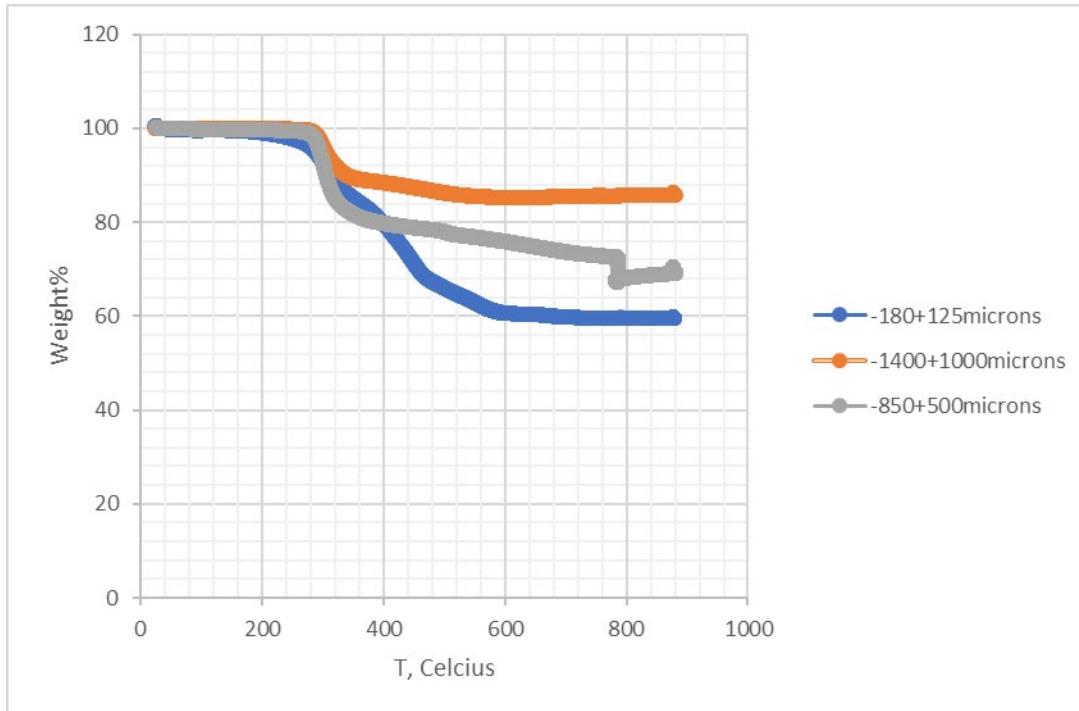


Figure 4.3: Mass loss for unreacted Printed Circuit Boards size classes

Figure 4.3 shows the mass loss for the different unreacted PCB size classes and a general trend is observed. The ash content within the PCB increases with an increase in size class. This is because larger size classes have a smaller surface area compared to the small size fractions. With a smaller surface area, it means that the large size classes contain substantial amounts of char and re-enforcements. The smaller size classes contain less ash content because materials within the PCB were properly liberated and the char or re-enforcements could have been lost in earlier stages of PCB preparation.

4.3 HYDROMETALLURGICAL PROCESSING

The results from the complete dissolution runs are presented in table 4.1 below, calculations on the amount of metal dissolved are explored further in the sections to follow (see appendix section B). As already explained, the experiment was triplicated and the average of the 3 runs was taken as the amount of copper present in the sample.

Table 4.1: Results from complete dissolution

Run	Average reported concentration (mg/L)	Old concentration (ppm)	Amount of metal (g) (50ml was used for experiments)	Metal fraction within the PCB (3,125g)

1	80.5	40250	1. 2.013	0.644
2	70.7	35350	1.768	0.566
3	99.9	49950	2.498	0.799

Average Amount of Metal = 2.0925g

Metal Fraction Within PCB = 0.6696

The average reported concentrations used are the average of the triplicated runs of a single sample that were performed by the ICP. The old concentration is calculated from the equation below,

$$Dilution = \frac{old\ concentration}{actual\ concentration} \quad (4.7)$$

When preparing the standards for ICP analysis, the samples were too concentrated and thus they were diluted, the dilution was 500. The actual concentration is the one that is determined by the ICP as the average reported concentration. To get the amount of dissolved metal per run, the following equation is used;

$$m = \frac{c}{1000000} \times v \quad (4.8)$$

The concentration is divided as a unit conversion step, the ppms are being expressed as g/ml and the volume used is 50ml. This is the volume that was used when conducting the experiments. To get the metal fraction within the PCB, the amount of metal dissolved in the experimental run is divided by the amount of PCB (3.125g) used when experimenting.

$$Metal\ fraction = \frac{Amount\ of\ dissolved\ metal(g)}{3.125g} \quad (4.9)$$

An example of calculating the metal fraction using the equations described is in the appendix section.

Table 4.2 shows the results of the leached copper for different runs under nitric acid conditions.

Table 4.2: Results of leached copper in nitric acid

Run	Average reported concentration (mg/L)	Old concentration (ppm)	Amount of metal (g) (50ml was used for experiments)	Metal fraction within the PCB (3,125g)

1	25.477	12738.333	0.637	0.204
2	27.980	13990.000	0.700	0.224
3	14.637	7318.333	0.366	0.117
4	13.100	6550.000	0.328	0.105
5	11.827	5913.333	0.296	0.095
6	11.743	5871.667	0.294	0.094
7	4.941	2470.500	0.124	0.040
8	1.089	544.500	0.027	0.009
9	29.110	14555.000	0.728	0.233
10	29.890	14945.000	0.747	0.239
11	4.907	2543.667	0.123	0.039
12	3.481	1740.500	0.087	0.028
13	1.768	883.833	0.442	0.014
14	1.316	658.167	0.033	0.010
15	0.973	486.667	0.024	0.008
16	0.590	295.000	0.015	0.005

From table 4.2, it is evident that most of the copper was recovered in run 10 where 0.2391 copper fraction was dissolved in solution. Conditions are; time = 2hours, temperature = 80°C, nitric acid concentration = 4M and particle size = 6mm.

Table 4.3 shows the results of the leached copper for different runs under sulphuric acid and hydrogen peroxide conditions.

Table 4.3: Results of leached copper in sulphuric acid and hydrogen peroxide

Run	Average reported concentration (mg/L)	Old concentration (ppm)	Amount of metal (g) (50ml was used for experiments)	Metal fraction within the PCB (3,125g)
1	16.520	8260.000	0.413	0.132
2	18.027	9013.333	0.406	0.144
3	18.313	9156.667	0.458	0.147
4	10.617	5308.333	0.265	0.085

5	21.960	10980.000	0.549	0.176
6	5.603	2801.667	0.140	0.044
7	17.353	8676.667	0.433	0.139
8	12.470	6235.000	0.312	0.100
9	12.253	6126.667	0.306	0.098
10	6.111	3055.333	0.153	0.049
11	12.417	6208.333	0.310	0.099
12	8.197	4098.500	0.205	0.066
13	12.817	6408.333	0.320	0.103
14	7.032	3516.000	0.176	0.056
15	11.887	5943.333	0.297	0.095
16	6.121	3060.500	0.153	0.049

From table 4.3, it is evident that most of the copper was recovered in run 5 where 0.1757 copper fraction was dissolved in solution.

It is seen that under sulphuric acid and hydrogen peroxide conditions, most recovery of copper was in run 5; time = 8hours, temperature = 25⁰C, sulphuric acid concentration = 1.2M and hydrogen peroxide volume % = 20%.

The results for the recovery of copper were also analyzed using Minitab to see which parameters were significant in the recovery process and to also see if there were any interactions amongst parameters.

4.3.1 Nitric acid media

Table 4.4 show the yield of Copper (Cu) under nitric acid leaching conditions as analyzed by Minitab.

4.3.1.1 Copper Yield

Table 4.4: Coded Coefficients

Term	Effect	Coef	SE	
			Coef	T-Value
Constant		0,09141	*	*
Time	0,03876	0,01938	*	*
Temperature	0,11433	0,05717	*	*
Particle Size	-0,004450	-0,002225	*	*
Nitric Acid Concentration	0,09539	0,04770	*	*
Time*Temperature	-0,011148	-0,005574	*	*
Time*Particle Size	-0,001487	-0,000744	*	*
Time*Nitric Acid Concentration	-0,008872	-0,004436	*	*
Temperature*Particle Size	0,005090	0,002545	*	*
Temperature*Nitric Acid Concentration	0,05727	0,02864	*	*
Particle Size*Nitric Acid Concentration	0,009947	0,004974	*	*
Time*Temperature*Particle Size	0,004714	0,002357	*	*
Time*Temperature*Nitric Acid Concentration	-0,04091	-0,02046	*	*
Time*Particle Size*Nitric Acid Concentration	0,005670	0,002835	*	*
Temperature*Particle Size Nitric Acid Concentration	0,002545	0,001273	*	*
Time*Temperature*Particle Size*Nitric Acid Concentration	-0,002003	-0,001001	*	*
Term	P-Value	VIF		
Constant	*			
Time	*	1,00		
Temperature	*	1,00		
Particle Size	*	1,00		
Nitric Acid Concentration	*	1,00		
Time*Temperature	*	1,00		
Time*Particle Size	*	1,00		
Time*Nitric Acid Concentration	*	1,00		
Temperature*Particle Size	*	1,00		
Temperature*Nitric Acid Concentration	*	1,00		
Particle Size*Nitric Acid Concentration	*	1,00		
Time*Temperature*Particle Size	*	1,00		
Time*Temperature*Nitric Acid Concentration	*	1,00		
Time*Particle Size*Nitric Acid Concentration	*	1,00		
Temperature*Particle Size*Nitric Acid Concentration	*	1,00		
Time*Temperature*Particle Size*Nitric Acid Concentration	*	1,00		

Table 4.5: Regression Equation in Uncoded Units

$$\begin{aligned}
\text{Yield-Cu} = & 0,01881 && - 0,000454 \text{ Time} && - 0,000928 \text{ Temperature} \\
& + 0,005301 \text{ Particle Size} \\
& - 0,03595 \text{ Nitric Acid Concentration} && + 0,000248 \text{ Time*Temperature} \\
& - 0,002193 \text{ Time*Particle Size} & + & 0,005582 \text{ Time*Nitric Acid Concentration} \\
& - 0,000114 \text{ Temperature*Particle Size} \\
& + 0,001378 \text{ Temperature*Nitric Acid Concentration} \\
& - 0,001789 \text{ Particle Size*Nitric Acid Concentration} \\
& + 0,000024 \text{ Time*Temperature*Particle Size} \\
& - 0,000149 \text{ Time*Temperature*Nitric Acid Concentration} \\
& + 0,000527 \text{ Time*Particle Size*Nitric Acid Concentration} \\
& + 0,000036 \text{ Temperature*Particle Size*Nitric Acid Concentration} \\
& - 0,000004 \text{ Time*Temperature*Particle Size*Nitric Acid Concentration}
\end{aligned}$$

The copper model in table 4.5 above shows the significance of each parameter and the significance of the interaction between parameters towards the copper yield. In the model, there are positive and negative coefficients associated with the parameters. If we look at the time, for instance, it has a negative coefficient and what this means is that for time to give a maximum contribution on the yield of copper; it should be negative (-1). Time being negative means using the low level (of 2 hours).

Particle size, on the other hand, has a positive coefficient and the opposite is also true in its case. However, attention should also be placed on the interaction of parameters. Looking at the interaction of time and particle size, it has a negative coefficient, and what does this mean? To get a positive value out of the time and particle size interaction term, either time or particle size has to be negative and the other positive.

If in this case, we decide to use high level on time (+1) and low level (-1) on particle size, we would still get an overall positive coefficient but it would be contradicting the contribution of the individual parameters. What happens in that particular situation is that we need to look at which coefficient has the most contribution, whether the individual parameters are more significant than the interaction of the parameters. We can determine the influential parameters by looking at which parameters have the biggest value (absolute) in the model or from the Pareto chart. On the Pareto chart, significant parameters are those that pass the *critical value line*. As such, the most influential parameter will be the one with the highest absolute value, and the one that surpasses the critical value line the most on the Pareto chart.

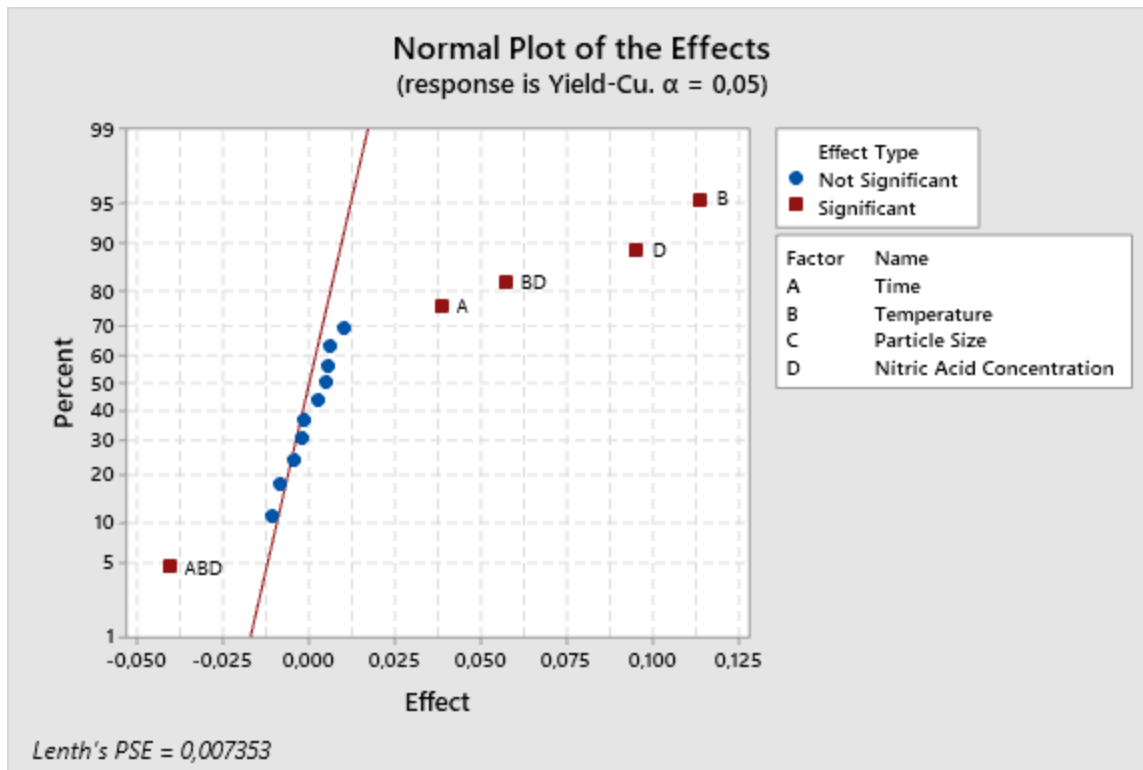


Figure 4.4: Normal plot of the effects

Figure 4.4 above, it provides a visual representation of the parameters and which are more significant than others. From this normal plot, it is seen that time, temperature, nitric acid concentration, temperature, and nitric acid concentration interaction and the interaction between time, temperature, nitric acid concentration; are the most influential parameters on the yield of copper. That is because they are the interactions that pass the critical value line, with temperature having the most significance on the copper recovery.

If we look at the interaction of nitric acid concentration and temperature, it is seen from the normal plot that it is an influential parameter. From the model we determine that the individual parameters have negative coefficients while their interaction has a positive coefficient. This means that to get the maximum out of these parameters, they must be set at a low level. It is however different for their interaction, to get the maximum from the yield term; both parameters can either be positive or be negative. From the copper yield graph under nitric acid conditions, we determined that run 10 resulted in most of the copper being dissolved in solution. Run 10 conditions are such that temperature and nitric acid are at their positive values. This means that the interaction term is more valuable than the individual terms.

4.3.2 Sulphuric acid media

The results below show the yield of 3 different metals copper under sulphuric acid and hydrogen peroxide leaching conditions which are showed above. There is a need to use hydrogen peroxide because sulphuric acid alone does not dissolve the metal components out of the PCB and into solution.

4.3.2.1 Copper Yield

Table 4.6: Coded Coefficients

Term	Effect
Constant	
Hydrogen Peroxide volume %	0,04934
Sulphuric acid concentration	0,002948
Temperature	0,007211
Time	0,04403
Hydrogen Peroxide volume %*Sulphuric acid concentration	0,004212
Hydrogen Peroxide volume %*Temperature	-0,016238
Hydrogen Peroxide volume %*Time	0,005518
Sulphuric acid concentration*Temperature	0,003786
Sulphuric acid concentration*Time	0,003765
Temperature*Time	0,004968
Hydrogen Peroxide volume %*Sulphuric acid concentration*Temperature	-0,018772
Hydrogen Peroxide volume %*Sulphuric acid concentration*Time	0,000328
Hydrogen Peroxide volume %*Temperature*Time	-0,013862
Sulphuric acid concentration*Temperature*Time	0,011967
Hydrogen Peroxide volume %*Sulphuric acid concentration*Temperature*Time	-0,02258

Term	Coef	SE Coef
Constant	0,09885	*
Hydrogen Peroxide volume %	0,02467	*
Sulphuric acid concentration	0,001474	*
Temperature	0,003606	*
Time	0,02201	*
Hydrogen Peroxide volume %*Sulphuric acid concentration	0,002106	*
Hydrogen Peroxide volume %*Temperature	-0,008119	*
Hydrogen Peroxide volume %*Time	0,002759	*
Sulphuric acid concentration*Temperature	0,001893	*
Sulphuric acid concentration*Time	0,001883	*
Temperature*Time	0,002484	*
Hydrogen Peroxide volume %*Sulphuric acid concentration*Temperature	-0,009386	*
Hydrogen Peroxide volume %*Sulphuric acid concentration*Time	0,000164	*
Hydrogen Peroxide volume %*Temperature*Time	-0,006931	*
Sulphuric acid concentration*Temperature*Time	0,005984	*
Hydrogen Peroxide volume %*Sulphuric acid concentration*Temperature*Time	-0,01129	*

Term	T-Value	P-Value
Constant	*	*
Hydrogen Peroxide volume %	*	*
Sulphuric acid concentration	*	*
Temperature	*	*
Time	*	*
Hydrogen Peroxide volume %*Sulphuric acid concentration	*	*
Hydrogen Peroxide volume %*Temperature	*	*
Hydrogen Peroxide volume %*Time	*	*
Sulphuric acid concentration*Temperature	*	*
Sulphuric acid concentration*Time	*	*
Temperature*Time	*	*
Hydrogen Peroxide volume %*Sulphuric acid concentration*Temperature	*	*
Hydrogen Peroxide volume %*Sulphuric acid concentration*Time	*	*
Hydrogen Peroxide volume %*Temperature*Time	*	*
Sulphuric acid concentration*Temperature*Time	*	*
Hydrogen Peroxide volume %*Sulphuric acid concentration*Temperature*Time	*	*

Term	VIF
Constant	

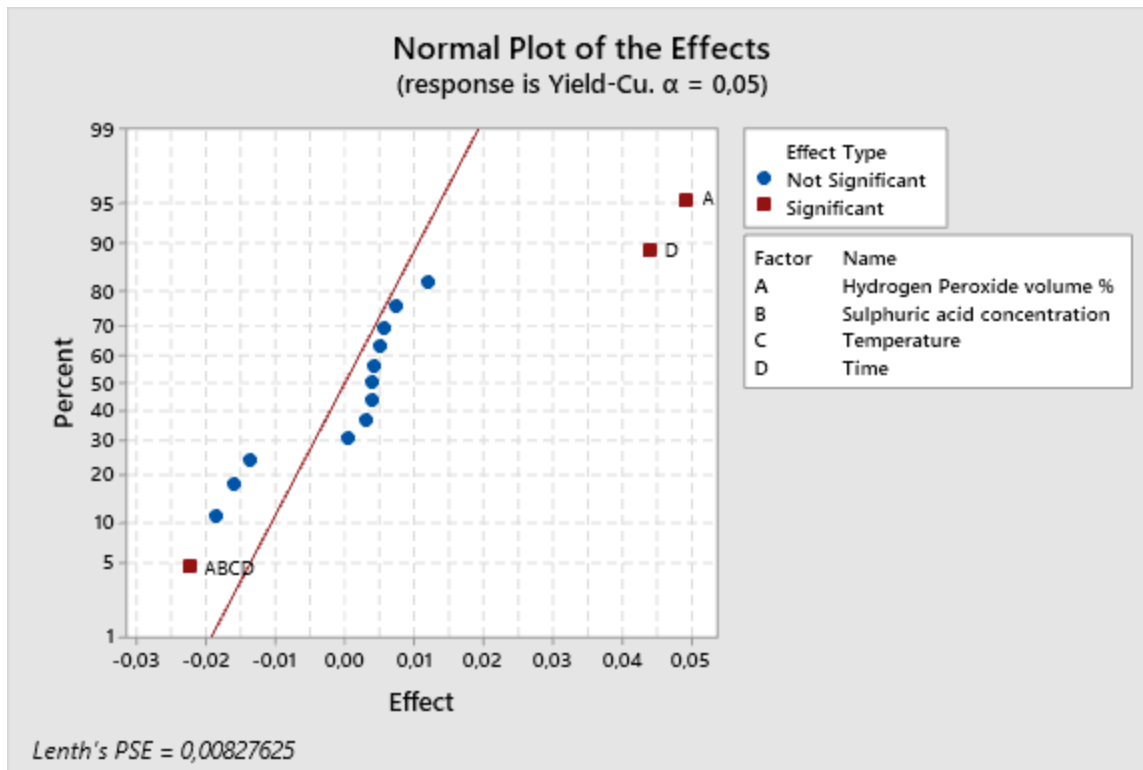


Figure 4.5: Normal plot of the effects

From the copper yield model and the normal plot, it is seen that the most influential parameters for maximum copper yield are hydrogen peroxide volume % and time. Also, the interaction of all the parameters passes the critical value line. The influential individual parameters have more significance than the influence brought about by the interaction of all the parameters. From the model, it is seen that hydrogen peroxide volume % and time have a positive coefficient while the interaction amongst all the parameters has a negative coefficient.

As iterated in the copper yield section under nitric acid conditions, choosing to use a negative (low level) or a positive (high level) for a parameter that can bring about the positive contribution to the overall yield whether it is positive or negative is dependent on whether it is most influential acting alone or when interacting with other parameters. Although the focus on the study was on the recovery of copper, the appendix section B has results and analysis of the hydrometallurgical processing of other trace metals (Nickel and Iron) under different leaching conditions.

When comparing the acid mediums under which the PCBs were leached, it was seen that, in a general view; nitric acid conditions bring about more dissolution of the target metals. Under nitric acid conditions, copper, iron, and nickel fractions dissolved were 0.2391, 0.0047, and 0.0006 respectively. Under sulphuric acid and hydrogen peroxide, copper, iron, and nickel metal fractions dissolved were 0.17568, 0.00364, and 0.00046

respectively. This is because nitric acid is more corrosive than sulphuric acid and hydrogen peroxide. However, due to nitric acid being more expensive and extremely harsh to the environment, sulphuric acid and hydrogen peroxide conditions are preferred for the leaching of PCBs. This study will be no different, further experiments will be done under sulphuric acid conditions.

From the screening experiments, individual parameters that were most significant were identified and investigated further. Significant individual parameters were time, temperature, and hydrogen peroxide volume percent. Under both acidic conditions, the size of the waste PCBs proved not to be a significant parameter. This is because the sizes that were used (2mm and 6mm) fall under the same size range in terms of size impact on metal recovery when dealing with PCBs. As such, the size will also be investigated, but this time going to much lower size classes. The central composite design (CCD) will be used as a design of experiment.

Table 4.8: Parameters and their levels

Control factors	Levels				
	Star point (- α)	Minimum level (-)	Center point (0)	Maximum level (+)	Star point (+ α)
Hydrogen peroxide volume %	0	6	12	18	24
Temperature ($^{\circ}$ C)	12.5	30	47.5	65	82.5
Time (min)	30	120	210	300	390
Particle size (mm)	0.125	0.75	1.375	2	2.65

Constants:

- Sulphuric acid concentration (1.2M)
- Agitation speed (500rpm)

Table 4.9: Central composite Design

Runs	Hydrogen peroxide volume %	Temperature	Time	Particle size
1	-	-	-	-

2	+	-	-	-
3	-	+	-	-
4	+	+	-	-
5	-	-	+	-
6	+	-	+	-
7	-	+	+	-
8	+	+	+	-
9	-	-	-	+
10	+	-	-	+
11	-	+	-	+
12	+	+	-	+
13	-	-	+	+
14	+	-	+	+
15	-	+	+	+
16	+	+	+	+
17	$-\alpha$	0	0	0
18	α	0	0	0
19	0	$-\alpha$	0	0
20	0	α	0	0
21	0	0	$-\alpha$	0
22	0	0	α	0
23	0	0	0	$-\alpha$
24	0	0	0	α
25	0	0	0	0
26	0	0	0	0
27	0	0	0	0

On the tables to follow, the average reported concentrations is the average of the triplicated runs of a single sample that were performed by the ICP. Equations on how to calculate old concentrations, amount of metal and metal fraction are showed on the earlier parts of the section.

Table 4.10: Results of leached copper in sulphuric acid and hydrogen peroxide

Runs	Average reported concentration (mg/L)	Old concentration (ppm)	Amount of metal (g)	Metal fraction within the PCB (3.125g)
1	17,0	8500	0,425	0,136
2	30,2	15100	0,755	0,242
3	15,7	7850	0,393	0,126
4	21,9	10950	0,548	0,175
5	15,8	7900	0,395	0,126
6	24,9	12450	0,623	0,199
7	2,93	1465	0,073	0,023
8	10,5	5250	0,263	0,084
9	11,7	5850	0,293	0,094
10	18,5	9250	0,463	0,148
11	14,8	7400	0,370	0,118
12	16,1	8050	0,403	0,129
13	19,9	9950	0,498	0,159
14	21,7	10850	0,543	0,174
15	25,6	12800	0,640	0,205
16	25,1	12550	0,628	0,201
17	0,557	278,6	0,014	0,004
18	29,6	14800	0,740	0,237
19	19,6	9800	0,490	0,157
20	3,46	1730	0,087	0,028
21	28	14000	0,700	0,224
22	3,08	1540	0,077	0,025
23	2,41	1205	0,060	0,019
24	21,4	10700	0,535	0,171
25	25,8	12900	0,645	0,206
26	27,5	13750	0,688	0,220
27	25,4	12700	0,635	0,203

Using runs 25 to 27, the error associated with our measurements can be determined as follows:

$$\text{Average Metal Fraction} = 0.2099$$

$$\text{Absolute error} = 0.22 - 0.2032 = 0.0168$$

$$\%Error = \frac{0.0168}{0.2099} \times 100 = 8.004\%$$

$$\%Copper\ recovery = \frac{0.755}{2.0925} \times 100 = 36.1\%$$

The metal fraction of copper recovered along with the parameters and their corresponding minimum, center, maximum and star points are analyzed using Minitab. From the analysis of variance table, a few deductions about the data can be drawn.

Table 4.11: Analysis of Variance

Source	DF	Adj SS	Adj MS	F-Value	P-Value
Model	14	0,101133	0,007224	2,12	0,099
Linear	4	0,051999	0,013000	3,82	0,032
Hydrogen peroxide vol %	1	0,028140	0,028140	8,27	0,014
Temperature	1	0,010977	0,010977	3,23	0,098
Time	1	0,006001	0,006001	1,76	0,209
Particle size	1	0,006881	0,006881	2,02	0,180
Square	4	0,018612	0,004653	1,37	0,302
Hydrogen peroxide vol %*Hydrogen peroxide vol %	1	0,005093	0,005093	1,50	0,244
Temperature*Temperature	1	0,014038	0,014038	4,13	0,065
Time*Time	1	0,004504	0,004504	1,32	0,272
Particle size*Particle size	1	0,010105	0,010105	2,97	0,110
2-Way Interaction	6	0,028643	0,004774	1,40	0,290
Hydrogen peroxide vol %*Temperature	1	0,001067	0,001067	0,31	0,586
Hydrogen peroxide vol %*Time	1	0,000363	0,000363	0,11	0,749
Hydrogen peroxide vol %*Particle size	1	0,002845	0,002845	0,84	0,378
Temperature*Time	1	0,000344	0,000344	0,10	0,756
Temperature*Particle size	1	0,008712	0,008712	2,56	0,135
Time*Particle size	1	0,015312	0,015312	4,50	0,055
Error	12	0,040808	0,003401		
Lack-of-Fit	10	0,040649	0,004065	51,08	0,019
Pure Error	2	0,000159	0,000080		
Total	26	0,141940			

Table 4.12: Model Summary

S	R-sq	R-sq(adj)	R-sq(pred)
0,0583150	71,25%	37,71%	0,00%

Table 4.13: Regression Equation in Uncoded Units

%Cu dissolved	= -0,091 + 0,0265 Hydrogen peroxide vol %
	+ 0,00533 Temperature + 0,000061 Time
	+ 0,005 Particle size
	- 0,000430 Hydrogen peroxide vol %*Hydrogen peroxide vol %
	- 0,000084 Temperature*Temperature - 0,000002 Time*Time
	- 0,0548 Particle size*Particle size
	- 0,000078 Hydrogen peroxide vol %*Temperature
	- 0,000009 Hydrogen peroxide vol %*Time
	- 0,00356 Hydrogen peroxide vol %*Particle size
	- 0,000003 Temperature*Time
	+ 0,00213 Temperature*Particle size
	+ 0,000550 Time*Particle size

From the analysis of the variance table, it was seen which parameters and which interactions were significant. The lack of fit checks if the model fits all the data and if there is a possibility of higher-order terms which are perhaps not shown by the model represented. The table shows that there is a lack of fit with the model and thus meaning that there are high order terms that are not represented by the model. For a p-value greater than 0.10, it means that there is no lack of fit and thus no higher-order terms were omitted. An R^2 value of greater than 80% also suggests that the model provided fits the data well and from the table above, the R^2 value is 71.25% and further indicating that the model presented does not adequately fit the data.

Two types of response surface plots are presented to represent the findings of the study. A contour plot and a surface plot, both showing %Copper recovered Vs time, temperature, particle size, and hydrogen peroxide volume percent. The graphs show the range of the region where the percentage of copper recovered is most high. Since the graphs essentially show the same information, the surface plots are in the appendix section (see appendix section B).

Figures 4.6 to 4.12 show the contour plot of percentage copper recovered vs time, temperature, particle size, and hydrogen peroxide volume percentage.

Contour Plots of %Cu dissolved

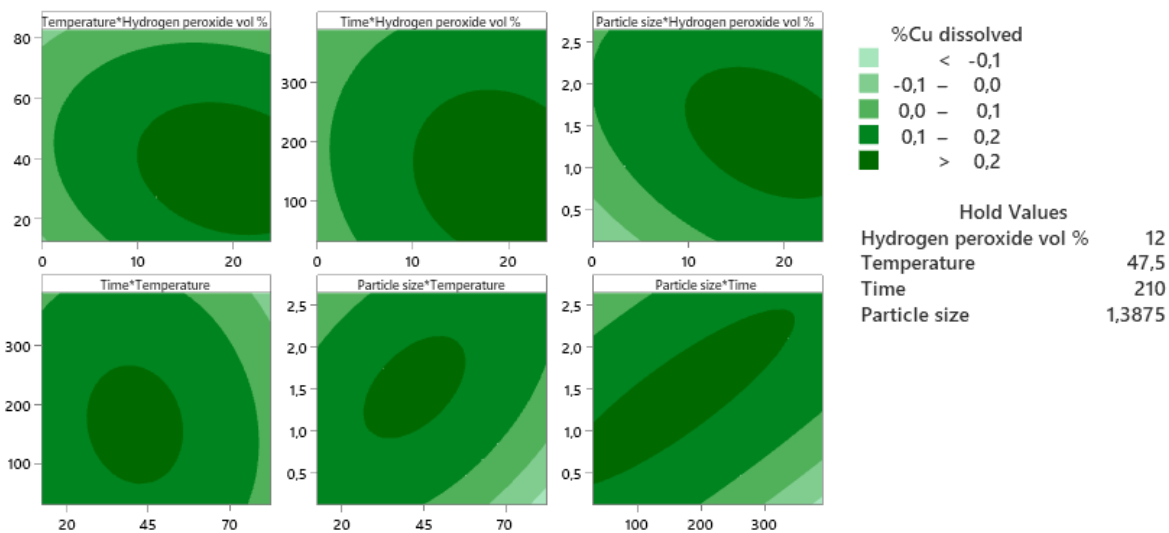


Figure 4.6: Percentage copper recovered

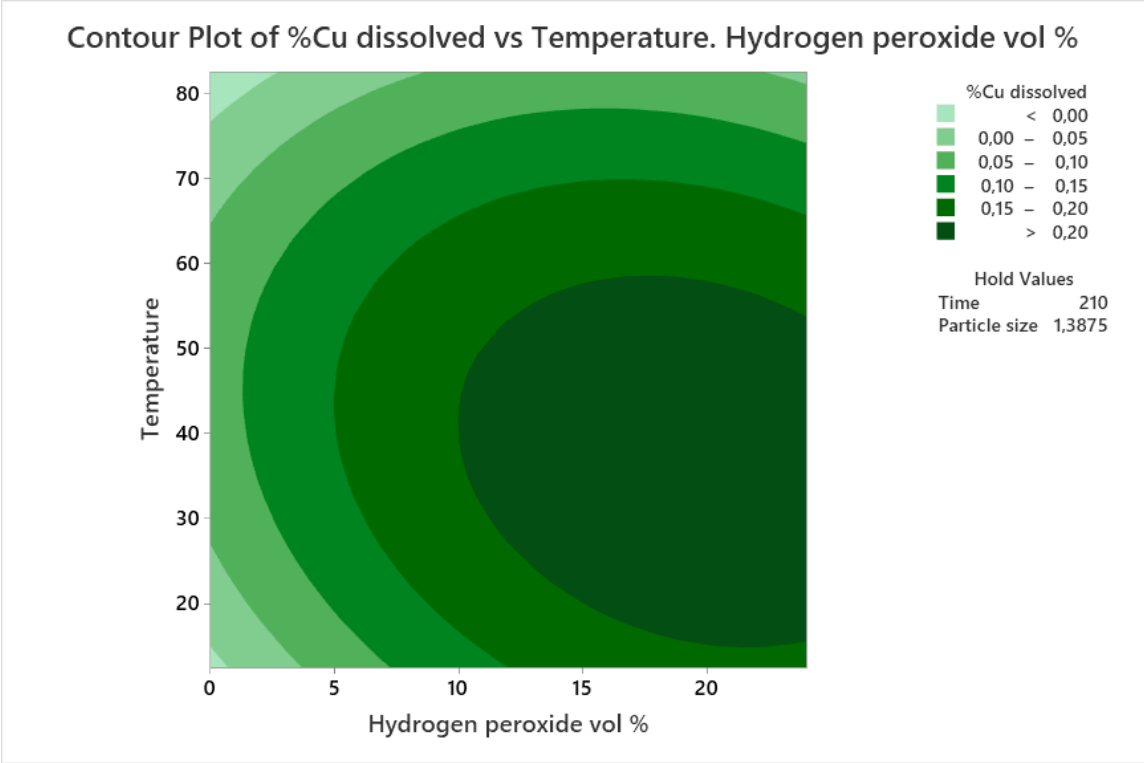


Figure 4.7: Percentage copper recovered

From figure 4.7 above, the dark green zone shows a range of which greater than 20% of copper can be dissolved (recovered) while time and particle size are kept constant at 210 minutes and 1.3875 microns respectively.

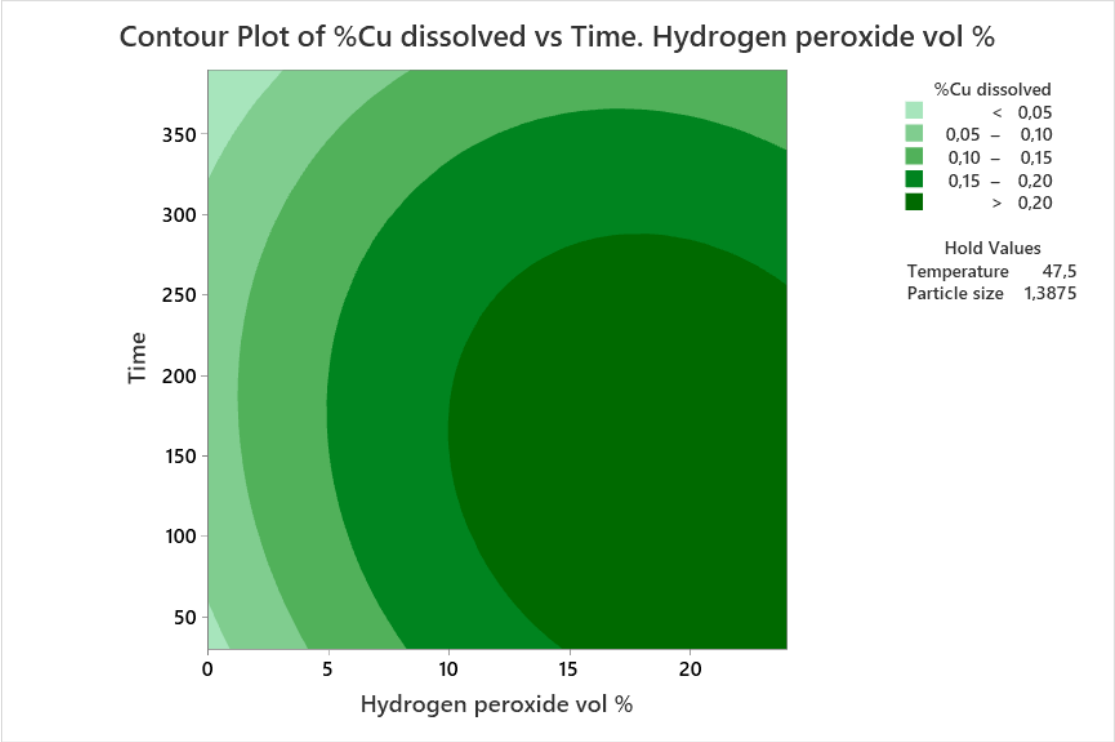


Figure 4.8: Percentage copper recovered

From figure 4.8 above, the dark green zone shows a range of which greater than 20% of copper can be dissolved (recovered) while temperature and particle size are kept constant at 47.5°C and 1.3875 microns respectively.

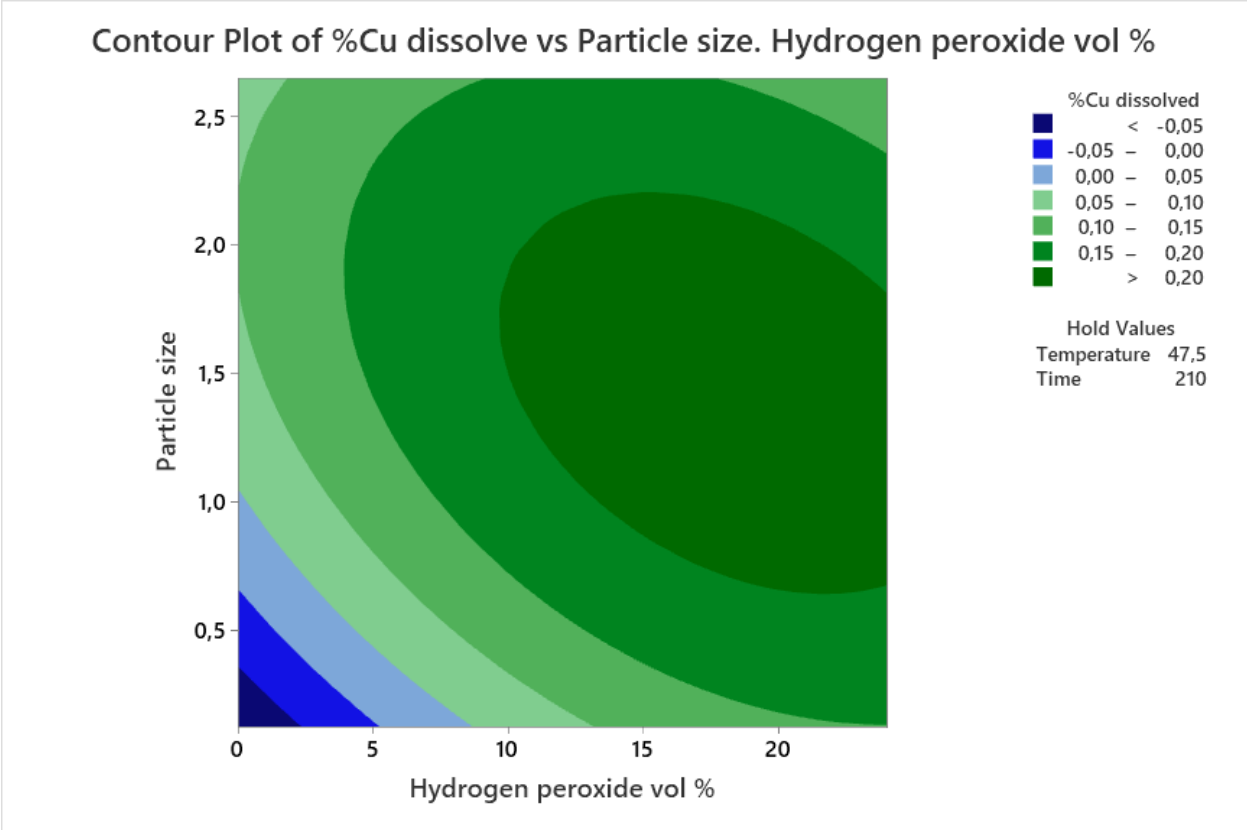


Figure 4.9: Percentage copper recovered

From figure 4.9 above, the dark green zone shows a range of which greater than 20% of copper can be dissolved (recovered) while temperature, time, and particle size are kept constant at 47.5°C and 210 minutes respectively.

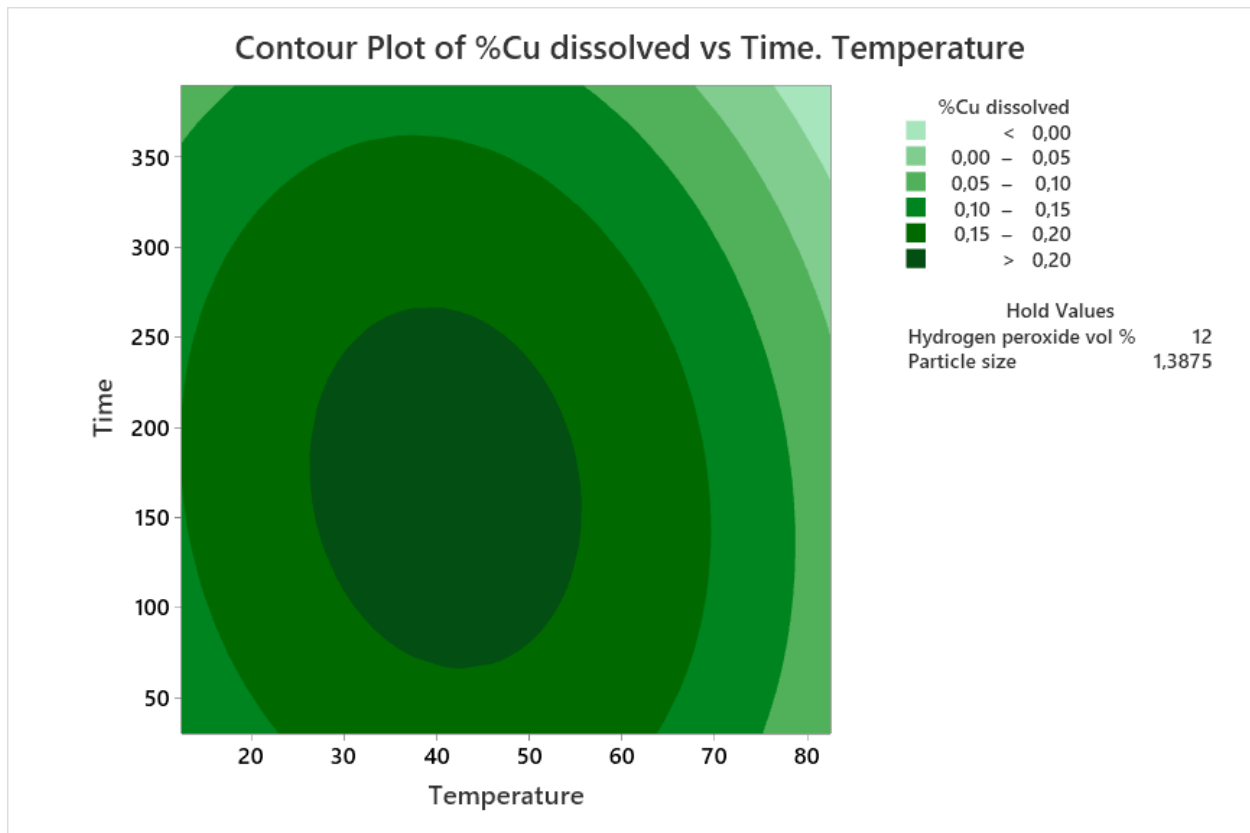


Figure 4.10: Percentage copper recovered

From figure 4.10, the dark green zone shows a range of which greater than 20% of copper can be dissolved (recovered) while hydrogen peroxide volume % and particle size are kept constant at 12% and 1.3875 microns respectively.

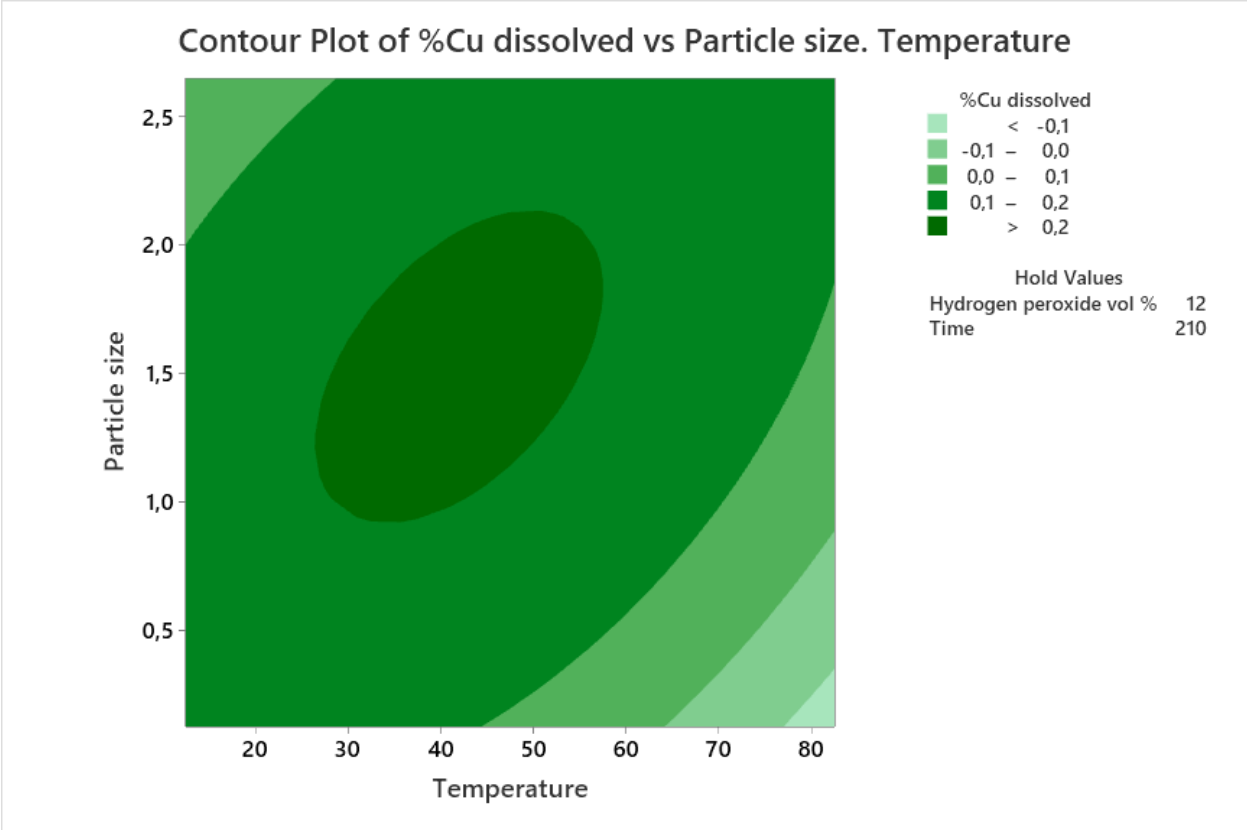


Figure 4.11: Percentage copper recovered

From figure 4.11, the dark green zone shows a range of which greater than 20% of copper can be dissolved (recovered) while hydrogen peroxide volume % and time are kept constant at 12% and 210 minutes respectively.

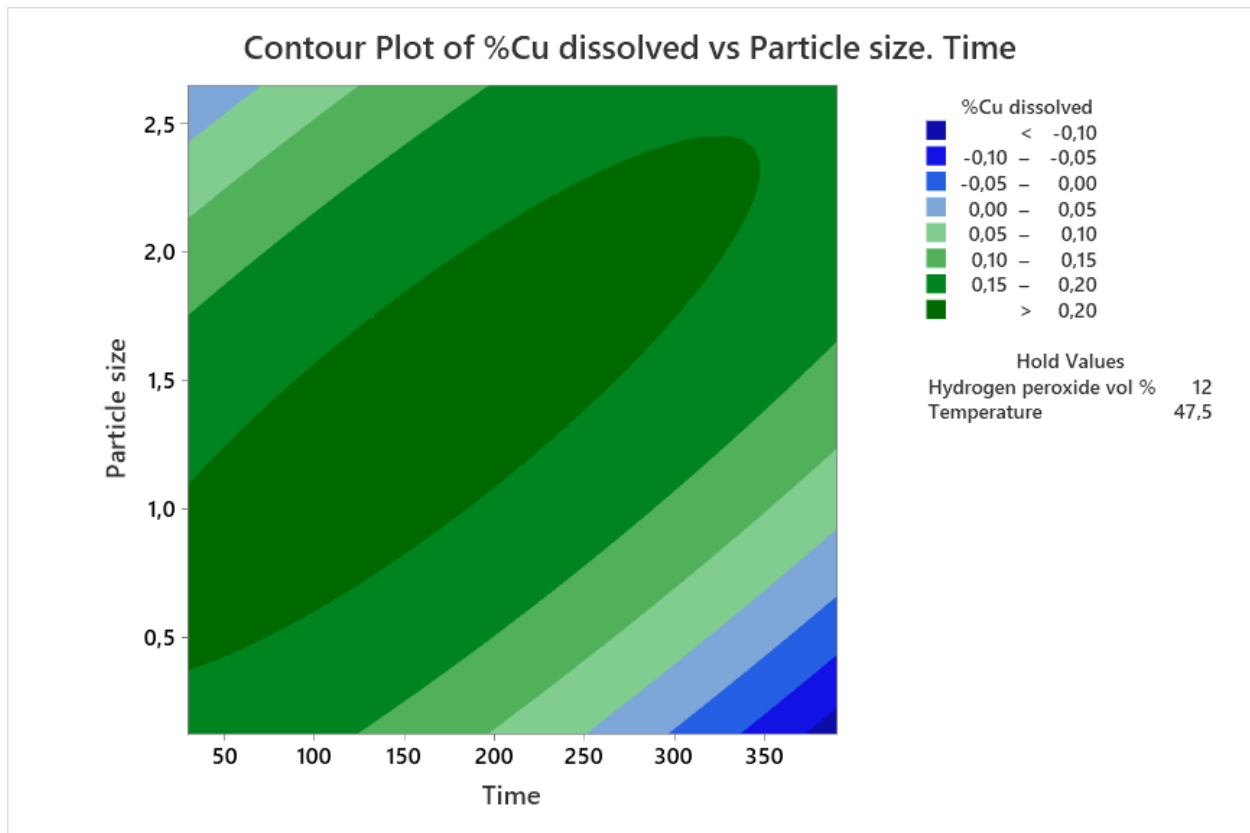


Figure 4.12: Percentage copper recovered

From figure 4.12, the dark green zone shows a range of which greater than 20% of copper can be dissolved (recovered) while hydrogen peroxide volume% and temperature are kept constant at 12% and 47.5°C respectively.

The surface plots show the same set of results as the contour plots and they are found in the appendix section of the paper.

Apart from the contour and surface plots, we also have the optimization plots which give the optimum values of the parameters such that the highest percentage of copper is recovered.

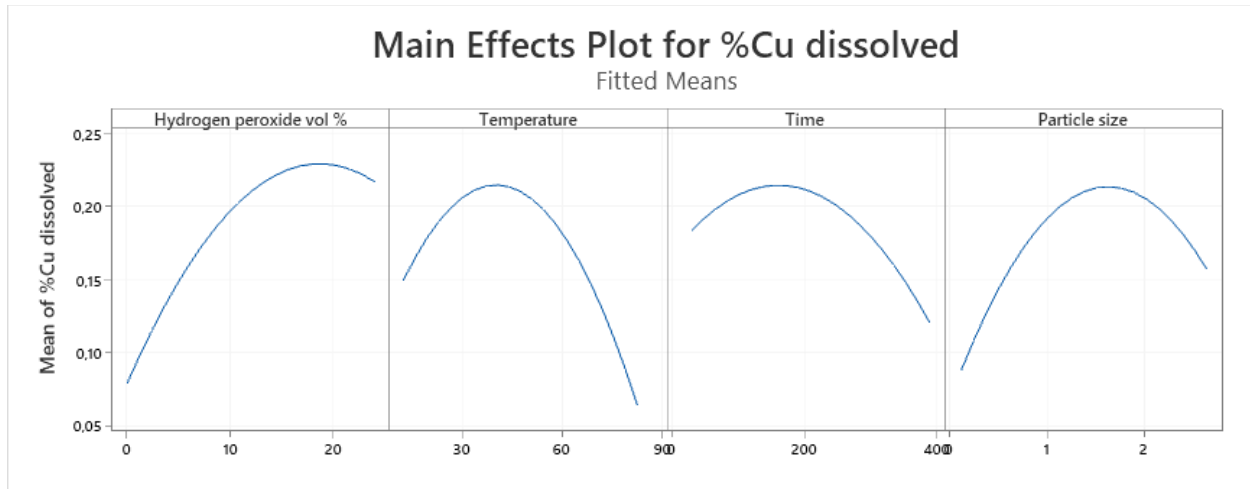


Figure 4.13: Main effects plot for % Copper dissolved

The main effects plot above show the optimal conditions for each parameter to attain maximum copper recovery. These optimal values correspond with the holding values of the same parameters on the contour plots. For hydrogen peroxide volume %, temperature, time, and particle size, these optimal values are 12%, 45°C, 210 minutes, and 1.375 microns.

Factorial plots show the interaction and relationship amongst parameters.

CHAPTER 5

5.1 CONCLUSIONS

When this study was being carried out, the objectives were to investigate the type of material being studied by performing a sieve analysis. It would involve the PCBs being depopulated and being crushed by a Zerma crusher. Also, investigate the effects of different leaching agents (nitric acid and sulphuric acid with hydrogen peroxide) and investigate the effect of other leaching process conditions such as leaching time, particle size, hydrogen peroxide volume percent, and temperature. Lastly, to investigate the characterization of e-waste by a TGA. The conclusions below directly address the objectives of the study.

Nitric acid was found to be a more effective leaching agent than sulphuric acid with hydrogen peroxide. And reasons, why it was not explored further are explained in the results and analysis section (Chapter 4). The sieve analysis suggests that the sample is of coarse material and was found not to be well represented. TGA analysis of unreacted PCBs of different size classes found that the ash content within the PCBs increased with an increase in size class. From the TGA analysis, unreacted PCBs have a lower moisture content than the reacted PCBs. The opposite is true in terms of ash content. Most copper recovery (0.2416g) was found under run 2 conditions (hydrogen peroxide at maximum, temperature, time and particle size all at minimum). Hydrogen peroxide volume percent is the most influential parameter for the recovery of copper. The contour plots show regions where greater than 20% of copper can be recovered from a PCB sample weighing 3.125g. Two parameters are plotted against one another while the other two are kept constant. The main effects plot shows optimal conditions for each parameter to attain max copper recovery. For hydrogen peroxide volume %, temperature, time, and particle size, these optimal values are 12%, 45°C, 210 minutes, and 1.375 microns.

The potential industrial applications of this study are limited as there are a few companies capable of recycling and reuse of the waste they manage. The main reason is the investments companies need to enable the facilities that they already have to carry out the extraction of valuable minerals and also that the recovery processes vary greatly for different minerals (e-waste is vastly heterogeneous and when companies recycle it, their technologies are limited to targeting just one mineral within the e-waste). However, the main stakeholders in e-waste (government and electronic equipment producers) are actively concerned with managing e-waste and have a huge role to play in ensuring the manifestation of the e-waste formal sector.

5.2 RECOMMENDATIONS

For further studies on E-waste (PCB) Processing, it is recommended that the PCB should be obtained from the same model of devices. This is because the mineral content in the PCBs varies slightly from the different makers. I was not able to obtain PCBs from the same model of devices because of availability. The chemical engineering school had a limited amount of waste PCBs and thus others had to be sourced from different departments and it was hard to obtain just one model from the various departments. Also, I would recommend that during the physical separation stages (depopulating of PCBs); an alternative to a soldering gun should be used to remove the pins because the soldering gun removes not only the thin pins but a substantial amount of minerals (tin) as well. I could not implement this recommendation because there was no other alternative to depopulating the PCBs with the equipment I had. And lastly, for better control over the temperature during the experiments, a water bath that is closable is recommended. This recommendation was not implemented because such equipment was not available at the school.

REFERENCES

- A. Finlay, D. L. (2008). E-waste assessment South Africa. *e-Waste Assessment South Africa*. November, 24-53.
- Abdelbasir, S. M., Hassan, S. S. M., Kamel, A. H., & El-Nasr, R. S. (2018). Status of electronic waste recycling techniques: a review. *Environmental Science and Pollution Research*, 25(17), 16533–16547. <https://doi.org/10.1007/s11356-018-2136-6>
- Africa, S. S. (2018). *Only 10% of Waste Recycled in SA*. www.statssa.gov.za/?p=11527, 12th May 2019
- Ari, V. (2016). A Review of Technology of Metal Recovery From Electronic Waste. In *A Review of Technology of Metal Recovery From Electronic Waste*, 121–158.
- Associates, P. C. (2006). Electronic waste recovery study. *Electronic Waste Recovery Study*, March, 4-13
- Bizzo, W. A., Figueiredo, R. A., & De Andrade, V. F. (2014). Characterization of printed circuit boards for metal and energy recovery after milling and mechanical separation. *Materials*, 7(6), 4555–4566. <https://doi.org/10.3390/ma7064555>
- Crashers, M. (2011). *Electronic e-waste disposal facts*. www.moneycrashers.com/electronic-e-waste-recycling-didposal-facts/, 7th June 2019
- Deveci, H., & Yazici, E. Y. (2018). Physical separation and hydrometallurgy processes for treatment of WEEE. *Physical Separation and Hydrometallurgy Processes for Treatment of WEEE*, 1-15
- Diaz, L. A., Lister, T. E., Parkman, J. A., & Clark, G. G. (2016). Comprehensive process for the recovery of value and critical materials from electronic waste. *Journal of Cleaner Production*, 125, 236–244. <https://doi.org/10.1016/j.jclepro.2016.03.061>
- Gentina, J. C., & Acevedo, F. (2013). Application of bioleaching to copper mining in Chile. *Electronic Journal of Biotechnology*, 16(3), 31-55. <https://doi.org/10.2225/vol16-issue3-fulltext-12>
- Ilankoon, I. M. S. K., Ghorbani, Y., Nan, M., Herath, G., & Moyo, T. (2018). E-waste in the international context – A review of trade flows , regulations , hazards , waste management strategies and technologies for value recovery. *Waste Management*, 82, 258–275. <https://doi.org/10.1016/j.wasman.2018.10.018>
- Jha, Manis K., Lee, J. C., Kumari, A., Choubey, P. K., Kumar, V., & Jeong, J. (2011). Pressure leaching of metals from waste printed circuit boards using sulfuric acid. *Jom*, 63(8), 29–32.

<https://doi.org/10.1007/s11837-011-0133-z>

Jha, Manis Kumar, Kumar, V., Lee, J., & Resources, M. (2010). Leaching studies of tin from the solder of waste PCBs. *Leaching studies of tin from the solder of waste PCBs*, 1-15.

Kumar, M., Lee, J. C., Kim, M. S., Jeong, J., & Yoo, K. (2014). Leaching of metals from waste printed circuit boards (WPCBs) using sulfuric and nitric acids. *Environmental Engineering and Management Journal*, 13(10), 2601–2607. <https://doi.org/10.30638/eemj.2014.290>

Kwonpongsagoon, S. (2017). Environmental Impacts of Recycled Nonmetallic Fraction From Waste Printed Circuit Board. *International Journal of GEOMATE*, 51-72.
<https://doi.org/10.21660/2017.34.2584>

Lee, J., Kim, S., Kim, B., & Lee, J. (2018). Effect of Mechanical Activation on the Kinetics of Copper Leaching from Copper Sulfide (CuS). *Metals*, 8(3), 150-151. <https://doi.org/10.3390/met8030150>

Maryam Ghodrat, M. Akbar Rhamdhani, Geoffery Brooks, Syed Masood, G. C. (2016). Techno Economic Analysis of Electronic Waste Processing Through Black Copper Route. *Journal of Cleaner Production*, 126-133.

Media, C. (2018, October). *E-waste recycling sector still underdeveloped in South Africa*. www.engineeringnews.co.za/article/e-waste-recycling-sector-still-underdeveloped-in-South-Africa-2018-10-17, 21st February 2020.

Mmereki, D., Li, B., & Li, W. (2015). Waste electrical and electronic equipment management in Botswana : Prospects and challenges Waste electrical and electronic equipment management in Botswana : Prospects and challenges. *Journal of the Air & Waste Management Association*, 65(1), 11–26. <https://doi.org/10.1080/10962247.2014.892544>

Montgomery, D. C. (2017). Design and Analysis of Experiments Ninth Edition. *Design and Analysis of Experiments Ninth Edition*, 38-157. <https://lccn.loc.gov/2017002355>

Muzayanha, S. U., Yudha, C. S., Hasanah, L. M., & Tungga, L. (2020). Comparative study of various kinetic models on leaching of NCA cathode material. *Comparative Study of Various Kinetic Models on Leaching of NCA Cathode Material*. 20(6), 1291–1300. <https://doi.org/10.22146/ijc.49412>

Ogunniyi, I. O., Vermaak, M. K. G., & Groot, D. R. (2009). Chemical composition and liberation characterization of printed circuit board comminution fines for beneficiation investigations. *Waste Management*, 29(7), 2140–2146. <https://doi.org/10.1016/j.wasman.2009.03.004>

- Pietrelli, L., Francolini, I., Piozzi, A., & Vocciante, M. (2018). Metals recovery from printed circuit boards: The pursuit of environmental and economic sustainability. *Chemical Engineering Transactions*, 70(September), 271–276. <https://doi.org/10.3303/CET1870046>
- Popescu, I., Egedy, A., & Fogarasi, S. (2014). Kinetic modelling of copper leaching process using FeCl₃ for recycling waste electrical and electronic equipments. *Kinetic Modelling Of Copper Leaching Process Using FeCl₃ For Recycling Waste Electrical And Electronic Equipments*, 2-14.
- Juan, J., & Xu, Z. (2016). Constructing environment-friendly return road of metals from e-waste : Combination of physical separation technologies. *Renewable and Sustainable Energy Reviews*, 54, 745–760. <https://doi.org/10.1016/j.rser.2015.10.114>
- S. Charterjee, K. K. (2009). Effective Electronic Waste Management and Recycling Progress Involving Formal and non-formal Sectors. *International Journal of Physical Sciences*, 132-147.
- Sedlakova-kadukova, J. (2013). Influence of bacterial culture to copper bioleaching. *Influence of Bacterial Culture to Copper Bioleaching*. 1-14.
- Sethurajan, M., van Hullebusch, E. D., Fontana, D., Akcil, A., Deveci, H., Batinic, B., Leal, J. P., Gasche, T. A., Ali Kucuker, M., Kuchta, K., Neto, I. F. F., Soares, H. M. V. M., & Chmielarz, A. (2019). Recent advances on hydrometallurgical recovery of critical and precious elements from end of life electronic wastes - a review. *Critical Reviews in Environmental Science and Technology*, 49(3), 212–275. <https://doi.org/10.1080/10643389.2018.1540760>
- Tatarants, M., Yousef, S., Sidaraviciute, R., Denafas, G., & Bendikiene, R. (2017). Characterization of waste printed circuit boards recycled using a dissolution approach and ultrasonic treatment at low temperatures. *RSC Advances*, 7(60), 37729–37738. <https://doi.org/10.1039/c7ra07034a>
- Tuncuk, A., Stazi, V., Akcil, A., Yazici, E. Y., & Deveci, H. (2012). Aqueous metal recovery techniques from e-scrap: Hydrometallurgy in recycling. *Minerals Engineering*, 25(1), 28–37. <https://doi.org/10.1016/j.mineng.2011.09.019>
- Zeng, X., Zheng, L., Xie, H., Lu, B., Xia, K., Chao, K., Li, W., Yang, J., Lin, S., & Li, J. (2012). Current Status and Future Perspective of Waste Printed Circuit Boards Recycling. *Procedia Environmental Sciences*, 16, 590–597. <https://doi.org/10.1016/j.proenv.2012.10.081>
- Zhang, K., Schnoor, J. L., & Zeng, E. Y. (2012). E - Waste Recycling: Where Does It Go from Here? *Environmental Science and Technology*, 46, 10861–10867. <https://doi.org/10.1021/es303166s>

Zhang, L., & Xu, Z. (2016). A review of current progress of recycling technologies for metals from waste electrical and electronic equipment. *Journal of Cleaner Production*, (127), 19–36.
<https://doi.org/10.1016/j.jclepro.2016.04.004>

Zhang, L., & Xu, Z. (2016). A review of current progress of recycling technologies for metals from waste electrical and electronic equipment. In *Journal of Cleaner Production* (127,) 19–36.
<https://doi.org/10.1016/j.jclepro.2016.04.004>

Zhang, Y., Liu, S., Xie, H., Zeng, X., & Li, J. (2012). Current Status on Leaching Precious Metals from Waste Printed Circuit Boards. *Procedia Environmental Sciences*, 16, 560–568.
<https://doi.org/10.1016/j.proenv.2012.10.077>

APPENDICES

A

Section A of the appendix section contains results from the analysis of PCBs of different size classes that was done using the TGA prior to hydrometallurgical processing.

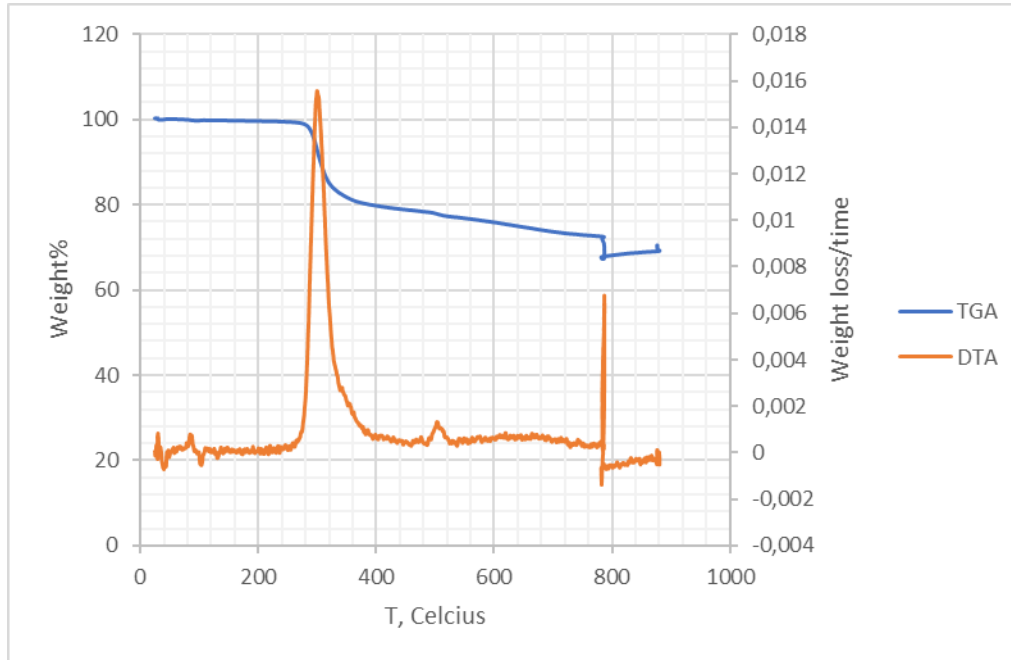


Figure A.1: Thermogravimetric analysis curve of unreacted PCBs of size class -850+500µm

Figure A.1 is a TGA curve of unreacted PCBs of size class -850+500µm.

The calculations of different contents within the PCB are calculated using the equations outlined above. Using the graph and the equations above, moisture content, volatile matter content, combustible material content and ash content are calculated.

$$W = 18.59225\text{mg}$$

$$R = 14.97544\text{mg}$$

$$S = 14.33932\text{mg}$$

$$T = 12.81431\text{mg}$$

With the constants above defined, the amounts of different fractions can be determined.

$$M = \frac{18.59225 - 14.97544}{18.59225} \times 100 = 19.45\%$$

$$O = \frac{14.97544 - 14.33932}{18.59225} \times 100 = 3.42\%$$

$$C = \frac{14.33932 - 12.81431}{18.59225} \times 100 = 8.20\%$$

$$A = \frac{12.81431}{18.59225} \times 100 = 68.92\%$$

From figure A.1, it is seen that there are two identifiable peaks, and both the decomposition stages occur in an inert environment. At 505⁰C, there is also a decomposition peak recorded, although it was small. All the peaks represent the decomposition of organic matter and the maximum decomposition temperature for the large peaks are 301⁰C and 786⁰C respectively. The decomposition temperature of 505⁰C falls within the range of temperature responsible for the decomposition of lead (400-600⁰C). The base material of PCBs is glass re-enforced epoxy and it decomposes at 300⁰C.

From the time the experiment to around 150⁰C, The DTG curve is unsettled, and this is due to the burning off of volatiles and evaporation of water. From the weight % curve, the mass loss is 31.1%. This means the residue content of the PCB is 68.92% and within the residue is where inorganic compounds are found.

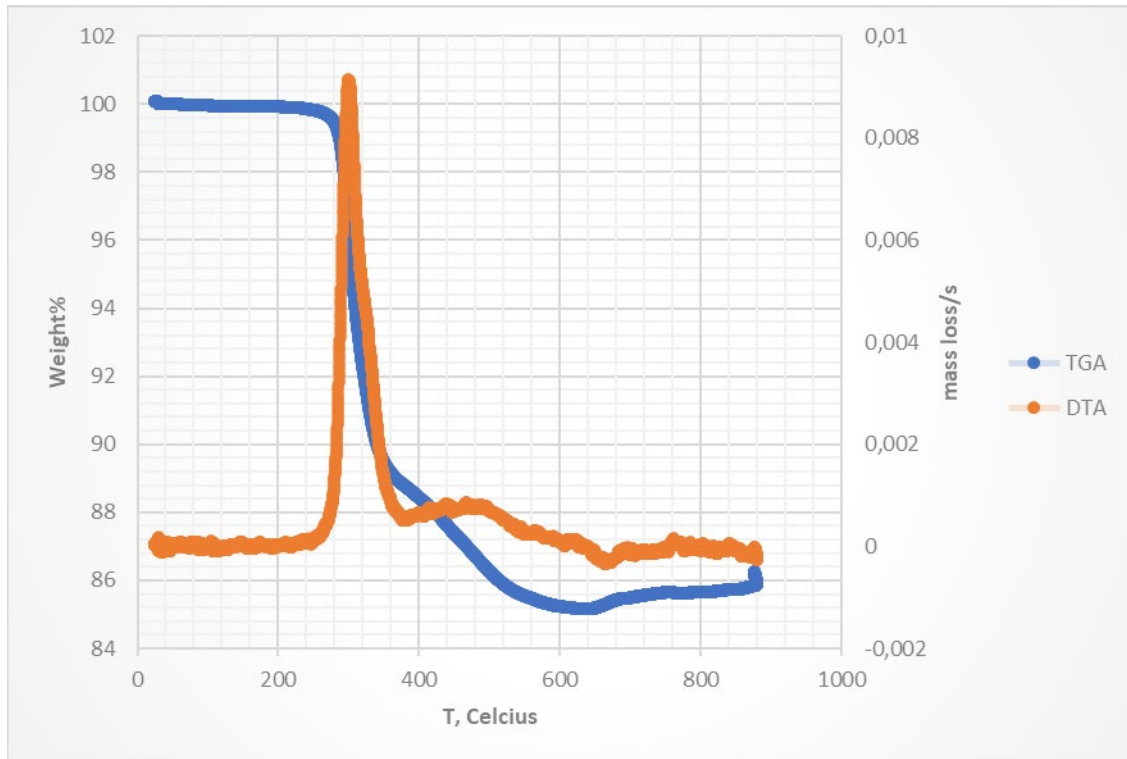


Figure A.2: TGA curve of unreacted PCBs of size class -1400+1000µm

The graph above is a TGA curve of unreacted PCBs of size class -1400+1000µm.

The calculations of different contents within the PCB are calculated using the equations outlined above. Using the graph and the equations above, moisture content, volatile matter content, combustible material content and ash content are calculated.

$$W = 20.6433\text{mg}$$

$$R = 18.31956\text{mg}$$

$$S = 17.76976\text{mg}$$

$$T = 17.69129\text{mg}$$

With the constants above defined, the amounts of different material can be determined.

$$M = \frac{20.6433 - 18.31956}{20.64336} \times 100 = 11.26\%$$

$$O = \frac{18.31956 - 17.76976}{20.64336} \times 100 = 2.66\%$$

$$C = \frac{17.76976 - 17.69129}{20.64336} \times 100 = 0.38\%$$

$$A = \frac{17.69129}{20.6433} \times 100 = 85.7\%$$

From figure A.2, there is one identifiable peak, and the decomposition stage occurs in an inert environment. The peak temperature of the decomposition is at 301⁰C. At 407⁰C, there is also a decomposition stage that is starting. This decomposition has a small peak at 477⁰C. All the peaks represent the decomposition of organic matter. The decomposition temperature of 407⁰C falls within the range of temperature responsible for the decomposition of lead (400-600⁰C). The base material of PCBs is glass re-enforced epoxy and it decomposes at 300⁰C.

From the time the experiment to around 150⁰C, The DTG curve is unsettled and this is due to the burning off volatiles and evaporation of water. From the weight % curve, the mass loss is 14.3%. This means the residue content of the PCB is 85.7% and within the residue is where inorganic compounds are found.

Performing a TGA analysis of the sample before leaching can be able to tell which size class has more metal presence. Size class with most metal content will experience minimal mass loss due to having less volatile matter (Bizzo et al., 2014).

B

Section B of the appendix section has results of the hydrometallurgical processing of e-waste, also results from Minitab.

An example of calculating the metal fraction using the equations described is in the section 4.3.

Using equation (4.7);

$$\text{old concentration} = 500 \times 25.4766667 = 12738.333\text{ppm}$$

Using equation (4.8);

$$m = \frac{12738.333}{1000000} \times 50 = 0.639\text{g}$$

Using equation (4.9);

$$\text{metal fraction} = \frac{0.639g}{3.125g} = 0.204$$

The research focused on the recovery of copper, but there were other base metals that were also recovered along with copper even though their recovery was in trace amounts. These metals are nickel and iron, tin could have also been recovered but the use of a soldering gun for depopulating the PCB boards got rid of tin in the PCB boards. The appendix section will contain results of the metals that were recovered in trace amounts and any other results that were not included in the main body of the research.

Table B.1 shows the results of the leached iron for different runs under nitric acid conditions.

B.1 HYDROMETALLURGICAL PROCESSING: Iron (Nitric Acid conditions)

Table B.1: Leached iron for different runs under nitric acid conditions

Run	Average reported concentration (mg/L)	Old concentration (ppm)	Amount of metal (g) (50ml was used for experiments)	Metal fraction within the PCB (3,125g)
1	0.4140	207	0.0104	0.0033
2	0.1357	67.8333	0.0034	0.0011
3	0.3643	182.1667	0.0091	0.0029
4	0.0393	19.6667	0.0010	0.0003
5	0.0387	19.3333	0.0010	0.0003
6	0.081	40.5	0.0020	0.0006
7	0.0563	28.1667	0.0014	0.0004
8	0.0263	13.1667	0.0006	0.0002
9	0.0586	29.3333	0.0014	0.0004
10	0.59	295	0.0148	0.0047
11	0.0357	17.8333	0.0009	0.0003
12	0.022	11	0.0006	0.0002
13	0.014	7	0.0004	0.0001
14	0.022	11	0.0006	0.0002
15	0.0177	8.8333	0.0004	0.0001
16	0.0233	11.6667	0.0006	0.0002

The contents of table B.1 above are more clearly expressed by the graph below

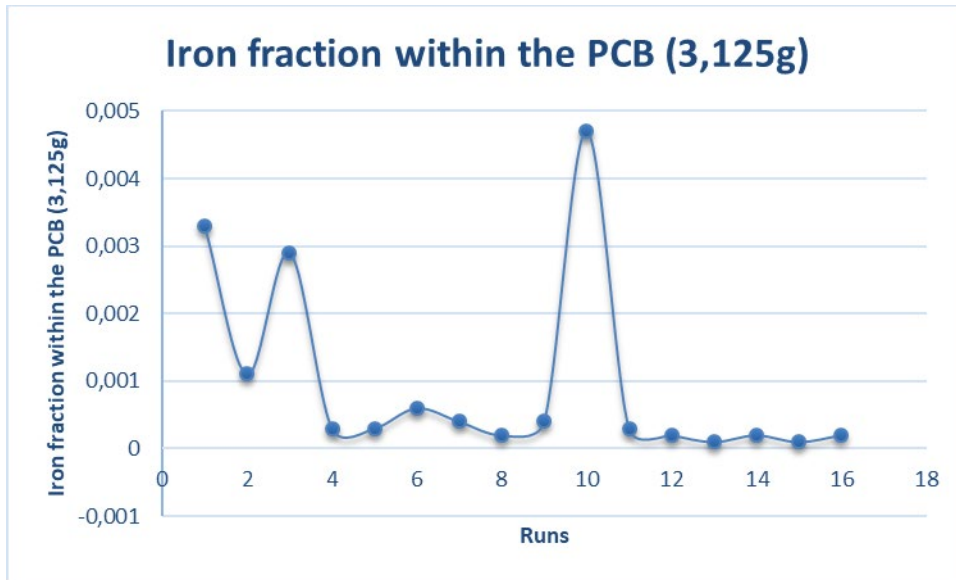


Figure B.1: Iron fraction within Printed Circuit Boards (3,125g)

From the iron fraction graph above, it is evident that most of the iron was recovered in run 10 where 0.0047 copper fraction was dissolved in solution.

B.2 HYDROMETALLURGICAL PROCESSING: Nickel (Nitric acid conditions)

Table B.2 shows the results of the leached nickel for different runs under nitric acid conditions.

Table B.2: Leached nickel for different runs under nitric acid conditions.

Run	Average reported concentration (mg/L)	Old concentration (ppm)	Amount of metal (g) (50ml was used for experiments)	Metal fraction within the PCB (3,125g)
1	0,0827	41.3333	0.0020	0.0006
2	0.0403	20.1667	0.0010	0.0003
3	0.0257	12.8333	0.0006	0.0002
4	0.0243	12.1667	0.0006	0.0002
5	0.0263	13.1667	0.0007	0.0002
6	0.0573	28.6667	0.0014	0.0004
7	0.041	20.5	0.010	0.0003
8	0.0273	13.6667	0.0007	0.0002

9	0.052	26	0.0013	0.0004
10	0.0427	21.3333	0.0010	0.0003
11	0.0347	17.3333	0.0009	0.0003
12	0.0197	9.8333	0.0005	0.0002
13	0.0177	8.8333	0.0004	0.0001
14	0.0193	9.6667	0.0005	0.0002
15	0.0117	5.8333	0.0003	0.00009
16	0.021	10.5	0.0005	0.0002

The contents of the table above are more clearly expressed by the graph below

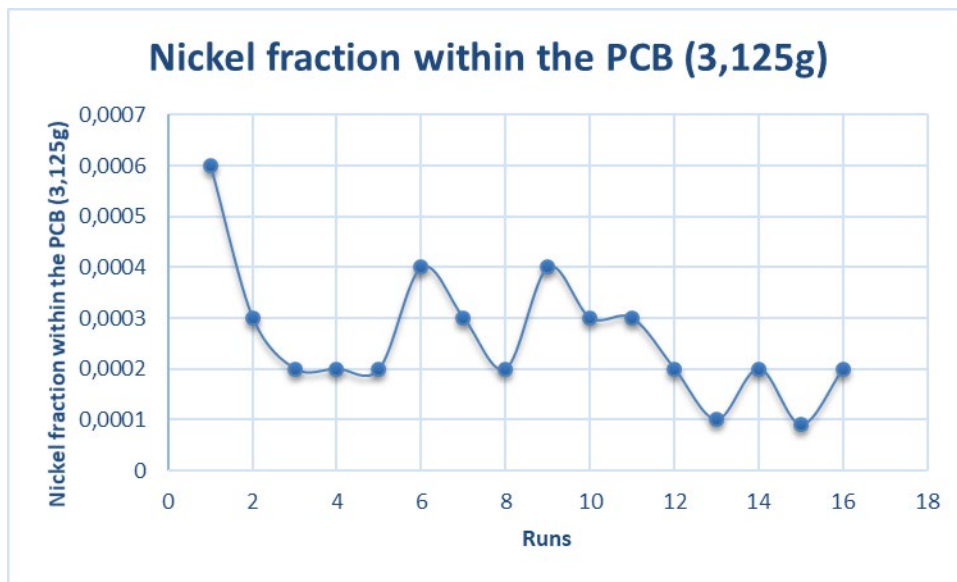


Figure B.2: Leached nickel for different runs under nitric acid conditions.

From the nickel fraction above, it is evident that most of the nickel was recovered in run 1 where 0.0006 nickel fraction was dissolved in solution.

For nickel, most recovery of the metal is in run 1 under the following conditions; time = 8hours, temperature = 80°C, nitric acid concentration = 4M and particle size = 2mm. Maximum iron is recovered in tun 10, its conditions are; time = 2hours, temperature = 80°C, nitric acid concentration = 4M and particle size = 6mm.

B.3 ANALYSIS IN MINITAB (Nitric acid leaching conditions)

The results were also analysed using Minitab:

B.3.1 Iron Yield

Table B.3: Coded Coefficients

Term	Effect	Coef	SE	
			Coef	T-Value
Constant		0,000968	*	*
Time	0,000376	0,000188	*	*
Temperature	0,001377	0,000688	*	*
Particle Size	-0,000056	-0,000028	*	*
Nitric Acid Concentration	0,000772	0,000386	*	*
Time*Temperature	0,000125	0,000063	*	*
Time*Particle Size	-0,001126	-0,000563	*	*
Time*Nitric Acid Concentration	-0,000407	-0,000203	*	*
Temperature*Particle Size	-0,000108	-0,000054	*	*
Temperature*Nitric Acid Concentration	0,000708	0,000354	*	*
Particle Size*Nitric Acid Concentration	0,000663	0,000331	*	*
Time*Temperature*Particle Size	-0,001123	-0,000562	*	*
Time*Temperature*Nitric Acid Concentration	-0,000490	-0,000245	*	*
Time*Particle Size*Nitric Acid Concentration	-0,000425	-0,000212	*	*
Temperature*Particle Size*Nitric Acid Concentration	0,000514	0,000257	*	*
Time*Temperature*Particle Size*Nitric Acid Concentration	-0,000565	-0,000283	*	*
Term	P-Value	VIF		
Constant	*			
Time	*	1,00		
Temperature	*	1,00		
Particle Size	*	1,00		
Nitric Acid Concentration	*	1,00		
Time*Temperature	*	1,00		
Time*Particle Size	*	1,00		
Time*Nitric Acid Concentration	*	1,00		
Temperature*Particle Size	*	1,00		
Temperature*Nitric Acid Concentration	*	1,00		
Particle Size*Nitric Acid Concentration	*	1,00		
Time*Temperature*Particle Size	*	1,00		
Time*Temperature*Nitric Acid Concentration	*	1,00		
Time*Particle Size*Nitric Acid Concentration	*	1,00		
Temperature*Particle Size*Nitric Acid Concentration	*	1,00		
Time*Temperature*Particle Size*Nitric Acid Concentration	*	1,00		

Table B.4: Regression Equation in Uncoded Units

$$\begin{aligned}
 \text{Yield-Fe} = & -0,000041 && - 0,000100 \text{ Time} && - 0,000001 \text{ Temperature} \\
 & + 0,000200 \text{ Particle Size} \\
 & + 0,000451 \text{ Nitric Acid Concentration} && + 0,000008 \text{ Time*Temperature} \\
 & - 0,000006 \text{ Time*Particle Size} && - 0,000086 \text{ Time*Nitric Acid Concentration} \\
 & - 0,000006 \text{ Temperature*Particle Size} \\
 & - 0,000017 \text{ Temperature*Nitric Acid Concentration} \\
 & - 0,000235 \text{ Particle Size*Nitric Acid Concentration} \\
 & - 0,000001 \text{ Time*Temperature*Particle Size} \\
 & + 0,000003 \text{ Time*Temperature*Nitric Acid Concentration} \\
 & + 0,000036 \text{ Time*Particle Size*Nitric Acid Concentration} \\
 & + 0,000009 \text{ Temperature*Particle Size*Nitric Acid Concentration} \\
 & - 0,000001 \text{ Time*Temperature*Particle Size*Nitric Acid Concentration}
 \end{aligned}$$

The iron model above shows the significance of each parameter and the significance of interaction between parameters towards the copper yield. In the model, there are positive and negative coefficients associated with the parameters.

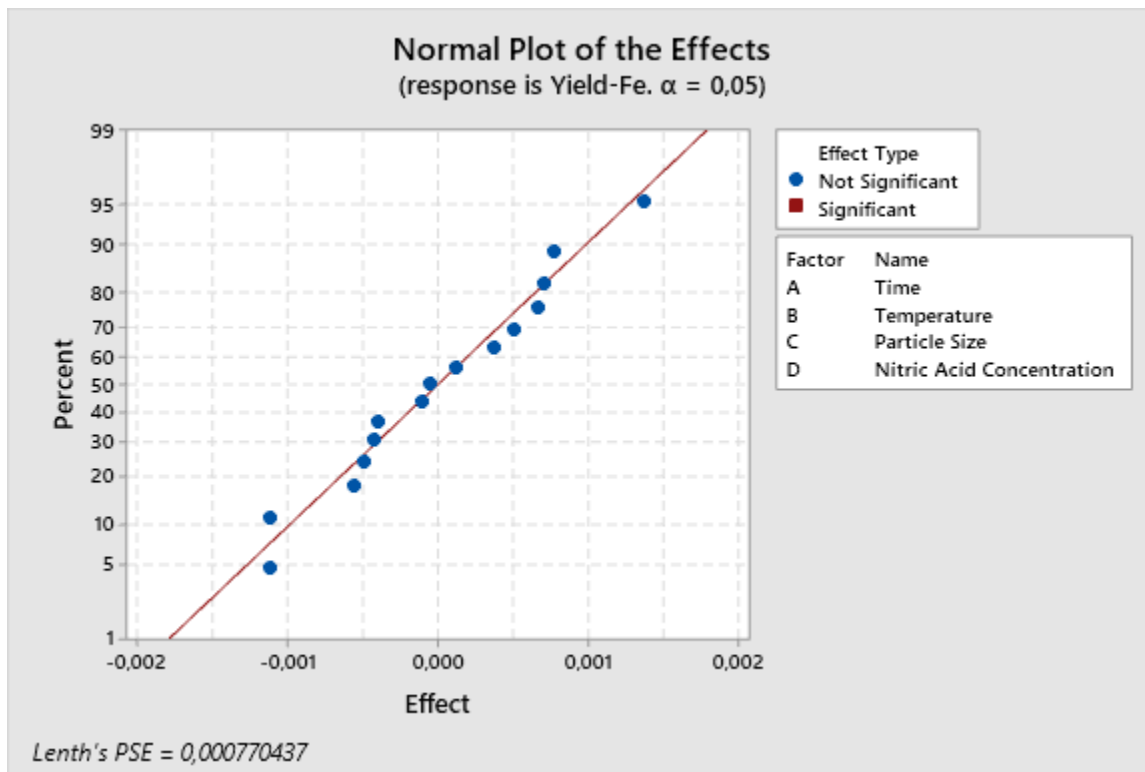


Figure B.3: Normal Plot effects

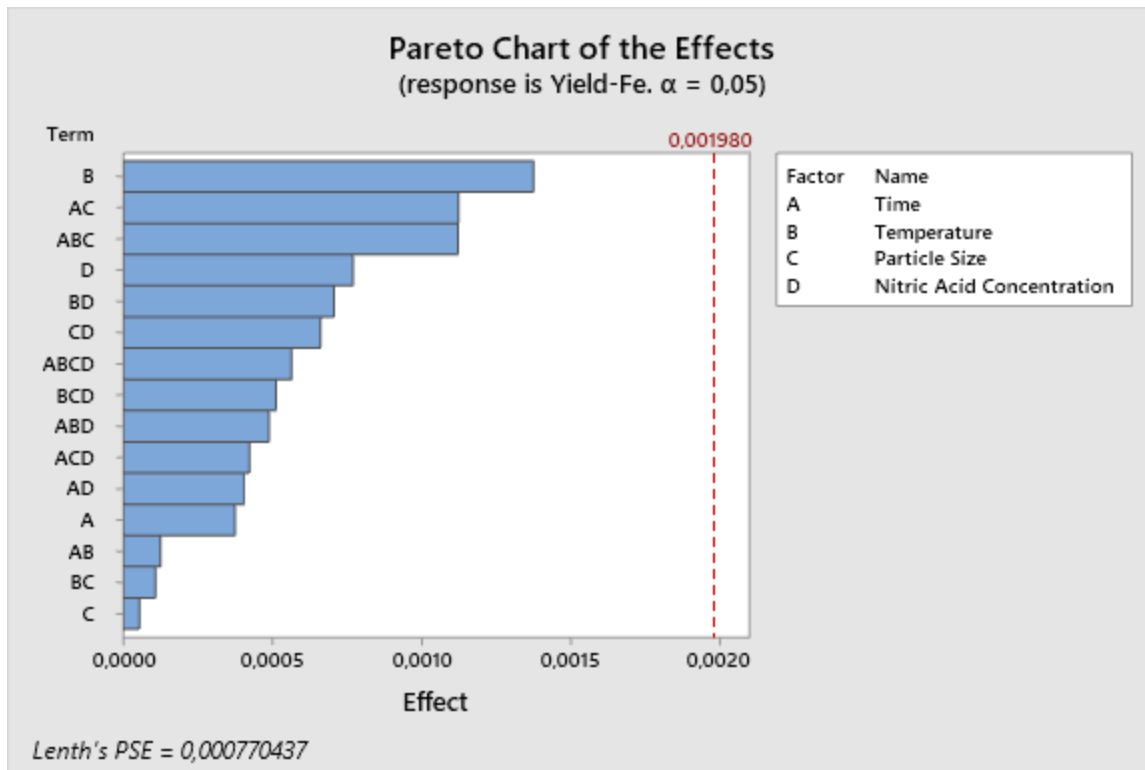


Figure B.4: Pareto Chart of the effects

The Pareto chart shown in figure B.4 above shows that in the recovery of iron, none of the parameters being investigated are significant. Same applies to their interactions. None of the parameters and their interaction go passed the critical value line.

B.3.2 Nickle Yield

Table B.5: Coded Coefficients

Term	Effect	Coef	SE	
			Coef	T-Value
Constant		0,000272	*	*
Time	0,000106	0,000053	*	*
Temperature	0,000101	0,000051	*	*
Particle Size	-0,000040	-0,000020	*	*
Nitric Acid Concentration	0,000132	0,000066	*	*
Time*Temperature	-0,000059	-0,000030	*	*
Time*Particle Size	-0,000012	-0,000006	*	*
Time*Nitric Acid Concentration	0,000045	0,000022	*	*
Temperature*Particle Size	-0,000097	-0,000049	*	*
Temperature*Nitric Acid Concentration	0,000093	0,000046	*	*
Particle Size*Nitric Acid Concentration	0,000003	0,000001	*	*
Time*Temperature*Particle Size	-0,000024	-0,000012	*	*
Time*Temperature*Nitric Acid Concentration	0,000023	0,000011	*	*
Time*Particle Size*Nitric Acid Concentration	0,000005	0,000002	*	*
Temperature*Particle Size*Nitric Acid Concentration	-0,000071	-0,000036	*	*
Time*Temperature*Particle Size*Nitric Acid Concentration	-0,000100	-0,000050	*	*
Term	P-Value	VIF		
Constant	*			
Time	*	1,00		
Temperature	*	1,00		
Particle Size	*	1,00		
Nitric Acid Concentration	*	1,00		
Time*Temperature	*	1,00		
Time*Particle Size	*	1,00		
Time*Nitric Acid Concentration	*	1,00		
Temperature*Particle Size	*	1,00		
Temperature*Nitric Acid Concentration	*	1,00		
Particle Size*Nitric Acid Concentration	*	1,00		
Time*Temperature*Particle Size	*	1,00		
Time*Temperature*Nitric Acid Concentration	*	1,00		
Time*Particle Size*Nitric Acid Concentration	*	1,00		
Temperature*Particle Size*Nitric Acid Concentration	*	1,00		
Time*Temperature*Particle Size*Nitric Acid Concentration	*	1,00		

Table B.6: Regression Equation in Uncoded Units

$$\begin{aligned}
 \text{Yield-Ni} = & -0,000365 & + 0,000133 & \text{Time} & + 0,000010 & \text{Temperature} \\
 & + 0,000099 & \text{Particle Size} & & & \\
 & + 0,000108 & \text{Nitric Acid Concentration} & - 0,000002 & \text{Time*Temperature} & \\
 & - 0,000024 & \text{Time*Particle Size} & - 0,000043 & \text{Time*Nitric Acid Concentration} & \\
 & - 0,000002 & \text{Temperature*Particle Size} & & & \\
 & - 0,000002 & \text{Temperature*Nitric Acid Concentration} & & & \\
 & - 0,000031 & \text{Particle Size*Nitric Acid Concentration} & & & \\
 & + 0,000000 & \text{Time*Temperature*Particle Size} & & & \\
 & + 0,000001 & \text{Time*Temperature*Nitric Acid Concentration} & & & \\
 & + 0,000011 & \text{Time*Particle Size*Nitric Acid Concentration} & & & \\
 & + 0,000001 & \text{Temperature*Particle Size*Nitric Acid Concentration} & & & \\
 & - 0,000000 & \text{Time*Temperature*Particle Size*Nitric Acid Concentration} & & &
 \end{aligned}$$

The nickel model above shows the significance of each parameter and the significance of interaction between parameters towards the copper yield. In the model, there are positive and negative coefficients associated with the parameters.

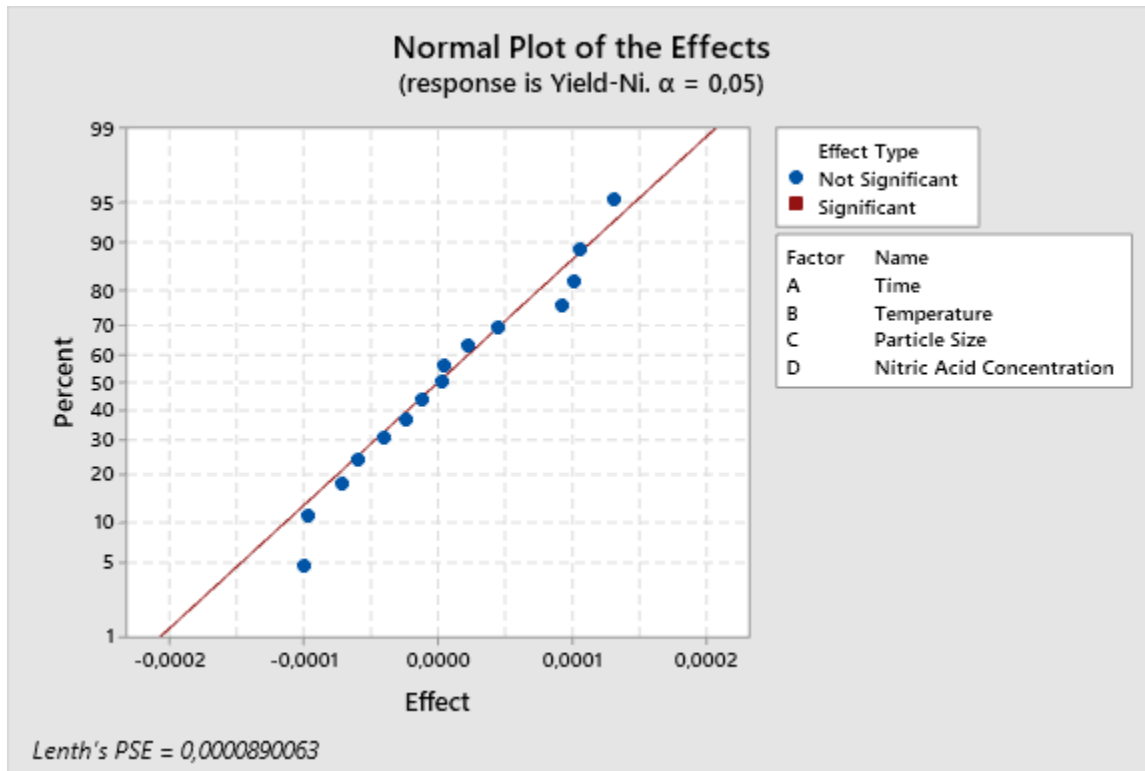


Figure B.5: Normal Plot of effects

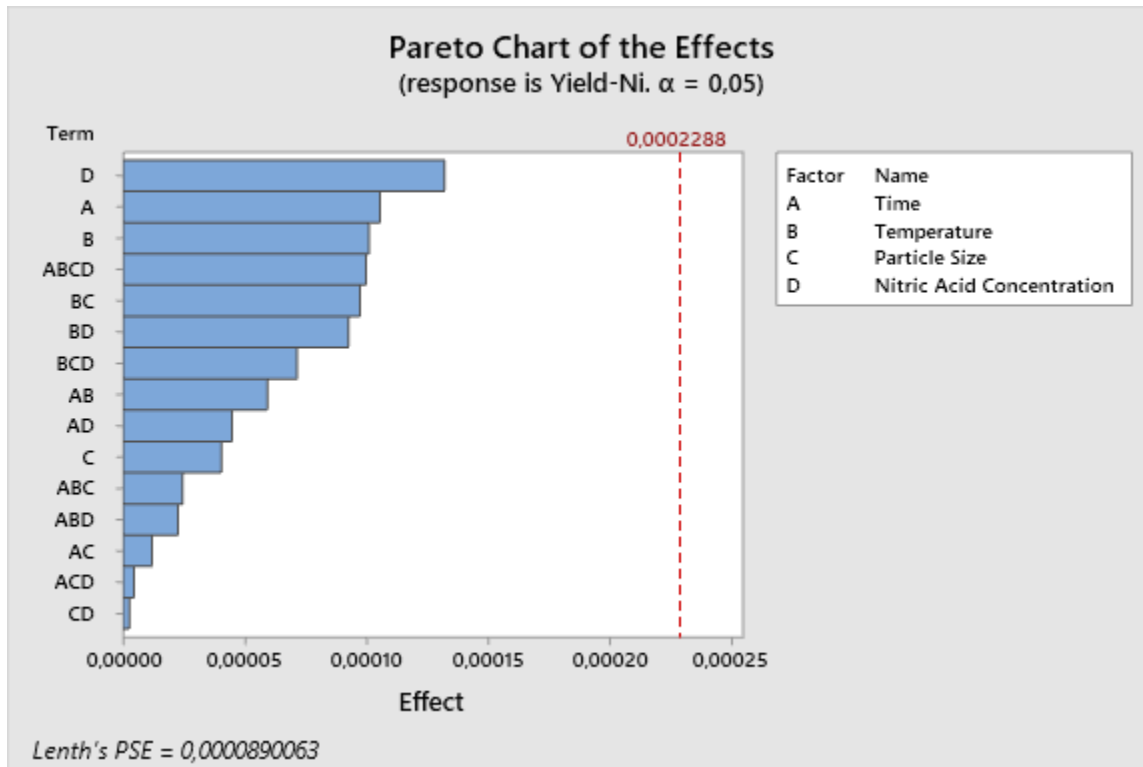


Figure B.6: Pareto Chart of the effects

The Pareto chart shown in figure B.6 above shows that in the recovery of nickel, none of the parameters and their interactions being investigated are significant; they do not go passed the critical value line.

B.4 HYDROMETALLURGICAL PROCESSING: Iron (H_2SO_4 and H_2O_2 conditions)

The table below shows the results of the leached iron for different runs under sulphuric acid and hydrogen peroxide conditions.

Table B.7: leached iron for different runs under sulphuric acid and hydrogen peroxide conditions

Run	Average reported concentration (mg/L)	Old concentration (ppm)	Amount of metal (g) (50ml was used for experiments)	Metal fraction within the PCB (3,125g)
1	0.06767	33.83333	0.00169	0.00054
2	0.07467	37.33333	0.00187	0.00060
3	0.07333	36.66667	0.00183	0.00059
4	0.45467	227.33333	0.01137	0.00364

5	0.11967	59.83333	0.00299	0.00096
6	0.06333	31.66667	0.00158	0.00051
7	0.40333	201.66667	0.01008	0.00323
8	0.15467	77.33333	0.00387	0.00124
9	0.332	166	0.0083	0.00266
10	0.04367	21.83333	0.00109	0.00035
11	0.19067	95.33333	0.00477	0.00153
12	0.328	164	0.0082	0.00262
13	0.09267	46.33333	0.00232	0.00074
14	0.2	100	0.005	0.00160
15	0.21333	106.66667	0.00533	0.00171
16	0.06567	32.83333	0.00164	0.00053

The contents of the table above are more clearly expressed by the graph below

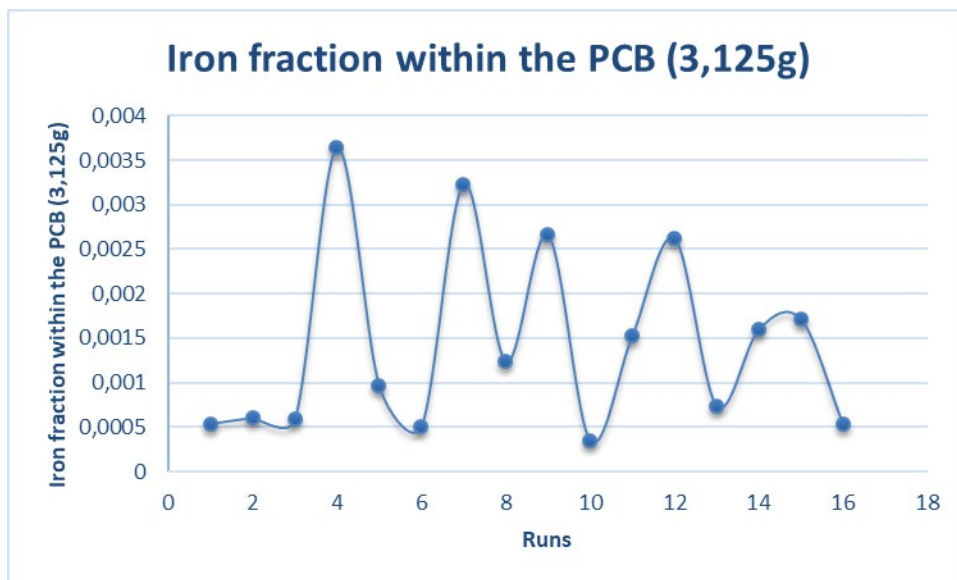


Figure B.7: Iron fraction within PCB (3,125g)

From the iron fraction above, it is evident that most of the iron was recovered in run 4 where 0.00364 iron fraction was dissolved in solution.

B.5 HYDROMETALLURGICAL PROCESSING: Nickel (H₂SO₄ and H₂O₂ conditions)

Table B.8 shows the results of the leached nickel for different runs under sulphuric acid and hydrogen peroxide conditions.

Table B.7: leached nickel for different runs under sulphuric acid and hydrogen peroxide conditions.

Run	Average reported concentration (mg/L)	Old concentration (ppm)	Amount of metal (g) (50ml was used for experiments)	Metal fraction within the PCB (3,125g)
1	0.051	25.5	0.00128	0.00041
2	0.03833	19.16667	0.00096	0.00031
3	0.034	17	0.00085	0.00027
4	0.047	23.5	0.00118	0.00038
5	0.00033	0.16667	0.000008	0.000003
6	0.01467	7.33333	0.00037	0.00012
7	-0.022	-11	-0.00055	-0.00018
8	0.03433	17.16667	0.00086	0.00028
9	0.058	29	0.00145	0.00046
10	0.01833	9.16667	0.00046	0.00015
11	0.049	24.5	0.00123	0.00039
12	-0.03767	-18.83333	-0.00094	-0.00030
13	0.02167	10.83333	0.00054	0.00017
14	-0.00733	-3.66667	-0.00018	-0.00006
15	-0.023	-11.5	-0.00058	-0.00018
16	0.02133	10.66667	0.00053	0.00017

The contents of the table above are more clearly expressed by the graph below

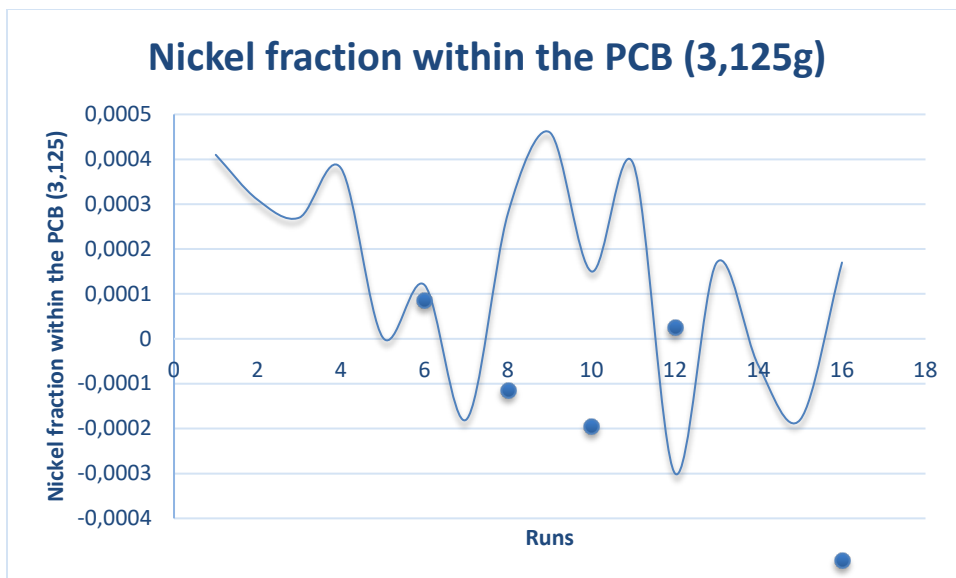


Figure B.8: Nickel fraction within the PCB (3,125)

From the nickel fraction above, it is evident that most of the nickel was recovered in run 9 where 0.00046 nickel fraction was dissolved in solution.

For iron, most recovery of the metal is in run 4 under the following conditions; time = 8hours, temperature = 80°C, sulphuric acid concentration = 0.8M and hydrogen peroxide volume % = 4%. Most nickel is recovered in run 9 where the conditions are as follows; time = 2hours, temperature = 80°C, sulphuric acid concentration = 1.2M and hydrogen peroxide volume % = 20%.

B.6 ANALYSIS IN MINITAB (Nickel (H₂SO₄ and H₂O₂ conditions)

B.6.1 Iron Yield

Table B.8: Coded Coefficients

Term	Effect
Constant	
Hydrogen Peroxide volume %	0,000108
Sulphuric acid concentration	-0,000890
Temperature	0,000252
Time	-0,000055
Hydrogen Peroxide volume %*Sulphuric acid concentration	0,000352
Hydrogen Peroxide volume %*Temperature	-0,000583
Hydrogen Peroxide volume %*Time	-0,000275
Sulphuric acid concentration*Temperature	-0,000167
Sulphuric acid concentration*Time	-0,000631
Temperature*Time	-0,000393
Hydrogen Peroxide volume %*Sulphuric acid concentration*Temperature	0,001248
Hydrogen Peroxide volume %*Sulphuric acid concentration*Time	0,000011
Hydrogen Peroxide volume %*Temperature*Time	-0,000804
Sulphuric acid concentration*Temperature*Time	0,000146
Hydrogen Peroxide volume %*Sulphuric acid concentration*Temperature*Time	-0,000114

Term	Coef	SE Coef
Constant	0,001439	*
Hydrogen Peroxide volume %	0,000054	*
Sulphuric acid concentration	-0,000445	*
Temperature	0,000126	*
Time	-0,000027	*
Hydrogen Peroxide volume %*Sulphuric acid concentration	0,000176	*
Hydrogen Peroxide volume %*Temperature	-0,000291	*
Hydrogen Peroxide volume %*Time	-0,000137	*
Sulphuric acid concentration*Temperature	-0,000084	*
Sulphuric acid concentration*Time	-0,000316	*
Temperature*Time	-0,000197	*
Hydrogen Peroxide volume %*Sulphuric acid concentration*Temperature	0,000624	*
Hydrogen Peroxide volume %*Sulphuric acid concentration*Time	0,000006	*
Hydrogen Peroxide volume %*Temperature*Time	-0,000402	*
Sulphuric acid concentration*Temperature*Time	0,000073	*
Hydrogen Peroxide volume %*Sulphuric acid concentration*Temperature*Time	-0,000057	*

Term	T-Value	P-Value
Constant	*	*
Hydrogen Peroxide volume %	*	*
Sulphuric acid concentration	*	*
Temperature	*	*
Time	*	*
Hydrogen Peroxide volume %*Sulphuric acid concentration	*	*
Hydrogen Peroxide volume %*Temperature	*	*
Hydrogen Peroxide volume %*Time	*	*
Sulphuric acid concentration*Temperature	*	*
Sulphuric acid concentration*Time	*	*
Temperature*Time	*	*
Hydrogen Peroxide volume %*Sulphuric acid concentration*Temperature	*	*
Hydrogen Peroxide volume %*Sulphuric acid concentration*Time	*	*
Hydrogen Peroxide volume %*Temperature*Time	*	*
Sulphuric acid concentration*Temperature*Time	*	*
Hydrogen Peroxide volume %*Sulphuric acid concentration*Temperature*Time	*	*

Term	VIF
Constant	

Table B.9: Regression Equation in Uncoded Units

$$\begin{aligned}
 \text{Yeild-Fe} = & -0,01013 & & + 0,000698 \text{ Hydrogen Peroxide volume \%} \\
 & + 0,01141 \text{ Sulphuric acid concentration} & + 0,000229 \text{ Temperature} & + 0,000846 \text{ Time} \\
 & - 0,000753 \text{ Hydrogen Peroxide volume \%*Sulphuric acid concentration} \\
 & - 0,000015 \text{ Hydrogen Peroxide volume \%*Temperature} \\
 & + 0,000002 \text{ Hydrogen Peroxide volume \%*Time} \\
 & - 0,000233 \text{ Sulphuric acid concentration*Temperature} \\
 & - 0,001044 \text{ Sulphuric acid concentration*Time} & & - 0,000005 \text{ Temperature*Time} \\
 & + 0,000016 \text{ Hydrogen Peroxide volume \%*Sulphuric acid concentration*Temperature} \\
 & + 0,000024 \text{ Hydrogen Peroxide volume \%*Sulphuric acid concentration*Time} \\
 & - 0,000000 \text{ Hydrogen Peroxide volume \%*Temperature*Time} \\
 & + 0,000010 \text{ Sulphuric acid concentration*Temperature*Time} \\
 & - 0,000000 \text{ Hydrogen Peroxide volume \%*Sulphuric acid concentration*Temperature*Time} \\
 & e
 \end{aligned}$$

The iron model above shows the significance of each parameter and the significance of interaction between parameters towards the iron yield

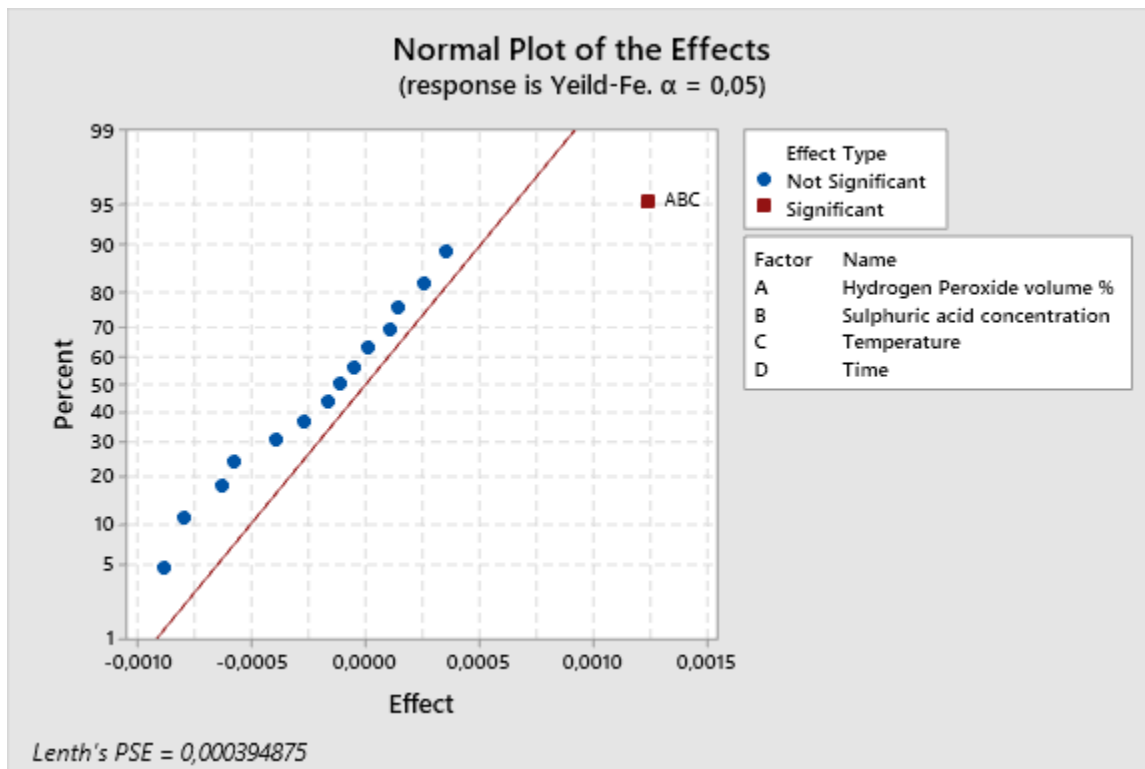


Figure B.9: Normal Plot of the effects

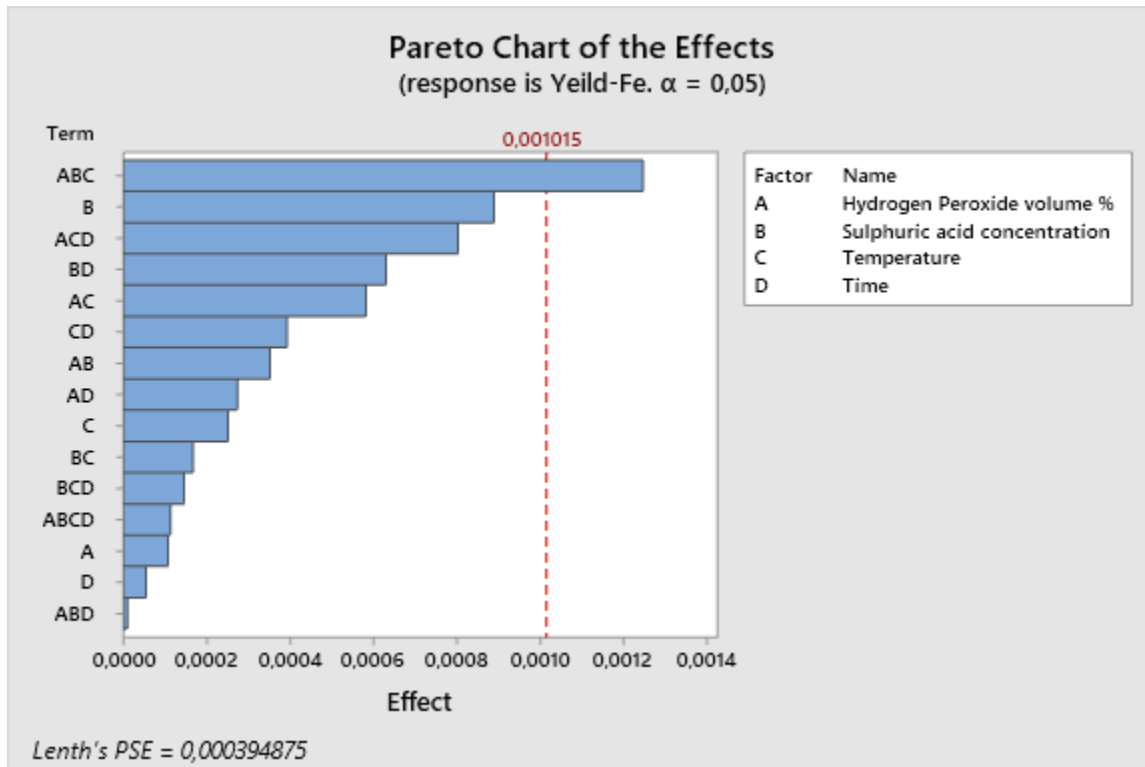


Figure B.10: Pareto Chart of the effects Iron, $\alpha=0,05$

From the Pareto chart, the interaction of hydrogen peroxide volume %, sulphuric acid concentration and temperature is the only significant factor as it passes the critical value line. However, the table of results showed just how little of the iron was being recovered and thus persuing its recovery is not economical.

B.6.2 Nickle Yield

Table B.10: Coded Coefficients

Term	Effect
Constant	
Hydrogen Peroxide volume %	0,000040
Sulphuric acid concentration	0,000092
Temperature	0,000218
Time	0,000096
Hydrogen Peroxide volume %*Sulphuric acid concentration	0,000094
Hydrogen Peroxide volume %*Temperature	0,000212
Hydrogen Peroxide volume %*Time	-0,000183
Sulphuric acid concentration*Temperature	0,000055
Sulphuric acid concentration*Time	-0,000069
Temperature*Time	0,000069
Hydrogen Peroxide volume %*Sulphuric acid concentration*Temperature	-0,000137
Hydrogen Peroxide volume %*Sulphuric acid concentration*Time	0,000042
Hydrogen Peroxide volume %*Temperature*Time	-0,000070
Sulphuric acid concentration*Temperature*Time	-0,000044
Hydrogen Peroxide volume %*Sulphuric acid concentration*Temperature*Time	0,000103

Term	Coef	SE Coef
Constant	0,000149	*
Hydrogen Peroxide volume %	0,000020	*
Sulphuric acid concentration	0,000046	*
Temperature	0,000109	*
Time	0,000048	*
Hydrogen Peroxide volume %*Sulphuric acid concentration	0,000047	*
Hydrogen Peroxide volume %*Temperature	0,000106	*
Hydrogen Peroxide volume %*Time	-0,000091	*
Sulphuric acid concentration*Temperature	0,000027	*
Sulphuric acid concentration*Time	-0,000034	*
Temperature*Time	0,000034	*
Hydrogen Peroxide volume %*Sulphuric acid concentration*Temperature	-0,000068	*
Hydrogen Peroxide volume %*Sulphuric acid concentration*Time	0,000021	*
Hydrogen Peroxide volume %*Temperature*Time	-0,000035	*
Sulphuric acid concentration*Temperature*Time	-0,000022	*
Hydrogen Peroxide volume %*Sulphuric acid concentration*Temperature*Time	0,000051	*

Term	T-Value	P-Value
Constant	*	*
Hydrogen Peroxide volume %	*	*
Sulphuric acid concentration	*	*
Temperature	*	*
Time	*	*
Hydrogen Peroxide volume %*Sulphuric acid concentration	*	*
Hydrogen Peroxide volume %*Temperature	*	*
Hydrogen Peroxide volume %*Time	*	*
Sulphuric acid concentration*Temperature	*	*
Sulphuric acid concentration*Time	*	*
Temperature*Time	*	*
Hydrogen Peroxide volume %*Sulphuric acid concentration*Temperature	*	*
Hydrogen Peroxide volume %*Sulphuric acid concentration*Time	*	*
Hydrogen Peroxide volume %*Temperature*Time	*	*
Sulphuric acid concentration*Temperature*Time	*	*
Hydrogen Peroxide volume %*Sulphuric acid concentration*Temperature*Time	*	*

Term	VIF
Constant	

Table B.11: Regression in Uncoded Units

$$\begin{aligned}
 \text{Yeild-Ni} = & 0,002574 && - 0,000209 \text{ Hydrogen Peroxide volume \%} \\
 & - 0,002392 \text{ Sulphuric acid concentration} && - 0,000061 \text{ Temperature} && - 0,000199 \text{ Time} \\
 & + 0,000191 \text{ Hydrogen Peroxide volume \%*Sulphuric acid concentration} \\
 & + 0,000004 \text{ Hydrogen Peroxide volume \%*Temperature} \\
 & + 0,000015 \text{ Hydrogen Peroxide volume \%*Time} \\
 & + 0,000054 \text{ Sulphuric acid concentration*Temperature} \\
 & + 0,000206 \text{ Sulphuric acid concentration*Time} && + 0,000007 \text{ Temperature*Time} \\
 & - 0,000004 \text{ Hydrogen Peroxide volume \%*Sulphuric acid concentration*Temperature} \\
 & - 0,000016 \text{ Hydrogen Peroxide volume \%*Sulphuric acid concentration*Time} \\
 & - 0,000000 \text{ Hydrogen Peroxide volume \%*Temperature*Time} \\
 & - 0,000006 \text{ Sulphuric acid concentration*Temperature*Time} \\
 & + 0,000000 \text{ Hydrogen Peroxide volume \%*Sulphuric acid concentration*Temperature*Time} \\
 & e
 \end{aligned}$$

The nickel model above shows the significance of each parameter and the significance of interaction between parameters towards the nickel yield.

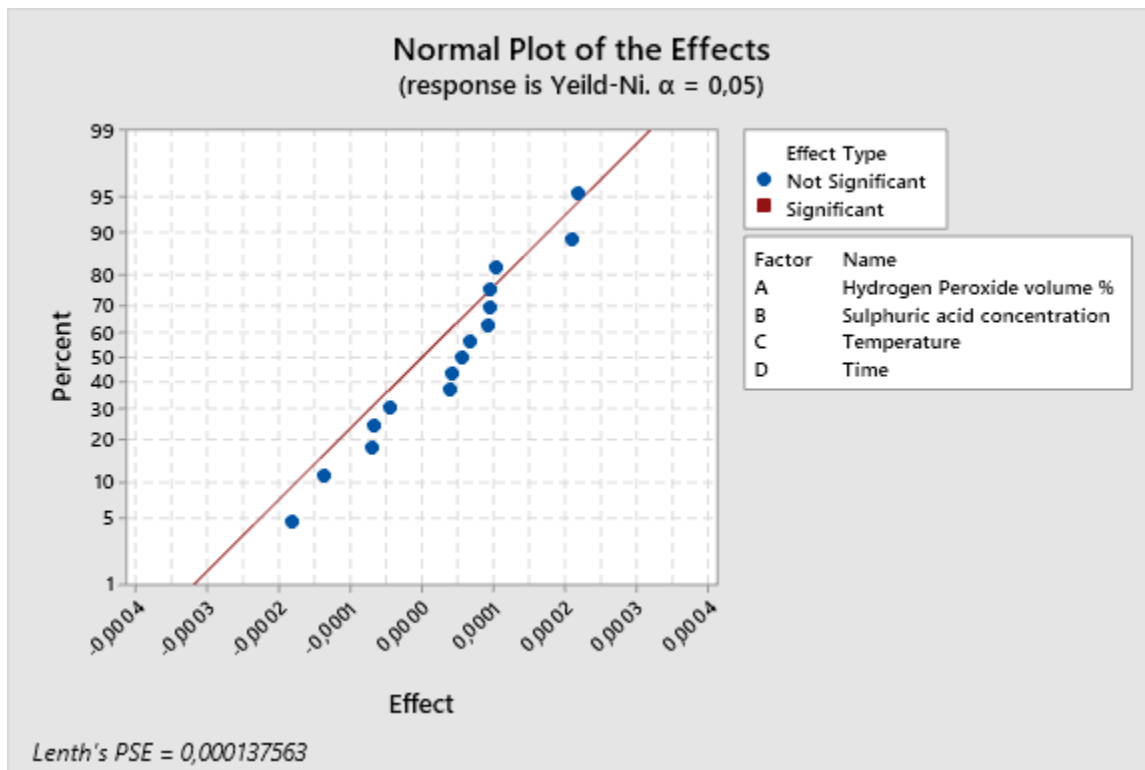


Figure B.11: Normal Plot of the effects Nickel, alpha=0,05

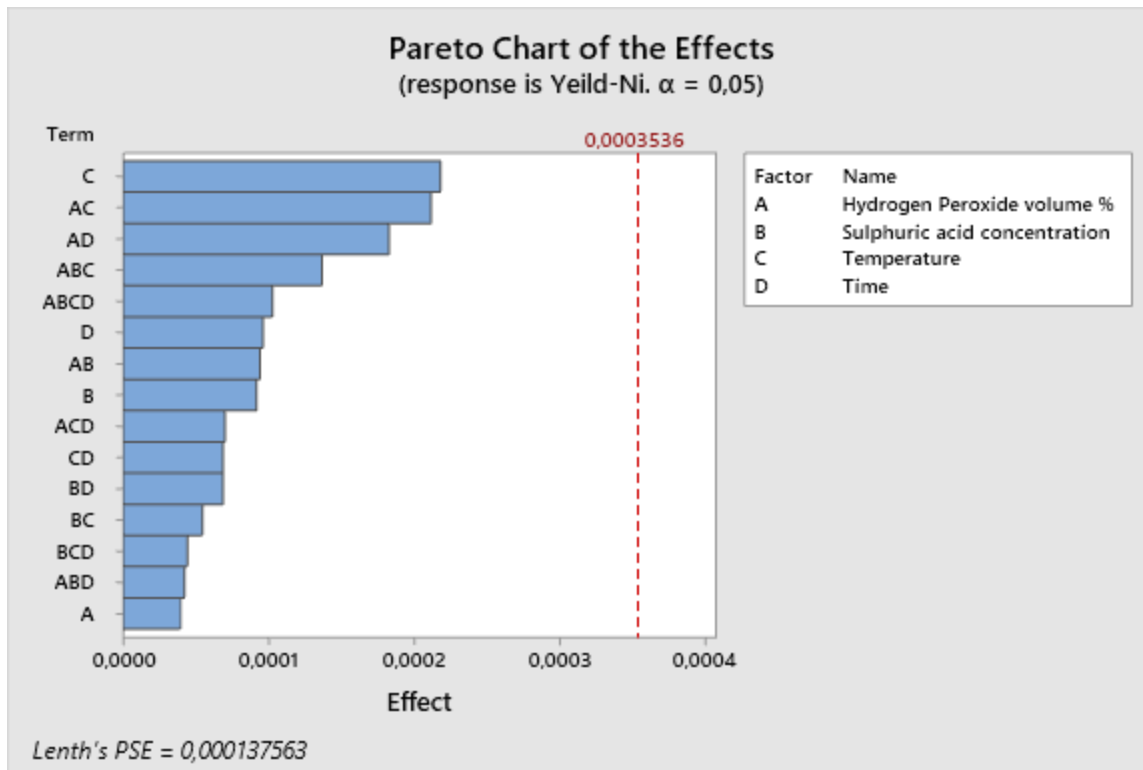


Figure B.12: Pareto Chart of the effects Nickel, alpha=0.05

The nickel Pareto chart shows that all the parameters and their interactions are insignificant towards the yield of nickel as none of them pass the critical value line. Even if they were significant, the amount of nickel that is being recovered from the leaching is so small that it is not economical to recover it.

In these tables and graphs above, it is observed that the amount of nickel and iron that is recovered from these leaching experiments conducted under both nitric acid and sulphuric acid with hydrogen peroxide conditions are small. Under both conditions, the highest amount of nickel and iron recovered was 0.0006 and 0.0047 respectively. Because of such low recoveries for nickel and iron, going forward the research will focus primarily on copper and how to optimize its recovery. The Pareto charts also indicate that the parameters and their interactions are not significant towards the recovery of nickel and iron.

B.7 SURFACE PLOTS

Graphs B.13 – B.19 show the surface plot of percentage copper recovered vs time, temperature, particle size and hydrogen peroxide volume percentage from using the central composite design.

Surface Plots of %Cu dissolved

Hold Values
 Hydrogen peroxide vol % 12
 Temperature 47,5
 Time 210
 Particle size 1,3875

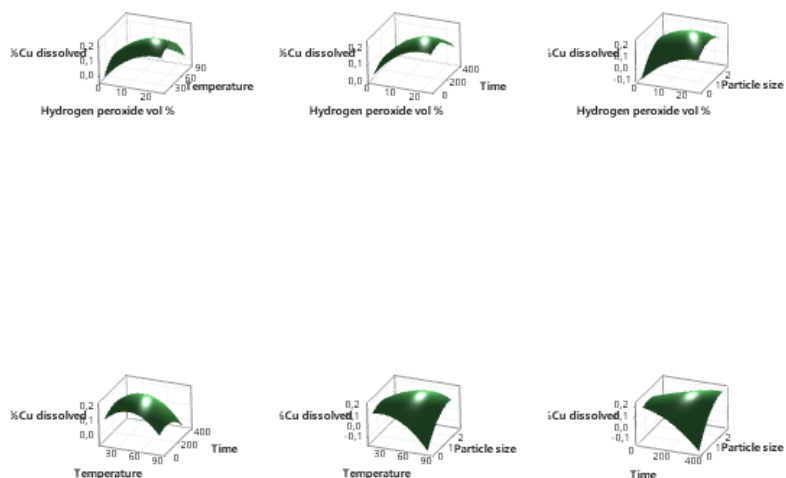


Figure B.13: Surface Plots of %Copper dissolved

Surface Plot of %Cu dissolved vs Temperature. Hydrogen peroxide vol %

Hold Values
Time 210
Particle size 1,3875

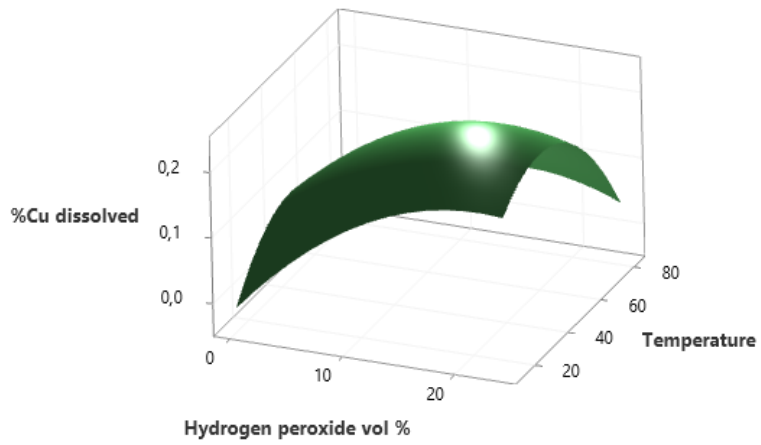


Figure B.14: Surface Plot of %copper dissolved Vs Temperature, Hydrogen peroxide volume%

Surface Plot of %Cu dissolved vs Time. Hydrogen peroxide vol %

Hold Values
Temperature 47,5
Particle size 1,3875

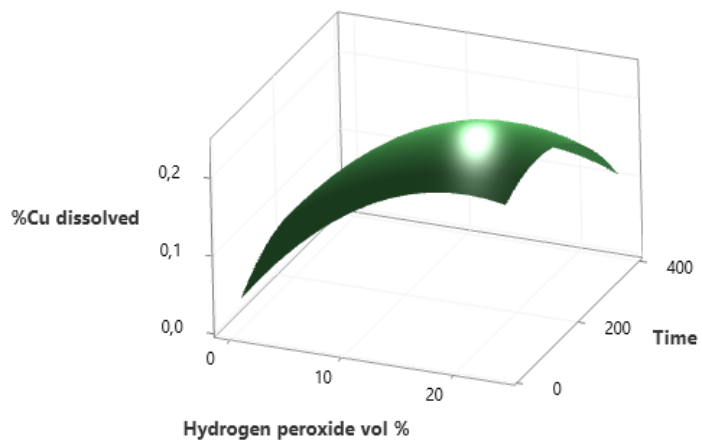


Figure B.15: Surface of %Copper dissolved Vs Time, Hydrogen peroxide volume%

Surface Plot of %Cu dissolved vs Particle size. Hydrogen peroxide vol

Hold Values
Temperature 47,5
Time 210

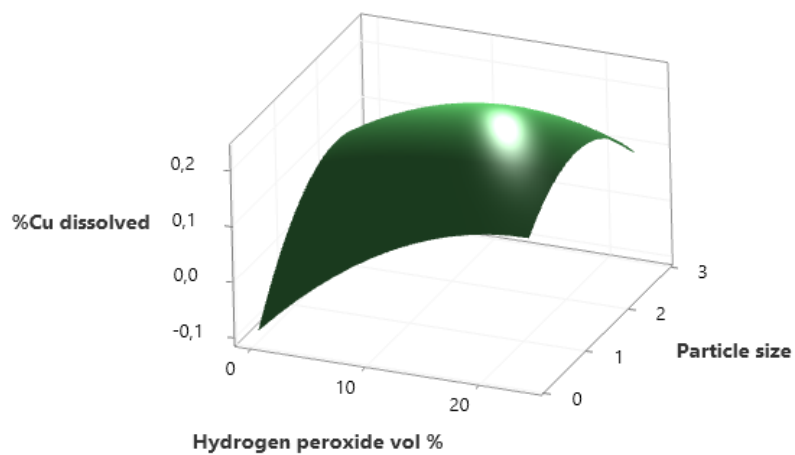


Figure B.16: Surface Plot of %Copper dissolved VS particle size. Hydrogen peroxide volume%

Surface Plot of %Cu dissolved vs Time. Temperature

Hold Values
Hydrogen peroxide vol % 12
Particle size 1,3875

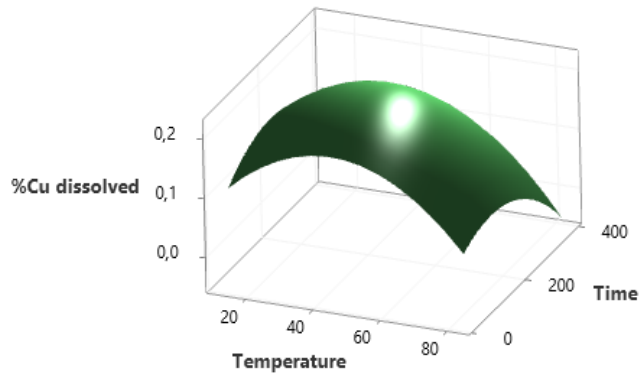


Figure B.17: Surface Plot of %Cu dissolved VS time. Temperature

Surface Plot of %Cu dissolved vs Particle size. Temperature

Hold Values
Hydrogen peroxide vol % 12
Time 210

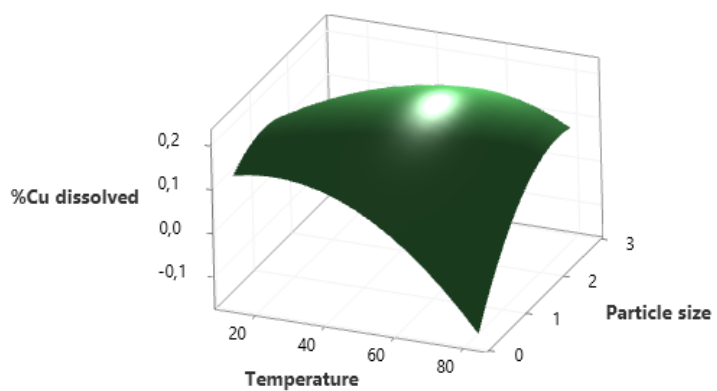


Figure B.18: Surface Plot of %Copper dissolved vs Particle size. Temperature

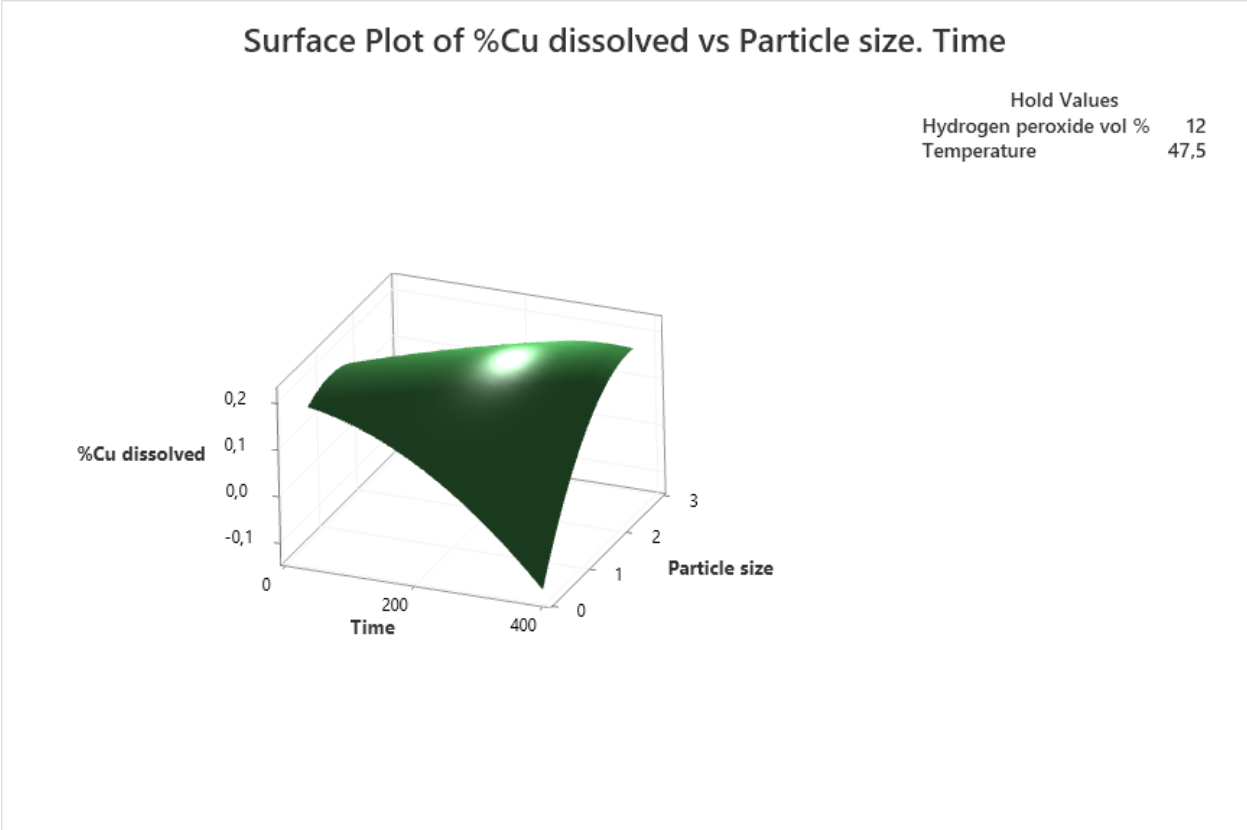


Figure B.19: Surface Plot of %Copper vs Particle size. Time

B.7.1 Interaction Plots

Figure B.20 shows the Interaction plots for recovering copper from waste PCBs using the Central Composite Design method.

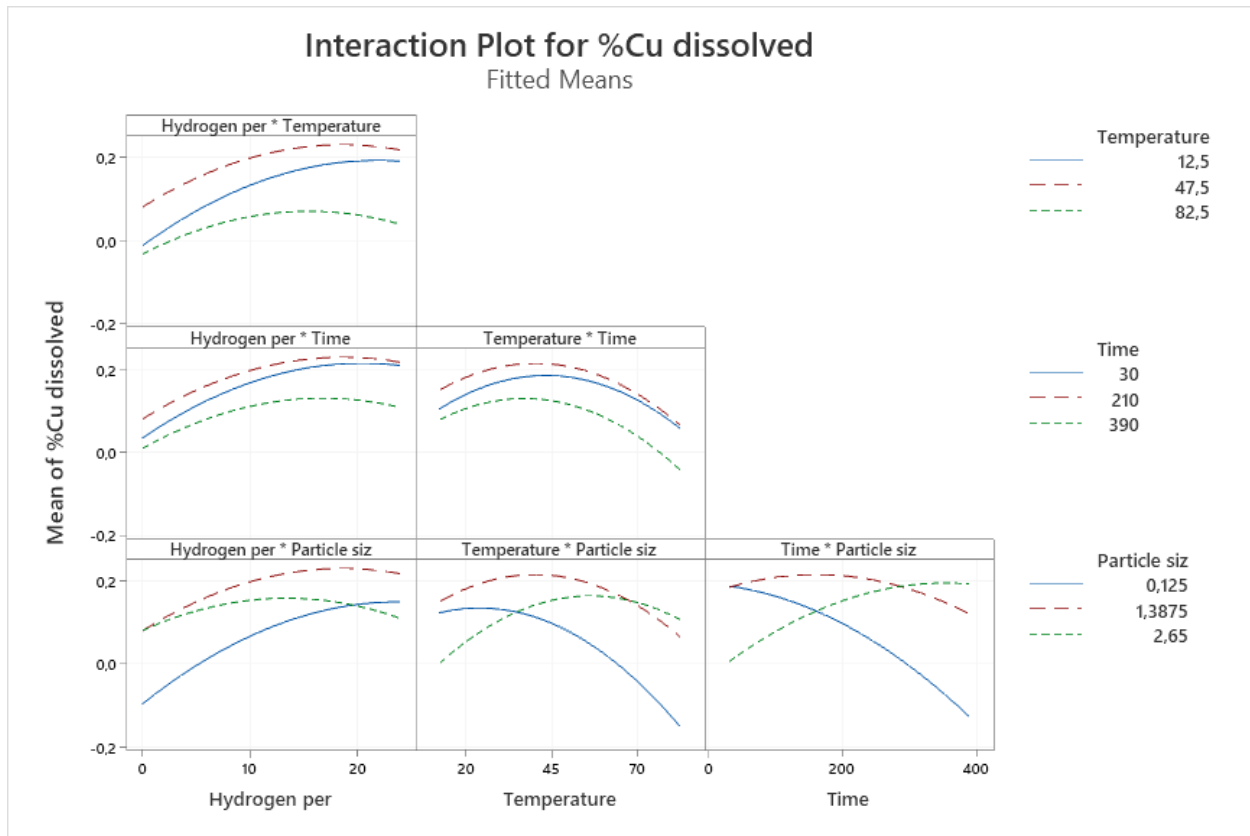


Figure B.20: Interaction Plot for %Copper dissolved

